Syntheses and Phase Equilibria of Orthorhombic Forms of ZrO_2

by

Osamu Ohtaka

Department of Material Physics,
Faculty of Engineering Science

A Thesis submitted in conformity with the requirements for the Degree of Doctor of Engineering in Osaka University

February 1989

Contents

Abstract

Zirconia (ZrO_2), which is monoclinic symmetry at room temperature in ambient pressure, has two high pressure polymorphs with orthorhombic symmetry (orthoⅠ and orthoⅡ). High pressure synthesis experiments of both phases were carried out.

It was found that orthoⅠ is quenchable only when very fine powder, the critical crystallite size is 60 nm, is used as a starting material and that stabilized tetragonal and cubic phases do not transform to orthoⅠ because of small differences in density among these three phases.

The stable region of orthoⅡ was obtained by phase equilibrium experiment. OrthoⅠ transforms to orthoⅡ at 15 GPa 800 ℃. Above 1000 ℃ orthoⅡ transforms to the cubic. OrthoⅡ of stabilized ZrO_2 was synthesized.

Enthalpies of phase transformation among high pressure phases were measured by calorimetry experiment. The entropies of phase transformation and slopes of the phase boundaries were calculated using the measured enthalpies and free energies calculated from the phase equilibrium data. The entropy of the monoclinic-orthoⅠ phase transformation has positive value and dP/dT has negative value. This result is reasonable when the crystal structures of both phases are compared. The orthoⅠ-orthoⅡ phase transformation has a negative value of entropy and a positive dP/dT. This is consistent with the results of synthesis experiment.

General Introduction

Zirconia (ZrO_2) is one of the major components of ceramic materials. In addition to its use as refractory materials, two more remarkable properties were pointed out recently; the transformation toughening which is described as 'ceramic steel' metaphorically and the electrolytic properties which are finding various uses such as an oxygen sensor. Consequently, ZrO_2 has received increasing attention lately in science and technology.

Its high temperature polymorphs, the tetragonal and the cubic phases, including partially and totally stabilized ZrO_2 by doping with small additions of CaO, Y_2O_3, MgO etc. have been investigated extensively. On the other hand, there are only a few studies of the high pressure phase of ZrO_2. ZrO_2 has two high pressure polymorphs. As both of the two phases have orthorhombic symmetries, in this paper, these terms "Ortho I " and "Ortho II " are used to identify the lower and the higher pressure phases respectively.

Ortho I was first introduced by Bocquillon and Sussee (1968). Because of the difficulty of quenching the phase, the studies of this phase were mainly performed by in-situ observations combining a diamond anvil pressure cell and X-ray diffractometer. Therefore, informations derived from quenched sample such as thermodynamical data are scarcely reported.

The toughening mechanism of ZrO_2 is explained by a phase transformation induced by a stress field. As ortho I was reported to appear on the fracture surface of stabilized ZrO_2 (Lenz and Heuer 1982), it is interesting to investigate the stability and

the mechanism of phase transformation of high pressure phase including stabilized ZrO_2.

OrthoII was found by Liu (1980). He synthesized the phase and showed that the phase has an orthorhombic cotunnite ($PbCl_2$) structure. The existence of the orthoII phase was confirmed by Ming (1985) and Block (1985). Block reported that this phase appears above 16.6 GPa at room temperature. While consistent results regarding the crystal structure have been reported, phase boundary between orthoI and orthoII is poorly understood because of the experimental difficulty under high pressure. Furthermore there is no thermodynamical data of this phase.

The author has made a series of experiments to determine stable regions of each phase and investigate the phase transformations. Furthermore, using synthesized sample, the thermodynamical approach to the high pressure polymorphs (monoclinic, orthoI and orthoII) was attempted through measuring the enthalpies of transition by drop calorimetry. The entropies of transition were evaluated by combining the phase equilibrium data.

In this paper the author reports the synthesis of orthoI including the effect of small amounts of additives such as Y_2O_3 and MgO in Chap.1, structure refinement of the orthoI by X-ray and neutron diffraction in Chap.2, the synthesis of orthoII in Chap.3 and thermodynamics of orthoI and orthoII in Chap.4, respectively.

Chapter 1. Synthesis of Ortho I

Introduction

The high pressure phase of ZrO_2 was first studied by Whitney (1962) and (1965). Considering the thermodynamical data of the monoclinic and the tetragonal, he indicated that the slope of the phase boundary (dP/dT) between these phases had a negative value, therefore, stable region of the tetragonal extended to higher pressure part of the monoclinic.

The high pressure phase with an orthorhombic symmetry was introduced by Bocquillon et al. (1968). They synthesized the high pressure phase of hafnia (HfO_2), which has an orthorhombic symmetry, and predicted that ZrO_2 also would have a high pressure phase with the orthorhombic symmetry because ZrO_2 and HfO_2 share same characters in many respects. However, it was difficult to quench the high pressure phase of ZrO_2 as a single phase, therefore, they only showed the region where this phase was recovered in P-T space (Boquillon and Sussee, 1969).

Because of the difficulty of quenching the phase, the studies of this phase were mainly performed by in-situ observations combining a diamond anvil pressure cell and X-ray diffractometer. By optical and X-ray powder diffraction techniques using a diamond anvil pressure cell, Block et al. (1985) reported that the monoclinic transforms to a high pressure phase at 3.3-4.4 GPa at room temperature. In their study, however, they identified the high pressure phase not as an orthorhombic but as a tetragonal which has lower symmetry than the tetragonal of the high temperature polymorph. These controversies regarding the crystal

symmetry of the phase arised from the fact that lattice parameters of ortho I are very close to that of the tetragonal and it is difficult to identify them by in-situ observation under pressure using X-ray diffraction method.

From the results of Raman spectrum observation under pressure, Arashi (1982) reported that the high pressure phase cannot be identified as a tetragonal. Using a diamond anvil pressure cell and single crystal X-ray diffraction method, Kudoh (1986) showed that this high pressure phase has an orthorhombic symmetry and its space group is Pbcm. Suyama (1986) succeeded in synthesizing the high pressure phase as a single phase and confirmed the result presented by Kudoh. While disputation regarding to the structure of this phase seems to have been settled, other informations such as thermodynamical data are rarely obtained.

Zirconia ceramics has received considerable interest in recent years in connection with its high strength and high fracture toughness. The toughening mechanism of ZrO_2 ceramics is explained by a phase transformation induced by a stress field (Gupta et al., 1981). Furthermore, Lenz and heuer (1982) and Dickerson et al. (1987) reported that a new ZrO_2 polymorph with an orthorhombic symmetry was observed on fracture surfaces of commercial partially stabilized ZrO_2 and the occurrence of orthorhombic ZrO_2 is a thin foil artifact; no orthorhombic ZrO_2 has been observed using X-ray diffraction from bulk specimens.

In view of this state of affairs, the investigation of the phase transformation at high pressure and the stability of the phases are considered to be important. Therefore, high pressure synthesis experiments were executed in order to obtain single

phase of ortho I both in good quality and quantity for the characterization and thermodynamical study.

Considering the results of previous researcher (Suyama et al. 1986), there seem to be two essential conditions to synthesize the ortho I ; starting material should be very fine powder and the synthesis should be carried out under hydrostatic pressure. For the purpose of obtaining hydrostatic pressure, small amount of water was added to starting material. As regards the grain size, some starting materials of different grain size were prepared and synthesis experiments were conducted to examine its effect.

Furthermore, synthesis of ortho I of partially and totally stabilized ZrO_2 was attempted to reveal the effects of a small amount of additives on ortho I . Their results are reported in this chapter.

Experimental

§ 1 Synthesis

1-1 Starting Material

To characterize ZrO_2 fine powder, dehydration of $Zr(OH)_4$ was undertaken and crystallized precipitate was examined by thermogravimetry (TG), differential thermal analysis (DTA) and X-ray powder diffraction (XRD). $Zr(OH)_4$ was prepared as follows: A solution of $ZrOCl_2$ was directly reacted with NH_4OH at pH 10. The resultant precipitate was decanted, washed with methanol, filtrated and dried at 110 ℃. The thermal analysis was carried out with a Rigaku thermoanalyser in air. About 40 mg of dried gel was placed in a platinum crucible and heated at the rate of 15 ℃ $*min^{-1}$. Finely powdered alumina was used as a reference material.

To study the grain size effects on the synthesis of ortho I, starting materials with various grain size were prepared by annealing for appropriate duration of time. Crystallite size was evaluated with full-width at half maximum (FWHM) of X-ray powder diffraction pattern.

Starting materials with small amount of additives are summarized in Table 1-1. The chemical analyses results of MgO doped ZrO_2 are listed in Table 1-2.

Transmission electron microscopy (TEM) was used to observe each grain before and after the high pressure synthesis, the concentration of additives was examined by energy dispersive X-ray fluorescence analyser equipped in the TEM.

1-2 High Pressure Synthesis

High pressure synthesis of ortho I was undertaken using a cubic anvil type apparatus. The apparatus consists of six anvils made of tungsten carbide, four of which are fixed to the anvil blocks on a horizontal plane as shown in Fig.1-1. The upper and the lower surfaces of these four anvil blocks contact with the surfaces of the upper and the lower pressing blocks, respectively. The other two anvils are located at the center of the upper and the lower pressing blocks along a vertical axis.

When a hydraulic press works, the upper pressing block advances vertically. Since the pressing block contacts with the anvil blocks at the angle of 45° ,the vertical movement of pressing block causes the horizontal movement of four anvil blocks. Six anvils synchronously move forwards with the same amount of displacements and compress the sample in center to produce high pressure.

The upper and the lower surfaces of four anvil blocks in horizontal plane are covered with teflon sheets for the purposes of both the electric insulation and the reduction of friction. Pyrophyllite is used as the pressure transmission media. The detailed procedure of the synchronization of anvils and the pretreatment of pyrophyllite was described by Endo(1970).

The magnitudes of pressure generated in the sample were calibrated by detecting the changes of the electric resistance of Bi at 2.55 GPa and Ba at 5.5 GPa. The relation between the load oil pressure in the hydraulic press of the apparatus and the pressure generated in the sample is shown in Fig.1-2. Pressures were interpolated from these two fixed points.

The temperature of the sample was evaluated from the electric current through the graphite heater and calibrated by inserting a Pt/Pt-13%Rh thermocouple in the cell under working pressure. No correction for pressure effects on the emf was made.

The starting material charged in a platinum capsule was inserted into a cell illustrated in Fig.1-3. BN sleeve was used as an insulator. For the purpose of obtaining hydrostatic pressure, small amount of water was added to starting material.

Table 1-1 ZrO_2 Fine Powder Used in the Experiments

symbol	additives	mol%	remarks
non-doped	-	-	Toso Co.
non-doped	-	-	precipitation
2Y	Y_2O_3	2	Toso Co.
4Y	Y_2O_3	4	Toso Co.
6Y	Y_2O_3	6	Toso Co.
2M	MgO	2	Osaka Cement Co.
4M	MgO	4	Osaka Cement Co.
6M	MgO	6	Osaka Cement Co.

Table 1-2 Chemical Analysis of MgO-ZrO_2

	MgO	SiO_2	Fe_2O_3	TiO_2	Na_2O
2MgO-	0.738 (2.23)	0.0004	0.005	0.0004	0.026
4MgO-	1.442 (4.29)	0.0003	0.003	0.0000	0.026
6MgO-	2.112 (6.20)	0.0020	0.005	0.0004	0.062

wt % (mol %)

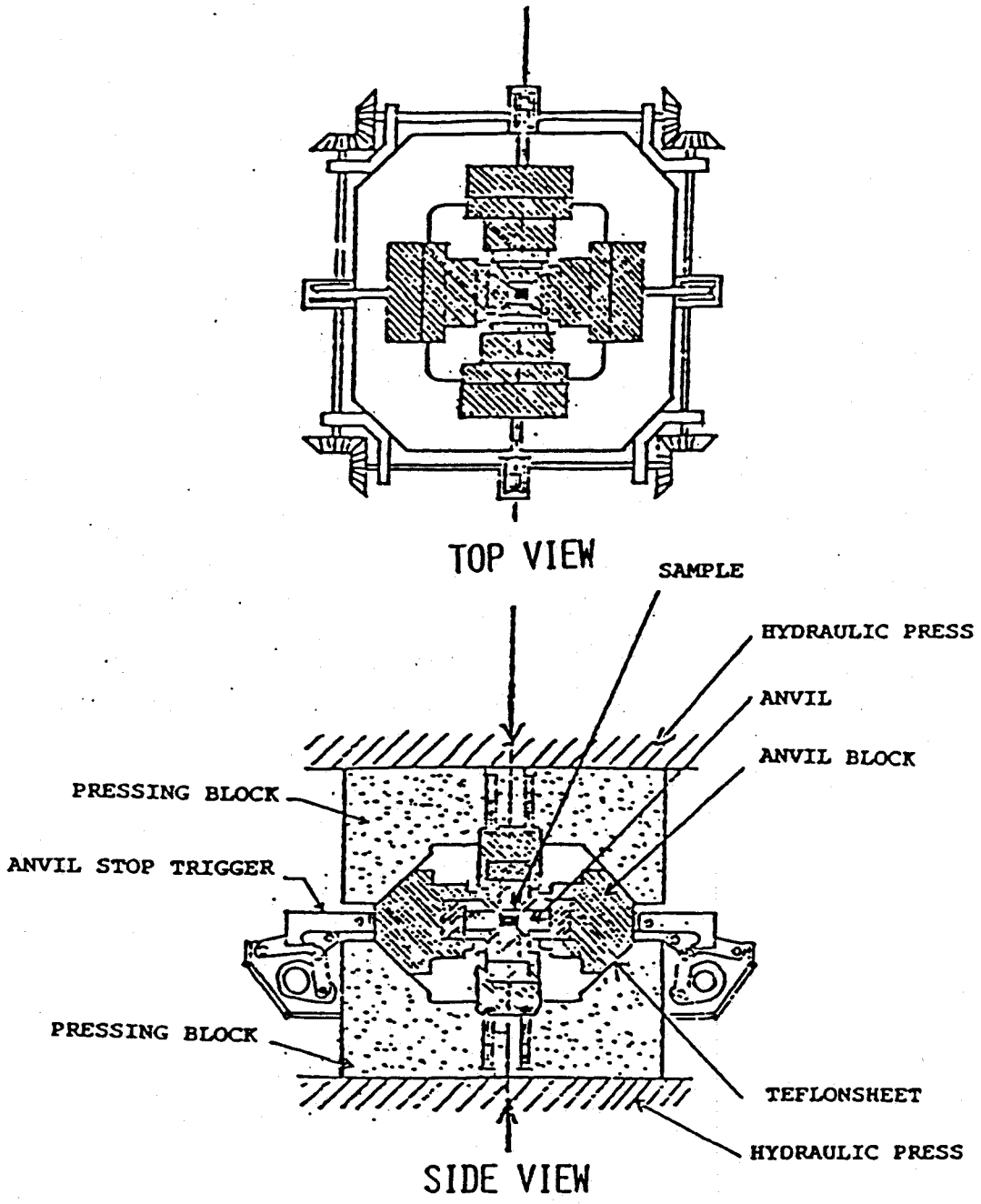

Fig.1-1 Schematic diagram of cubic anvil-type apparatus.

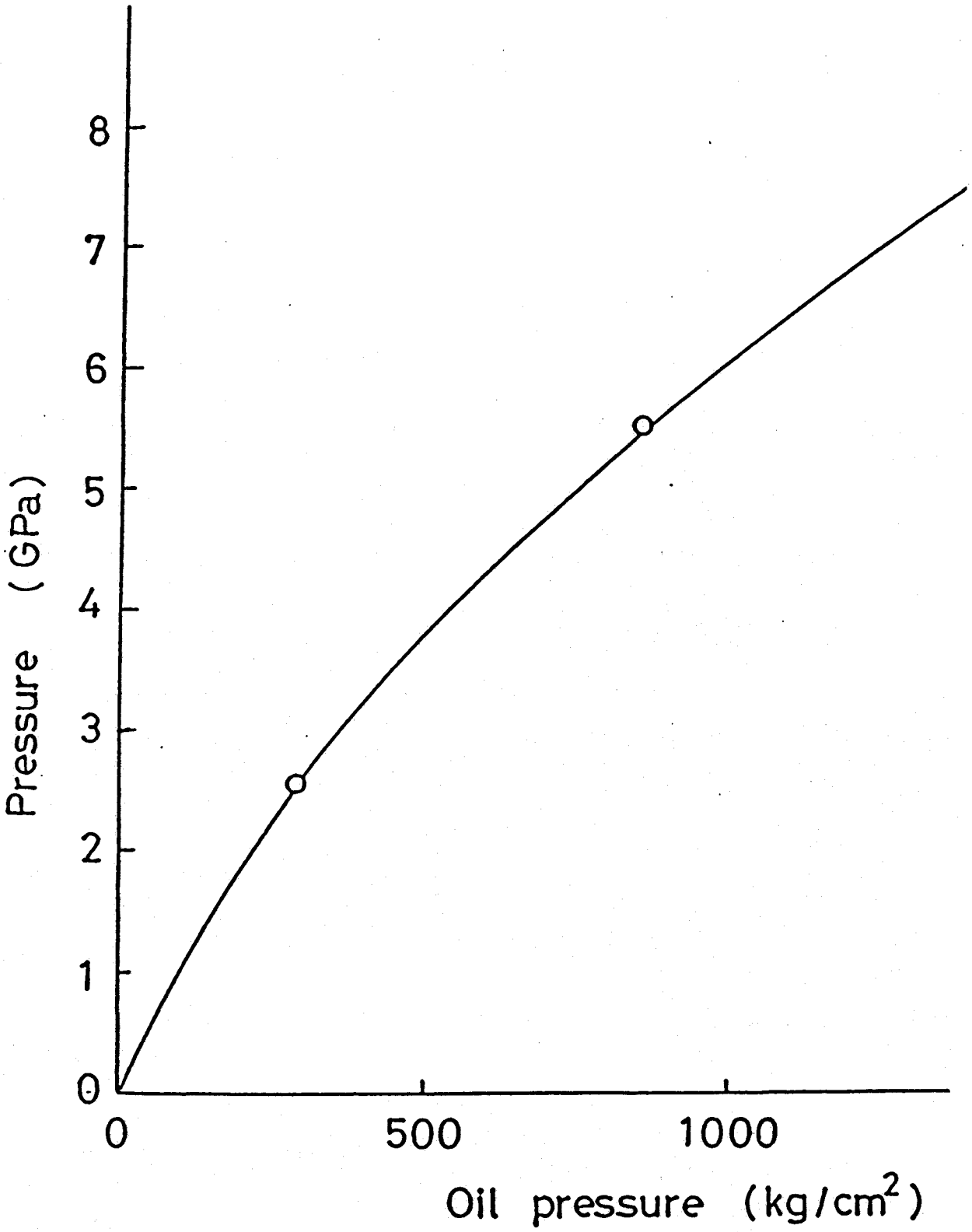

Fig.1-2 Relation between pressure inside the cell and load pressure.

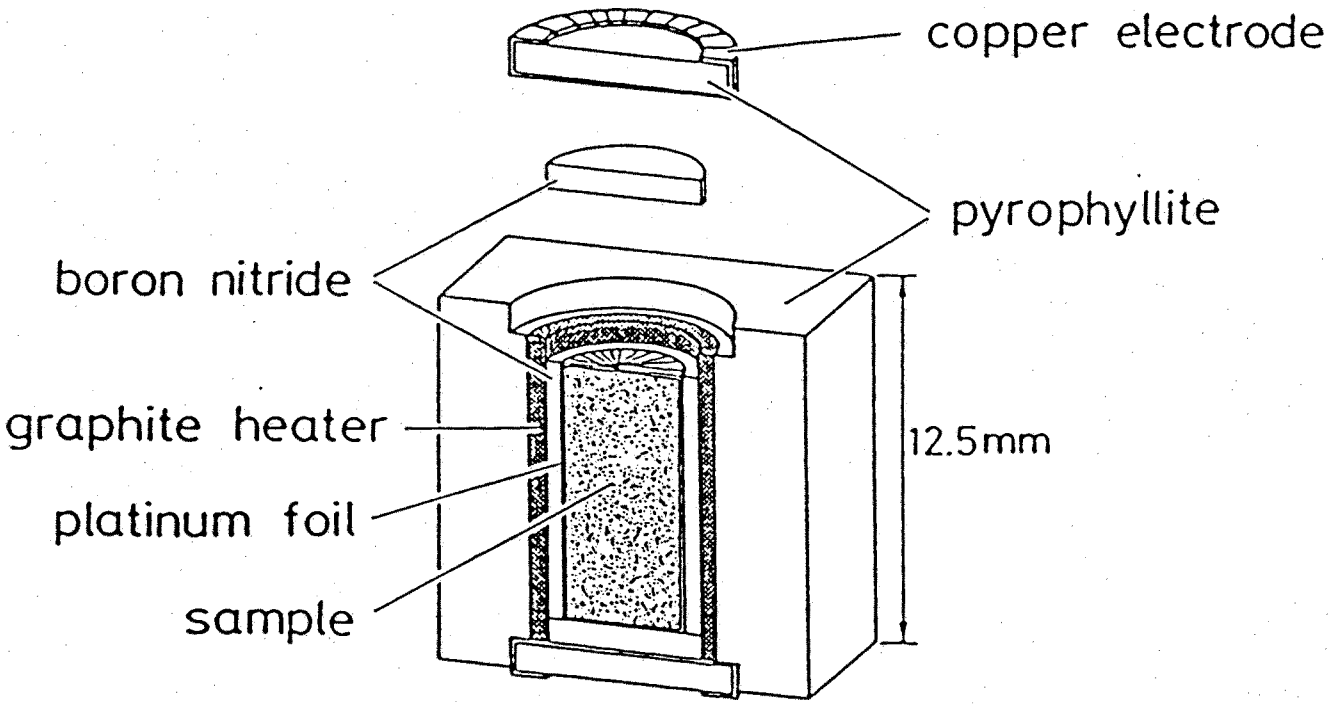

Fig.1-3 Cell assemblage for synthesis experiment with cubic anvil apparatus.

§ 2 Characterization

2-1 X-ray Diffraction

The identification of starting materials and products was carried out by means of X-ray powder diffractometry (XRD) with monochromatic CuKα radiation.

The crystallite size of samples was evaluated with FWHM of powder diffraction patterns using Scherrer's equation (Stokes, 1955);

$$B = \lambda / D \cos\theta + b \qquad (1\text{-}1)$$

where B is FWHM (radian), λ the wavelength (CuKα), D crystallite size (A) and b instrumental broadening width.

2-2 Raman Spectroscopy

The products consisted of the mixture of orthoⅠ and tetragonal in the synthesis experiments of 2Y-orthoⅠ and Mg-orthoⅠ. As is shown in Fig.1-4, the XRD patterns of both the two phases are quite similar and almost all the diffractions overlap each other. In addition to this, each peak is broadened because of the very small particle size, therefore, it is difficult to distinguish each phase out of their mixture by this method. On the other hand, the Raman bands of orthoⅠ reported by Arashi (1982) are clearly different from those of tetragonal (Keramidas and White, 1974). Therefore, Raman spectroscopy was used for identification of phases in this experiment.

The Raman spectra were recorded using a double monochromator (Jovin Yvon U-1000) and photon counting system at Osaka City

University. The 4416 A line of He-Cd continuous wave laser (45 mW) was used as excitation light.

2-3 Whole-Powder-Pattern Decomposition

In case of the synthesis of 2Y-ortho I , products consisted of the mixture of tetragonal and ortho I the profile of which overlapped each other. Therefore, appropriate pattern fitting technique must be applied to analyze XRD pattern. Recently, the whole-powder-pattern decomposition (WPPD) was developed (Pawley, 1981) and this method is useful to refine the lattice parameters of a sample which contains more than two phases (Toraya, 1986). The same technique was applied to the XRD pattern of 2Y-ZrO_2 powder treated under pressure.

Profile intensity data were collected at room temperature by a vertical type X-ray powder diffractometer (Rigaku, RAD-II A) with graphite-monochromatized CuKα radiation (40 kV, 40 mA) and the step-scan technique (step width = 0.02° in 2θ and fixed time = 20 s) in the 2θ range from 20° to 90° . Si powder was used as an internal standard, The computer program, WPPF, was applied to the collected data to draw a fitting profile of powder diffraction,

2-4 TEM Observation

Grain size of sample was observed by transmission electron microscopy (TEM) in Institute of Science and Industry Research, Osaka University. Since the samples were fine and nonagglomerated powders, they were dispersed directly on copper mesh. In case of stabilized ZrO_2, the concentration and its fluctuation of addi-

tives in each grain was estimated with Energy Dispersive X-ray (EDX) analyser.

Lattice image of 2Y-ZrO_2 which was dispersed directly in collodion (carbonized at 500 ℃) was observed using high resolution TEM in Tokyo Institute of Technology. Optical diffraction patterns were obtained by reflecting laser on the lattice images of the electron micrographs.

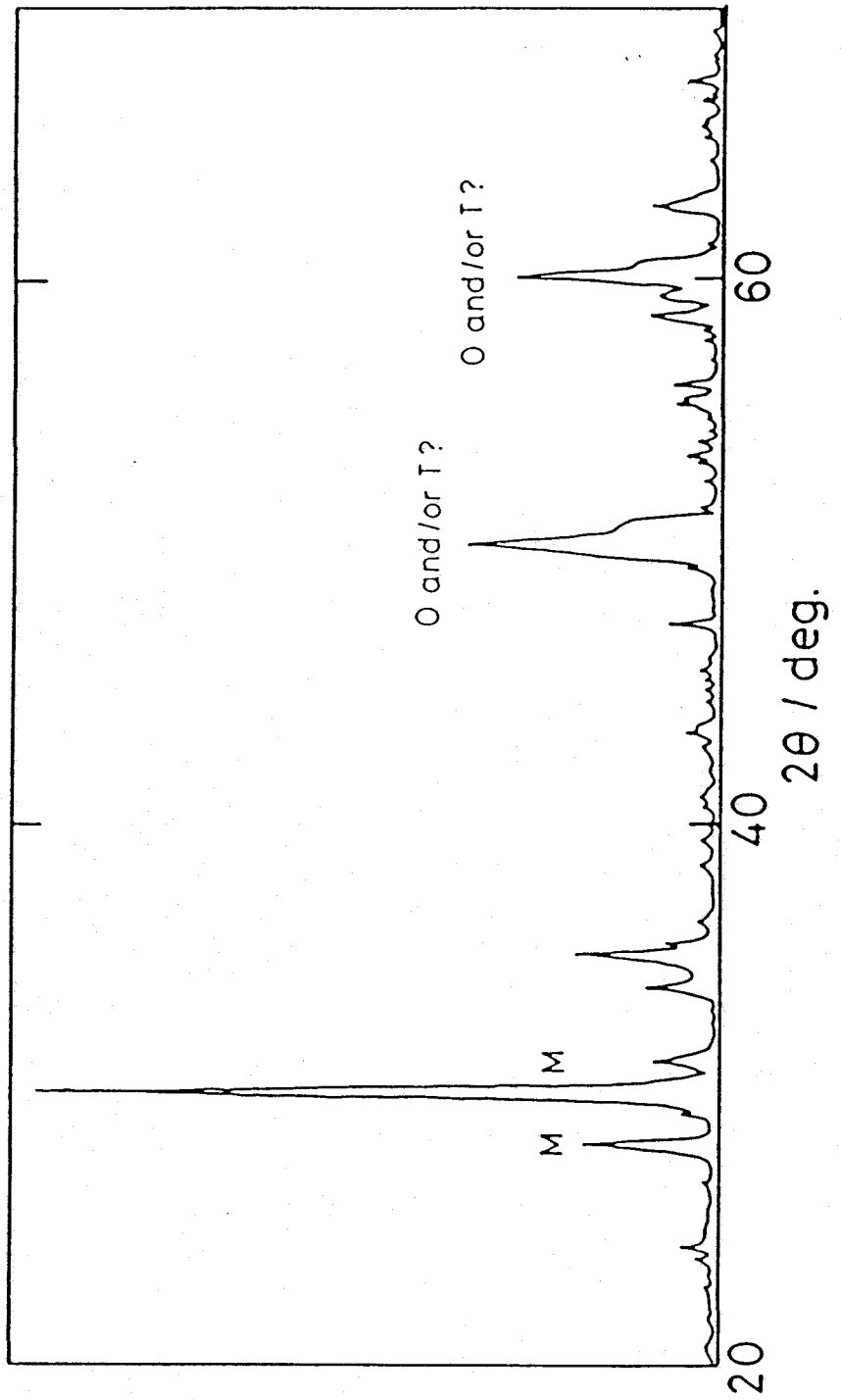

Fig.1-4 XRD pattern of 2Y-ortho I .

Results and Discussion

§ 1 Synthesis of Ortho I

1-1 Ultrafine Powder of ZrO_2

To characterize ZrO_2 fine powder $Zr(OH)_4$ was prepared by precipitation method and examined by TG, DTA and XRD. DTA and TG curves of 110℃ dried $Zr(OH)_4$ are illustrated in Fig.1-5. XRD patterns of samples collected from various temperature during the thermal analysis is shown in Fig.1-6.

While TG curve shows rapid decrease in weight, DTA curve shows an endothermic peak at the range from 100 to 150 ℃ and this is associated with the removal of absorbed water. XRD patterns collected from the first endothermic peak show a typical amorphous halo pattern. TG curve shows constant weight loss until 450 ℃ where drastic decrease occurs and very sharp exothermic peak appears in DTA curve. XRD patterns collected in this range of temperature shows gradual occurrence of the tetragonal peak and this is regarded as precursory stage of crystallization. Samples taken from the first exothermic peak temperature show the presence of the tetragonal ZrO_2. Therefore, this peak is assigned to the crystallization.

XRD pattern collected from the sample treated above 800 ℃ shows the appearance of the monoclinic phase and this corresponds to the slight exothermic peak around 800 ℃ on DTA curve.

Endothermic peak at 1180 ℃ is due to the monoclinic to the tetragonal phase transformation. The XRD pattern of recovered sample is that of the monoclinic without any trace of the tetragonal.

Comparing FWHM of XRD pattern, crystallite size is es-

timated. The crystallite size increased as the samples were subjected to higher temperature. As regards the sample recovered from 850 ℃ , using Scherrer's equation, the crystallite size of the monoclinic is calculated to be 20-25 nm while that of the tetragonal is 15-20 nm. This fact indicates that, as the crystal growth advances, the tetragonal transforms into the monoclinic because the monoclinic is thermodynamically stable in this temperature range, In other words, the tetragonal, which is high temperature polymorph of ZrO_2, exists at room temperature when its crystallite size is very small and critical crystallite size is estimated to be 15-20 nm. This phenomenon is due to the fact that the contribution of surface energy to the total free energy becomes relatively remarkable when crystallite size is small.

The notion of the critical crystallite size of ZrO_2 was introduced by Garvie (1965). According to his study, the free energy change of phase transformation is expressed by the following equations;

$$\begin{aligned} \Delta G_{t-m} &= G_m^c - G_t^c \\ &= G_m^c + U_m + V_m - (G_t^c + U_t + V_t) \end{aligned} \qquad (1\text{-}2)$$

where G^c is chemical free energy, U surface energy, V strain energy. The subscripts, m and t, refer to the monoclinic and the tetragonal phases, respectively. In case of free particle, strain energy is negligible, therefore, equation (1-2) comes to

$$\begin{aligned} \Delta G_{t-m} &= G_m^c + U_m - G_t^c - U_m \\ &= G_m^c + S_m \gamma_m - G_t^c - S_t \gamma_t \end{aligned} \qquad (1\text{-}3)$$

S is the molar surface(cal/mole) and γ the surface energy(cal/cm^2). In the region where metastable tetragonal phase appears, ΔG_{t-m} has a positive value because of the excess positive value of the surface energy though the chemical free energy of the tetragonal is higher than that of the monoclinic.

If the shape of each grain is assumed to be a sphere, then

$$S = 6 / (\rho D) \qquad (1\text{-}4)$$

ρ is density and D diameter of a crystallite. If D_c at which $\Delta G_{t-m} = 0$ is defined as a critical crystallite size,

$$D_c = 6 * (G_m^c - G_t^c)^{-1} * (\gamma_m/\rho_m - \gamma_t/\rho_t) \qquad (1\text{-}5)$$

Assuming the values of enthalpy and entropy of phase transformation are temperature-independent, $(G_t^c - G_m^c)$ at room temperature is calculated to be 1132 cal/mol with ΔH_{1478}=1420 cal/mol and ΔS_{1478}=0.96 cal/mol*K (after Hand Book of Chemistry and Physics). Substituting reported value of each parameter, ρ_m=5.56 and ρ_t=6.10 g/cm^3, D_c obtained in the present experiment and $(G_t^c - G_m^c)$ into equation (4), surface energy of the monoclinic is calculated to be 1200 to 1400 erg/cm^2. In Garvie's study, he estimated D_c=30 A and calculated γ_m=1770 erg/cm^2. This value, however, is too large when the surface energy of the tetragonal was considered because such a large difference in the surface energy is not likely to occur by the phase transformation. On the other hand, when the surface energies of the tetragonal and other oxides are compared (shown in Table 1-3),

our results is reasonable though 1400 erg/cm^2 seems a little too large.

1-2 Effect of Crystallite Size on the Synthesis of Ortho I

The results of high pressure synthesis of ortho I using starting materials of different crystallite size are summarized in Table 1-4. Ortho I was obtained above 4 GP in pressure and below 600 ℃ in temperature. This results are consistent with those of in-situ observation reported by Block et al.(1985). It became clear that ortho I could be quenched if a starting material with very small crystallite size was used. The critical size is about 60 nm. Further discussions, in which an influence of surface energy of particle is considered, will be made in Chapter4.

Table 1-3 Result of High Pressure Synthesis of Ortho I Using Starting Materials of Different Crystallite Size

heat treatment	crystallite size (nm)	synthesis conditions	product
Toso start	30	6GPa · 400℃ · 30min	ortho I
800℃ · 20hrs.	30	6GPa · 400℃ · 30min	ortho I
1000 · 20	45	6GPa · 400℃ · 30min	ortho I
1000 · 40	50	6GPa · 400℃ · 30min	ortho I
1000 · 80	63	6GPa · 400℃ · 30min	monoclinic

Table 1-4 Surface Energy

	temperature (℃)	surface energy (erg/cm²)	ref.
Al_2O_3 (liquid)	2080	700	#
Al_2O_3 (solid)	1850	905	#
MgO (solid)	25	1040	Jara (1952)
TiC (solid)	1100	1190	#
ThO_2	25	1150	Benson (1963)
UO_2	25	1030	Benson (1963)
ZrO_2 (tetra)	25	770	Livey (1963)
ZrO_2 (mono)	25	1200-1400	this study

#; in Introduction to Ceramics edited by Kingery,W.D. et al.

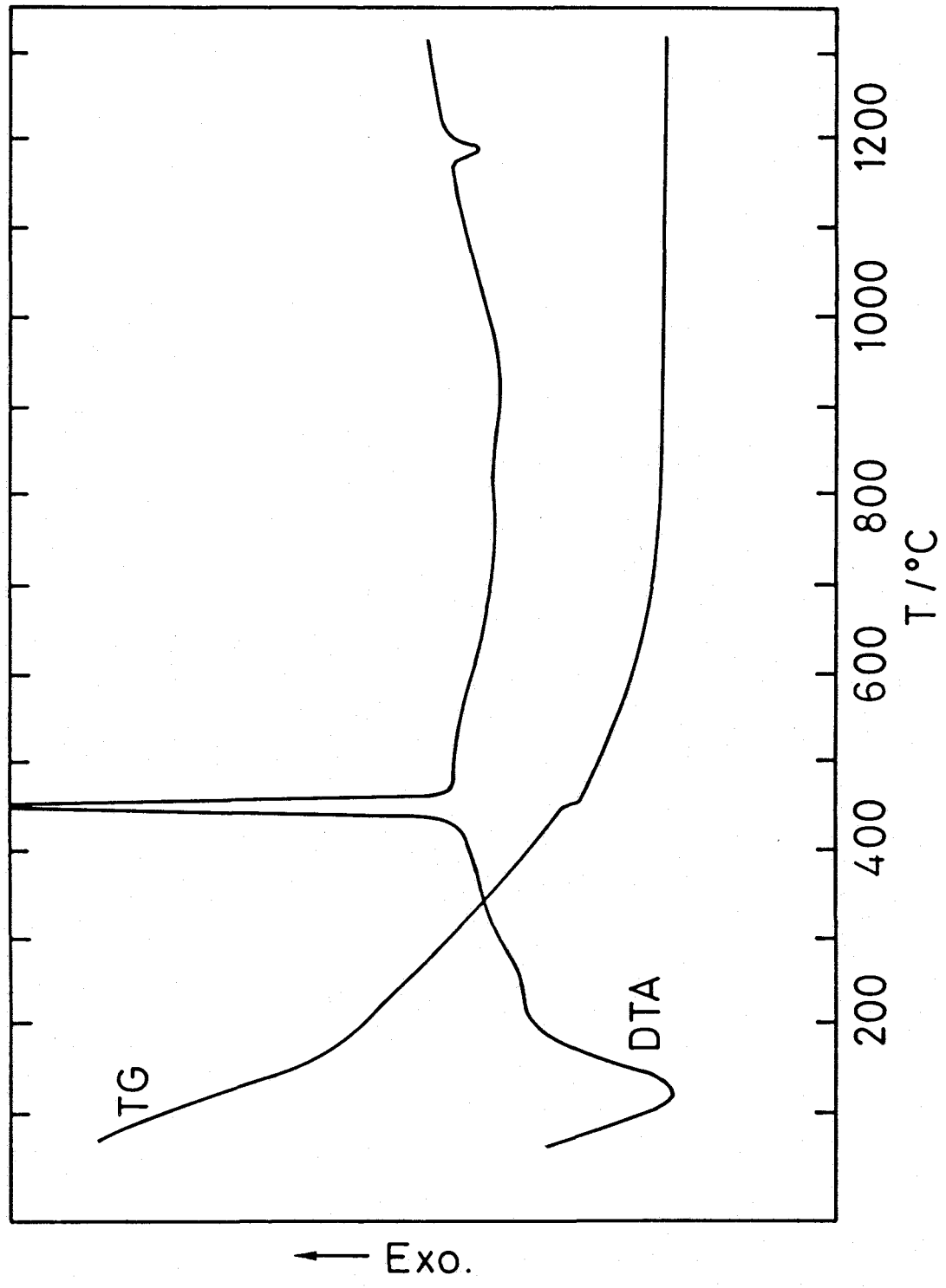

Fig.1-5 TG and DTA curves of precipitated $Zr(OH)_4$.

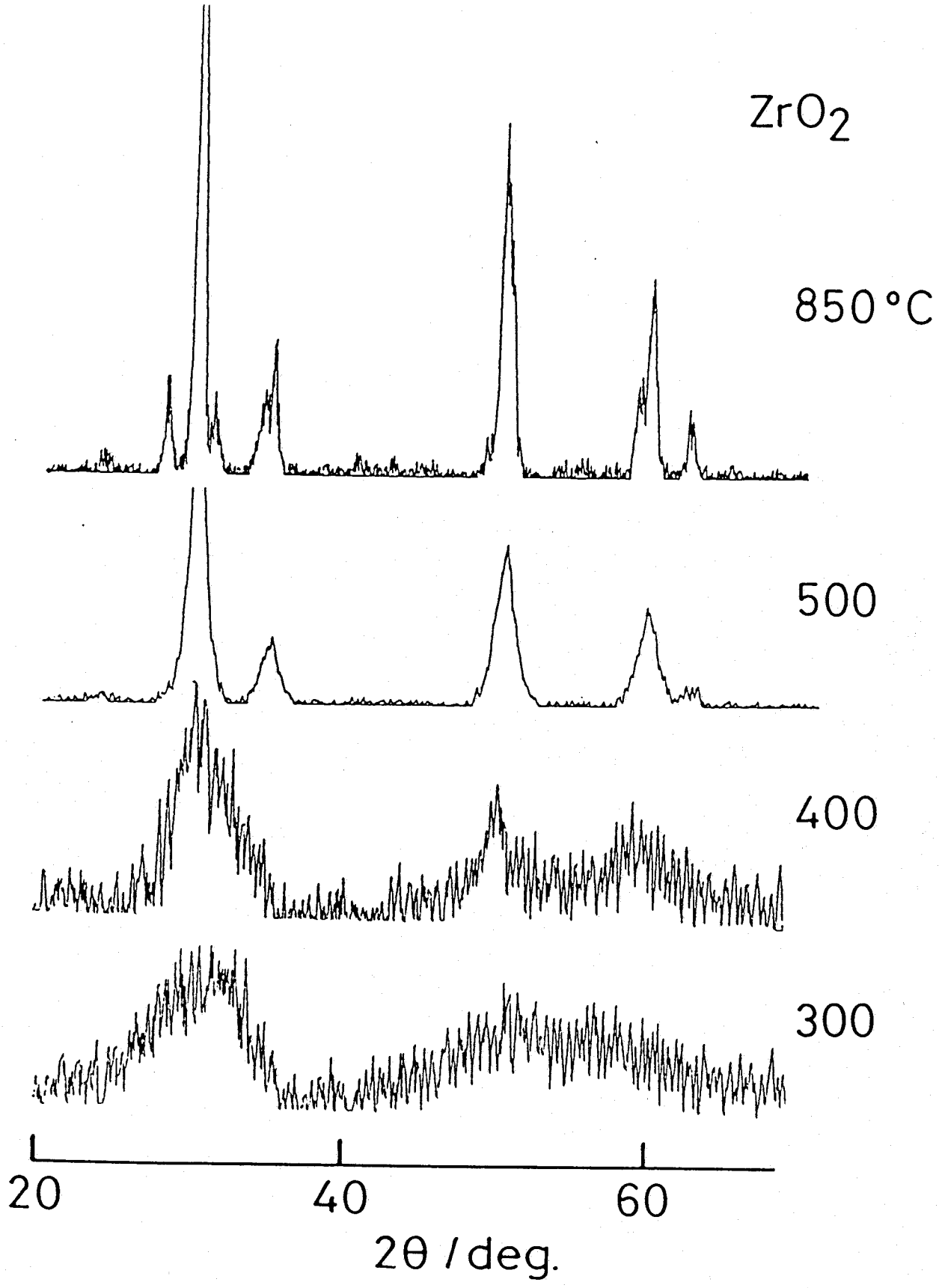

Fig.1-6 XRD pattern of ZrO_2 annealed at variuos temperature.

§ 2 Synthesis of Y_2O_3-Ortho I

2-1 Formation Diagram of 2Y-Ortho I

As for ortho I , Arashi et al(1982) observed the shifts of Raman spectra of non-doped ZrO_2 under pressures above 3.5 GPa. When the relation between pressure and amount of shift was interpolated to 1 atmosphere (shown in Fig.1-7), a fairly good consistency with the present results was seen. No peak shift attributed to the doping of Y_2O_3 was observed. Therefore, Raman spectra were used for the identification of the products.

Raman spectra of 2Y-ZrO_2 treated at 6 GPa and 600 ℃ for 60 min. is shown in Fig.1-8. Each spectrum is completely classified as being either the monoclinic, the tetragonal or ortho I .

Formation diagram of 2Y-ortho I is presented in Fig.1-9. The starting material was fine powder of 2Y-ZrO_2 (grain size was <30 nm) consisting of approximately 50-50 % the monoclinic and the tetragonal. 2Y-ortho I was synthesized by quenching in the ranges of temperatures from 400 ℃ and 600 ℃ and pressures >5 GPa; however, it always coexisted with the tetragonal.

The dominant product of ortho I was examined carefully by XRD (Fig.1-10). All diffraction lines except for those of the monoclinic phase were indexed assuming orthorhombic symmetry. Table 1-5 illustrates the similarity between the observed and the calculated d-spacing values.

2-2 TEM Observation

Analytical electron microscopy reveals that there was no difference in the particle size before and after treatment (Fig.1-11(A) and (B)). Results of EDX analysis show that Y_2O_3 is

equally doped into each particle, although quantitative determination are inaccurate because of the small grain size.

A high-resolution electron micrograph of the product is shown in Fig.1-12. Twins, characteristics of the monoclinic, are not seen, but the grain consists of a monophase. The lattice images cross at a right angle. When the lengths of segments intersected by the adjacent images are measured, the axial ratio of the crystal lattice can be calculated. The ratio coincides with that of c/a obtained from the lattice parameters, and consequently the photograph is considered parallel to the (001) plane of ortho I . An optical diffraction pattern and its index are also shown in Fig.1-12. The pattern is reasonably well indexed, assuming the axes indicated on the figure.

2-3 Quantitative Analysis

To reveal the cause of residual tetragonal phase, quantitative analysis was performed using the following equations:

$$C_M=[I_M(111)+I_M(11\bar{1})]/\,[I_M(111)+I_M(11\bar{1})+I_T(111)] \qquad (1\text{-}6)$$

$$C_1=(I_M^{181}+I_M^{192})/[4(I_T^{148}+I_T^{268})+I_M^{181}+I_M^{192}] \qquad (1\text{-}7)$$

$$C_2=I_M^{384}/(I_M^{384}+I_O^{406}) \qquad (1\text{-}8)$$

$$C_3=I_O^{406}/(I_O^{406}+1.3I_T^{268}) \qquad (1\text{-}9)$$

Equation (1) is a relation used widely in literatures (Toraya et al.,1984) in which the subscripts M and T represent the

monoclinic and the tetragonal phase, respectively. Equations (2), (3) and (4) are experimentally introduced for the present study (subscript O represents orthoI). Their adaptabilities were examined using standard samples of non-doped zirconia in which two phases were mixed in specific ratios.

Three kinds of mixtures of the monoclinic-tetragonal, whose ratios were 30:70, 50:50 and 70:30 respectively, were prepared as starting material. The sample enriched with the tetragonal was made by annealing for a few hours at 800 ℃ and that enriched with the monoclinic was prepared by grinding. The ground sample was annealed to release the strain caused by the grinding. There were no remarkable difference in crystallite size among these three samples.

The results of the quantitative analysis using Raman spectra are summarized in Table 1-6; after treatment at 5 and 6 GPa (room temperature), the amount of the tetragonal phase decreased slightly. This response is probably due to the transformation from the tetragonal to the monoclinic phases, which is generated by shearing stress accompanied by compression. When the starting material was treated under high pressure and temperature, the amount of the new orthoI corresponds to the decreased amount of the monoclinic; the tetragonal remains nearly constant. Consequently, it is said that only the monoclinic transforms into orthoI .

The density of orthoI is 6.17 Mg/m^3. This value is 1.5 % larger than that of the tetragonal (6.08 Mg/m^3). A small difference in density indicates that the tetragonal is fairly stable and the phase transformation to orthoI hardly occurs by compres-

sion. For further discussion on this subject, WPPD analysis was performed to determine precise lattice parameters and the result is presented in the next part.

In some cases, a small amount of the tetragonal decreased and apparently changed to ortho I . As stated earlier, this change is explained possibly by a foregoing phase transformation from the tetragonal to the monoclinic phase resulting from shearing stress and the subsequent change from the monoclinic to ortho I by compression.

2-4 WFFD analysis

Samples prepared for the WPPD analysis are summarized in Table 1-7. The sample A was used as a standard to give the unit cell parameters of non-doped tetragonal ZrO_2. The samples B and D were used as starting materials for synthesizing the high pressure form (samples C and E).

Refined unit cell parameters and calculated densities of sample A to E are given in Table 1-8. The final Rp and Rwp factors are given in Table 1-9, showing excellent fits except for the sample B. Relatively high R value of sample B is due to the anisotropy in the peak width of the monoclinic ZrO_2. Their accuracy is estimated to be < 0.0001 nm and sufficient to discuss the present problem; for example, the unit cell parameters a and c of the tetragonal in sample E are 0.36059 and 0.51779 nm, respectively, and well agree with those of the starting material (sample D in Table 1-8). A whole powder pattern fitting result for sample E is shown in Fig.1-13.

Variations of the unit cell parameters of the monoclinic and

the tetragonal zirconia with Y_2O_3 dopant are well in accordance with the generally observed tendency (Toraya 1987). The b axis of ortho I has the least change as is observed in that of the monoclinic. The transformation of the monoclinic into ortho I is considered to be displacive and the directions of the b and c axes are preserved during the transformation (Kudoh et al.1986). The little expansion in the b axes of the monoclinic and ortho I will, therefore, be due to the same structural configuration reason in both polymorphs.

Ortho I and the tetragonal have the same volume expansion in doping Y_2O_3 (Toraya, 1987). The monoclinic to ortho I transformation of ZrO_2 accompanies the increase of density by 0.25 to 0.26 Mg/m^3 (4.3 to 4.4 %). The tetragonal zirconia has slightly higher density than ortho I . The difference in density between the two phases is however, only 0.03 Mg/m^3, and has little effect on the transformation under pressure.

The stability of the tetragonal at higher pressure will be discussed in Chapter 3.

Table 1-5 d Values for 2Y-Ortho I

ortho I			2Y-ortho I	
dobs(nm)	hkl	I/I100	dobs(nm)	dcal(nm)
0.296	111	100	0.296	0.296
0.262	020	14	0.263	0.263
0.254	022	16	0.255	0.255
0.252	200	13	0.252	0.253
0.234	021	4	0.232	0.233
0.208	211	5	0.208	0.208
0.1829	022	19	0.183	0.183
0.1820	220	21	0.182	0.182
0.1790	202	13	0.180	0.179
0.1715	221	5	0.172	0.171
0.1656	130	6	0.166	0.165
0.1574	131	10	0.157	0.157
0.1537	113	15	0.154	0.154
0.1527	311	10	0.153	0.153
0.1479	222	6	0.148	0.148
a = 0.5042			a = 0.505	
b = 0.5257			b = 0.525	
c = 0.5092 nm			c = 0.509 nm	
V = 0.1350 nm^3			V = 0.135 nm^3	

Table 1-6
Amounts of Existing Phases in the Transformation of 2Y-ZrO_2

phase	composition(wt%)				
	starting material	5GPa R.T.	6GPa R.T.	5GPa 400℃	6GPa 400℃
M	30	60	60	60	70
T	70	60	60	60	70
O	0	0	0	10	25
M	70	75	75	25	20
T	30	25	25	45	50
O	0	0	0	30	30

M:monoclinic, T:tetragonal, and O:orthoI

Table 1-7 Samples and their Phases Identified

composition	sample	phase
non-doped ZrO_2	A	M + T
	B	M
	C	M + O
2mol% Y_2O_3 -doped ZrO_2	D	M + T
	E	M + T + O

Table 1-8 R_p and R_{wp} Factors

sample	R_p	R_{wp}
A	0.0228	0.0347
B	0.1046	0.1369
C	0.0394	0.0609
D	0.0511	0.0688
E	0.0367	0.0514

Table 1-9
Refined unit cell parameters and calculated densities of ZrO_2 polymorphs (Δ is the difference between the 2 mol% Y_2O_3-doped and non-doped ZrO_2)

	non-doped ZrO_2	2 mol% Y_2O_3-doped ZrO_2	Δ
monoclinic sample	B	D	
a/nm	0.51465	0.51605	0.00140
b/nm	0.52112	0.52117	0.00005
c/nm	0.53110	0.53203	0.00093
β /degree	99.219	99.050	-0.169
V/nm^3	0.14060	0.14131	0.00071
D/g cm^3	5.821	5.772	-0.049
ortho I sample	C	E	
a/nm	0.50939	0.50456	0.00063
b/nm	0.52580	0.52619	0.00039
c/nm	0.50885	0.50967	0.00082
V/nm^3	0.13483	0.13531	0.00048
D/g cm^3	6.070	6.028	-0.042
tetragonal sample	A	D	
a/nm	0.35944	0.36053	0.00109
b/nm	0.51911	0.51781	-0.00130
2xV/nm^3	0.13413	0.13461	0.00048
D/g cm^3	6.101	6.059	-0.042

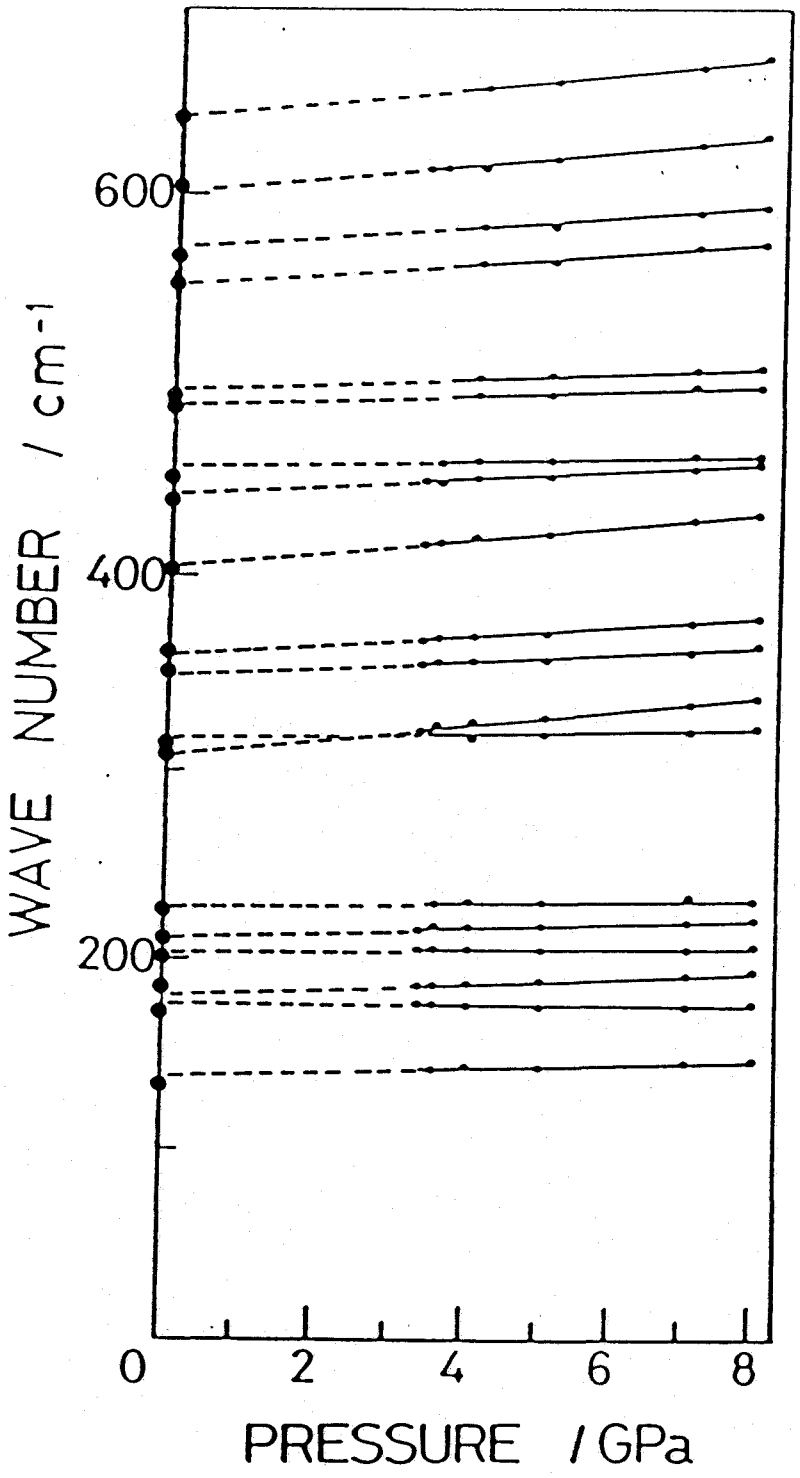

Fig.1-7 Pressure dependence of peak frequencies of Raman spectra measured for ZrO_2 (Arashi et al.,1982). Solid circles at ambient pressure show Raman spectra obtained from quenched 2Y-orthoI .

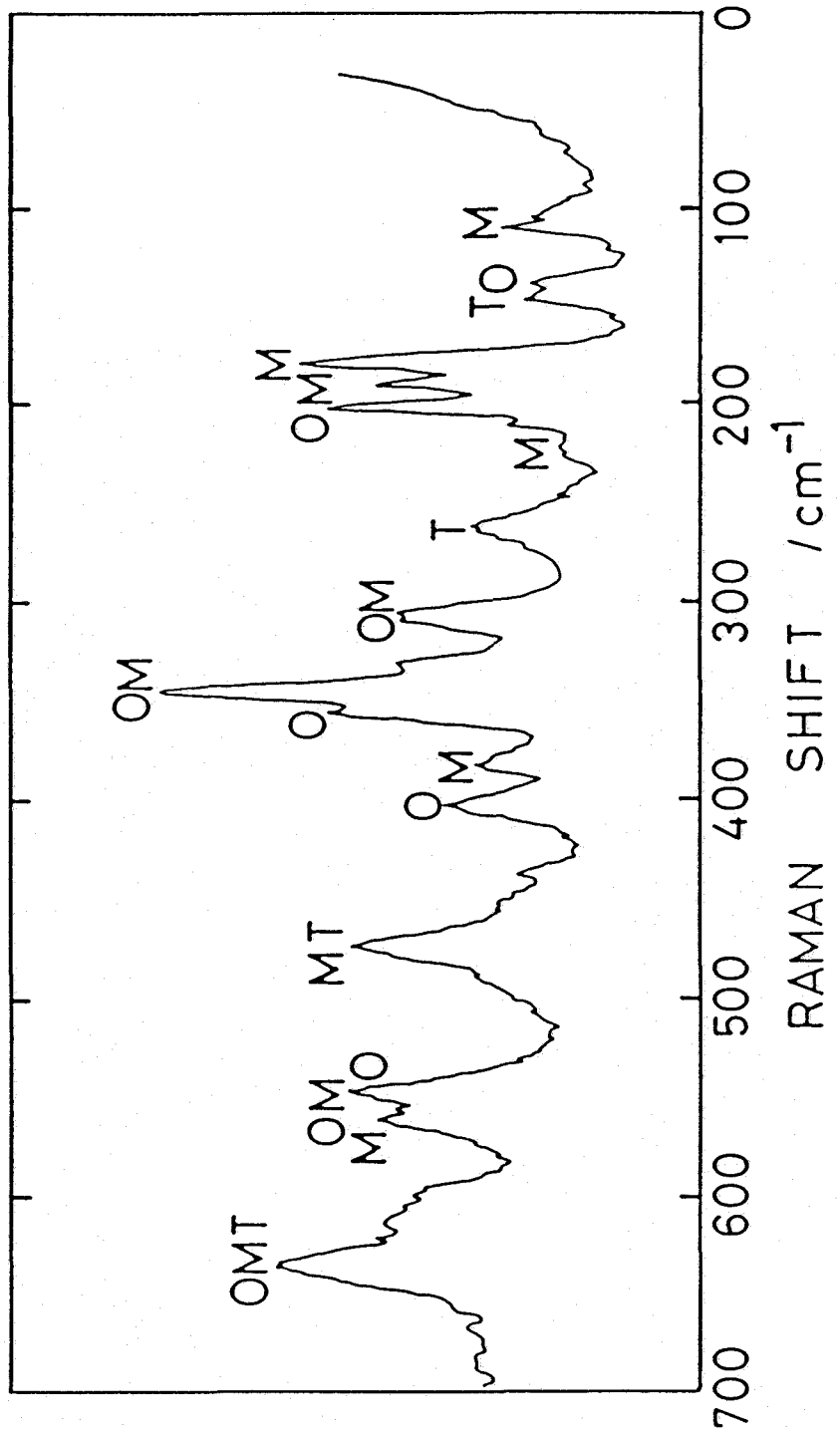

Fig.1-8 Raman spectra of 2Y-ZrO_2 treated at 600 GPa and 600 ℃ for 60 min.

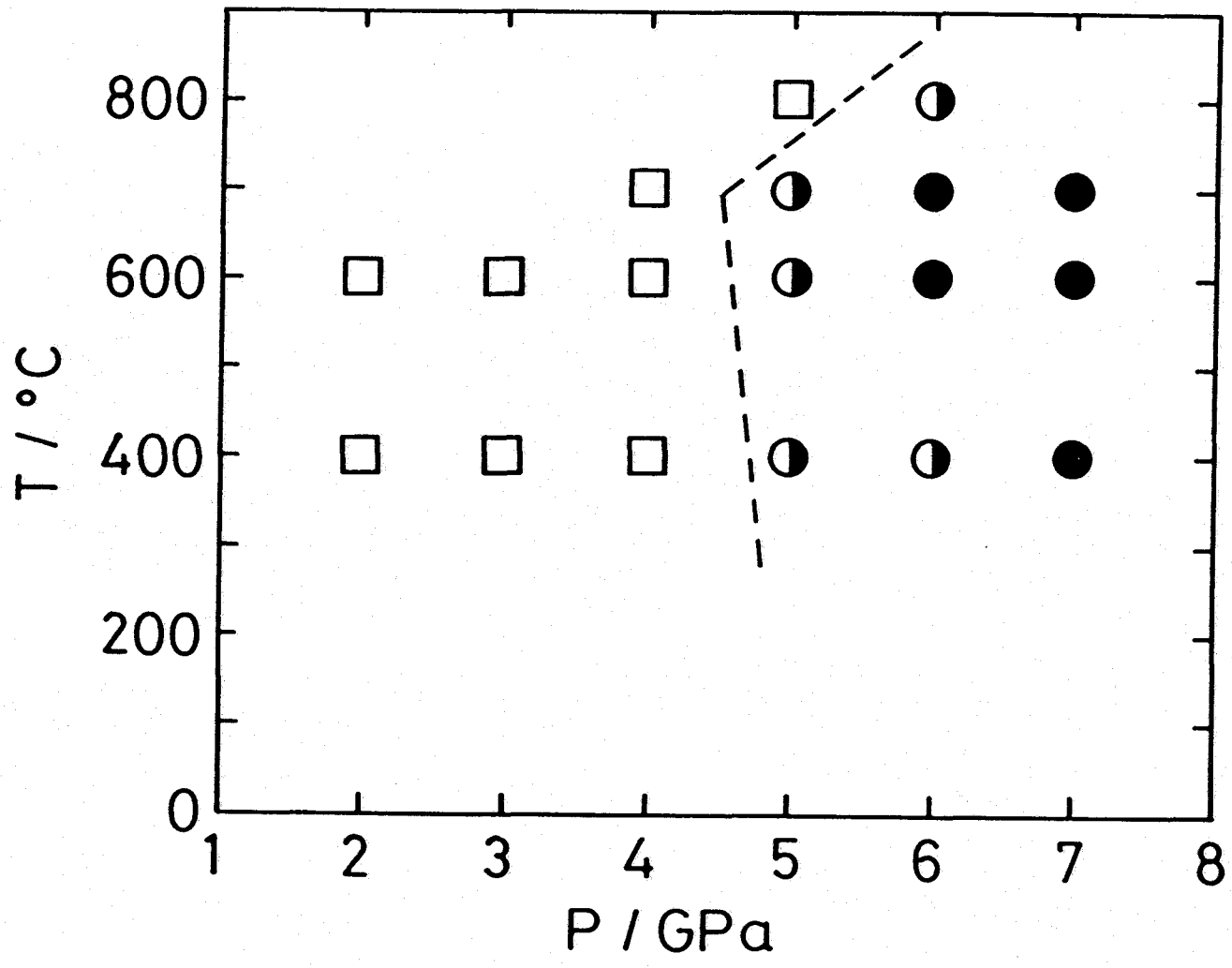

Fig.1-9 Phases of 2Y-ZrO_2 appearing under various temperature and pressure conditions: (●) coexistence of the tetragonal and ortho I ; (○) coexistence of the monoclinic, tetragonal and ortho I ; (□) coexistence of the monoclinic and tetragonal.

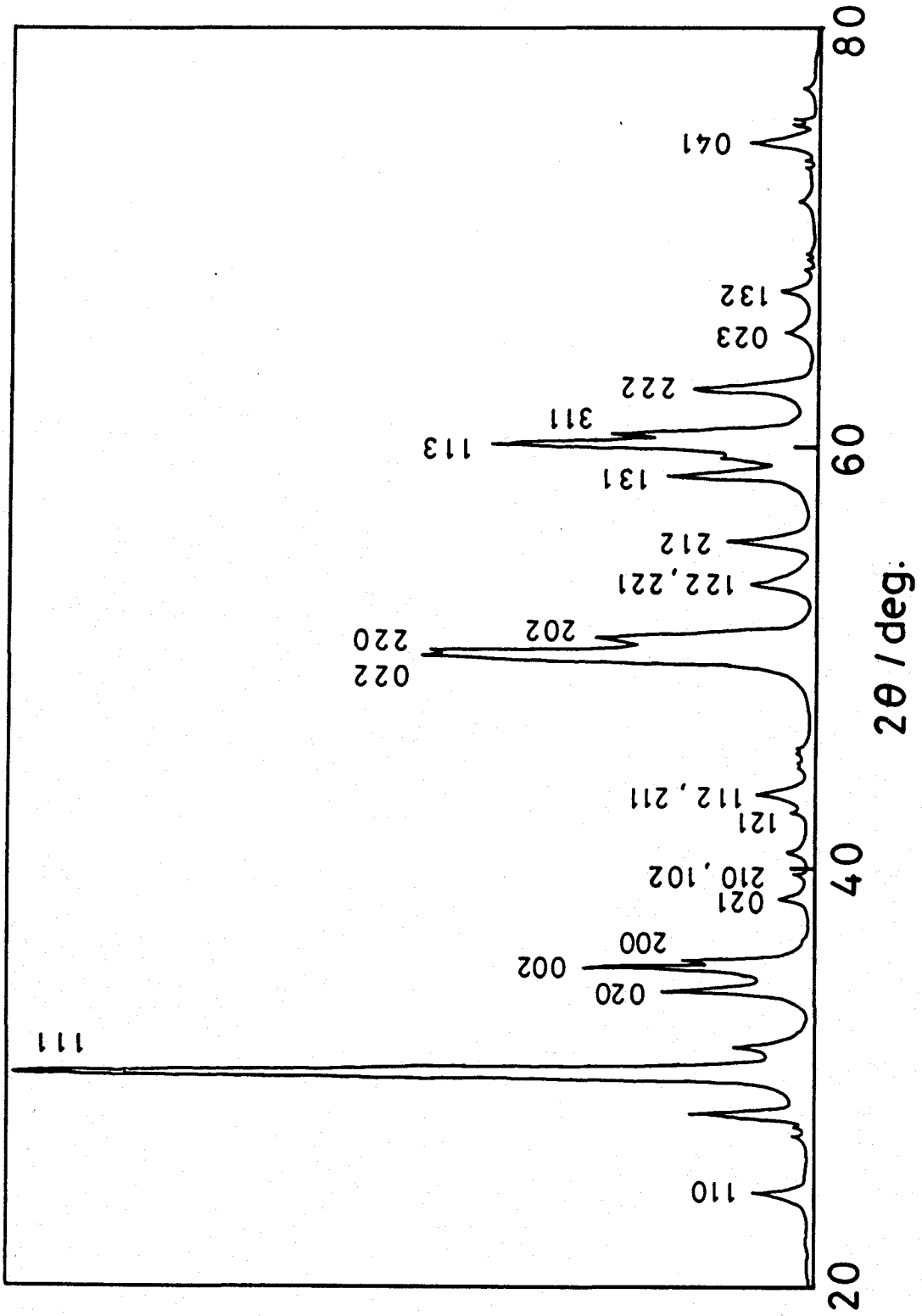

Fig.1-10 XRD pattern of 2Y-orthoI .

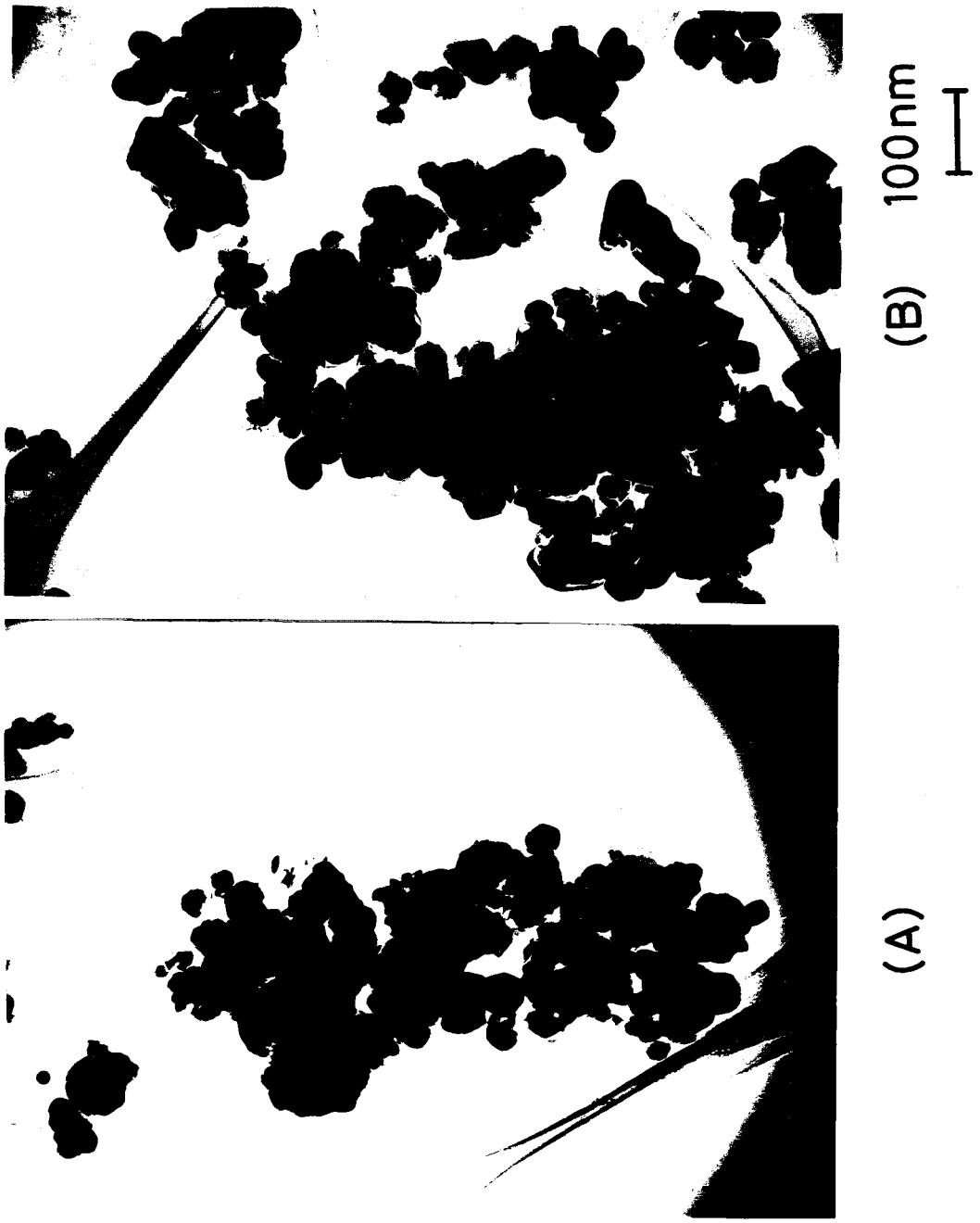

Fig.1-11 Electron micrographs of 2Y-ZrO_2 (A) before and (B) after treatments.

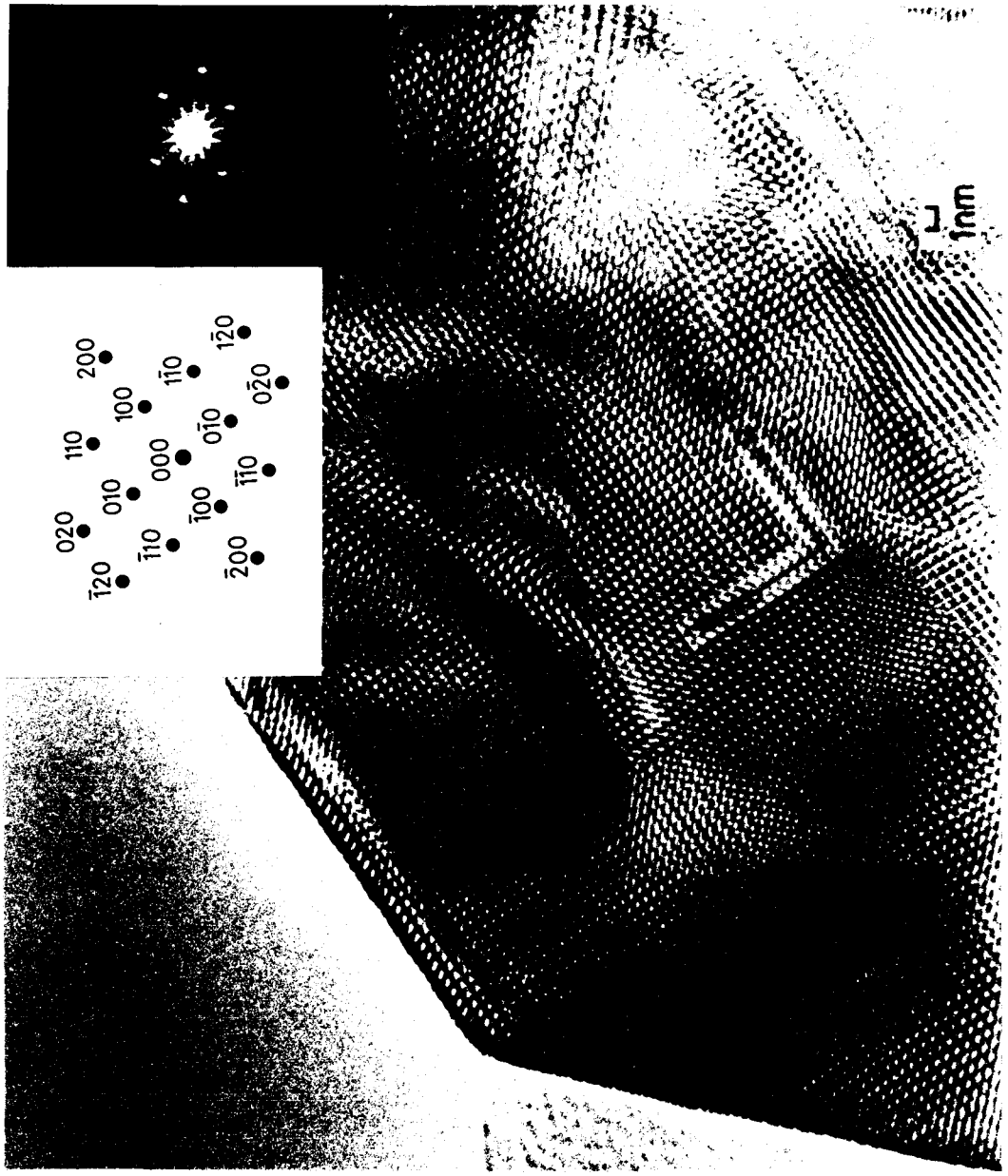

Fig.1-12 Bright-field TEM image of 2Y-orthoI on (001) plane; the diffraction pattern and its index are shown in inset.

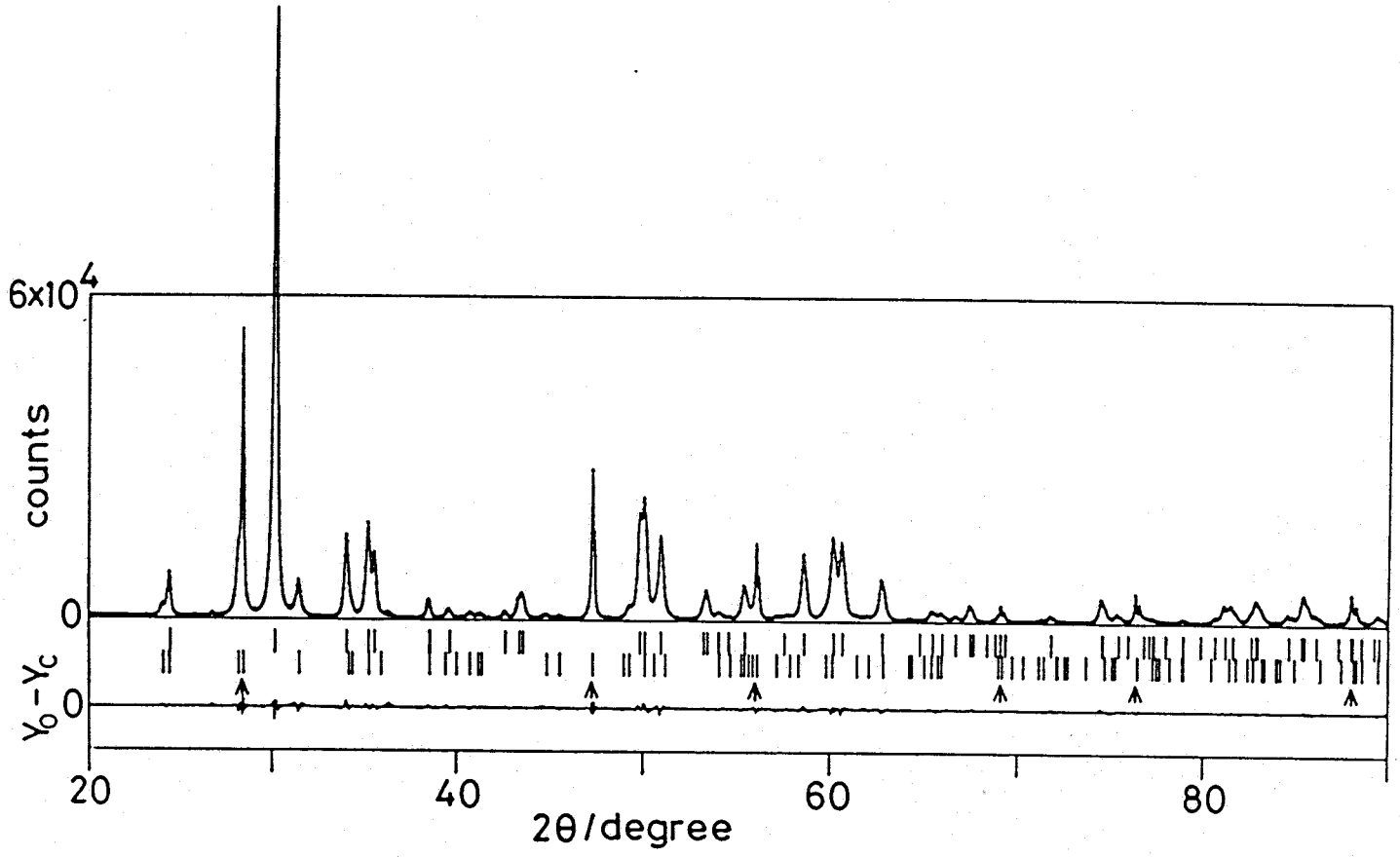

Fig.1-13 Whole-powder-pattern fitting result for the sample consisting of orthorhombic and monoclinic mixture. Symbol + is the observed profile intensity and solid line the calculated diffractions. The difference between the two intensities, Y_o-Y_c, are plotted at the bottom of diagram on the same scale. Positions (2 θ) of Bragg reflections are shown by vertical bars, in which upper column represents those of orthorhombic phase and lower column those of monoclinic. The arrows represent those of Si standard.

§ 3 Synthesis of MgO-ortho I

MgO-ZrO_2 used in this experiments are listed in Table 1-1. Heat-treatments were performed on these samples and examined by XRD. The results are illustrated in Fig.1-14 for 6 mol%-MgO. As the MgO concentration becomes higher, the amount of the residual tetragonal phase increase. However, the amount of the stabilized tetragonal phase is much smaller than that when Y_2O_3 is used as stabilizer. From the results of the synthesis experiments of Y-ortho I , it was foreseen that single phase of Mg-ortho I would be synthesized since ortho I is synthesized only from the monoclinic.

The results of the high pressure synthesis are listed in Table 1-10. Unexpectedly, the recovered products were either the mixture of ortho I and the monoclinic or the monoclinic single phase. As the MgO concentration increased, the amount of obtained ortho I decreased and the upper limit of the temperature ortho I appeared went down.

XRD patterns of recovered samples were found to be sharpened, which indicated the crystal growth during the high pressure synthesis. Therefore, TEM observation of the particles was carried out. TEM micrographs taken are shown in Figs.1-15(A)-(J). The extraordinary grain growth was observed and results are summarized in Table 1-11 in comparison with the case of non-doped ZrO_2. In case of 6 mol%MgO-ZrO_2, as the temperature of treatment was elevated, the grain became large while no grain growth was observed with non-doped ZrO_2. However, there is no difference in grain size between the samples treated at 6 GPa 600 ℃ (sample G and I). This fact implies that small grain grows as large as 100-

200 nm in 30 min. at 6 GPa 600 ℃ but that the rate of further grain growth (>200 nm) becomes remarkably slow. It was revealed that the grain growth of 6 mol%MgO-ZrO_2 caused with 6 GPa 600 ℃ 30 min. treatment is equivalent to that accompanied by 1300 ℃ 1 hr. calcination in air shown in Fig.1-15(K). It was revealed that ortho I was not obtained because of this extraordinary grain growth of Mg-ZrO_2 under high pressure. That is, grain size is too large for ortho I to be quenched.

This remarkable grain growth is tentatively explained as follows: There seems to be Mg^{2+} concentration gradient in a grain. Mg^{2+} is dominantly distributed at the surface of grains because of its low solubility to ZrO_2 and relatively low surface energy of MgO comparing to that of ZrO_2. This introduces high concentration of oxygen vacancy at the surface to keep charge balance, which raises the activity of the surface. When the sample with small amount of water is subjected to experimental conditions, the surface area is kept in hydrothermal conditions, and the reactivity of this surface area is believed to be much higher than that without doping MgO. Consequently grain growth is generated.

Dominant parameters which control the grain growth are the reactivity of surface (surface energy), duration of time, temperature and pressure. The reactivity of surface depends on the grain size and hydrothermal conditions which are controlled by pressure and temperature. Relatively low temperature and short duration of time makes long distance diffusion practically impossible. Therefore, as the grain growth proceeds to some extent and surface energy is decreased, the rate of the grain growth will

become significantly slow. This explains the reason that there is no difference in grain size between sample (G) and (I).

Table 1-10
Results of High Pressure Synthesis of Mg-Ortho I

sample (M:MgO mol%)	grain size (nm)	treatment GPa*℃ *min.	product
0	20-30	6*800*30	M
0	20-30	6*700*30	M
0	20-30	6*600*30	O
0	20-30	6*500*30	O
2	20-30	6*800*30	M
2	20-30	6*700*30	M
2	20-30	6*600*30	M
2	20-30	6*500*30	O>M
2	20-30	6*400*30	O>M
4	20-30	6*600*30	M
4	20-30	6*500*30	M>O
4	20-30	6*400*30	M>O
6	20-30	6*600*30	M
6	20-30	6*500*30	M
6	20-30	6*400*30	M>O
6	50-100	6*600*30	M
6	50-100	6*400*30	M>>O
6	100-150	6*600*30	M
6	100-150	6*400*30	M>>O
6	100-200	6*400*30	M>>>O

Table 1-11 Grain Growth of $MgO-ZrO_2$ under High Pressure

sample	MgO mol%	heat treatment	condition GPa*℃ *min.	grain size (nm)
A	0	as precipitated	none	<< 10
B	0	1000℃ 1day	none	50-100
C	0	1000℃ 1day	6*600*60	50-100
D	6	none	none	<10
E	6	none	6*350*30	50-100
F	6	none	6*400*30	50-150
G	6	none	6*600*30	100-200
H	6	1000℃ 5days	none	100-150
I	6	1000℃ 5days	6*600*60	100-200
J	6	1200℃ 1day	6*400*60	100-200
K	6	1300℃ 1hr.	none	# 100-200

SEM photo

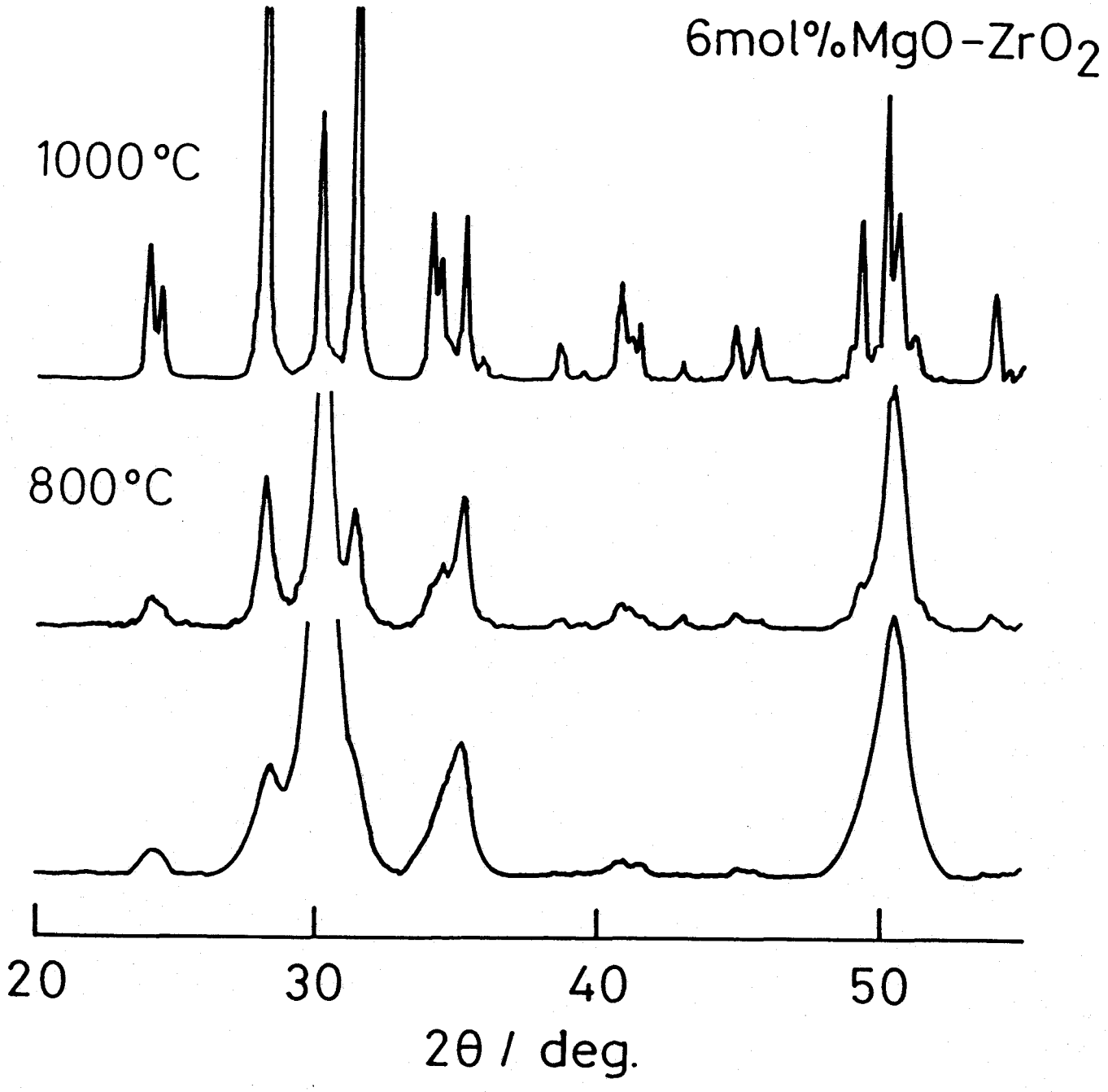

Fig.1-14 XRD pattern of 6 mol% MgO doped ZrO_2 annealed at various temperature.

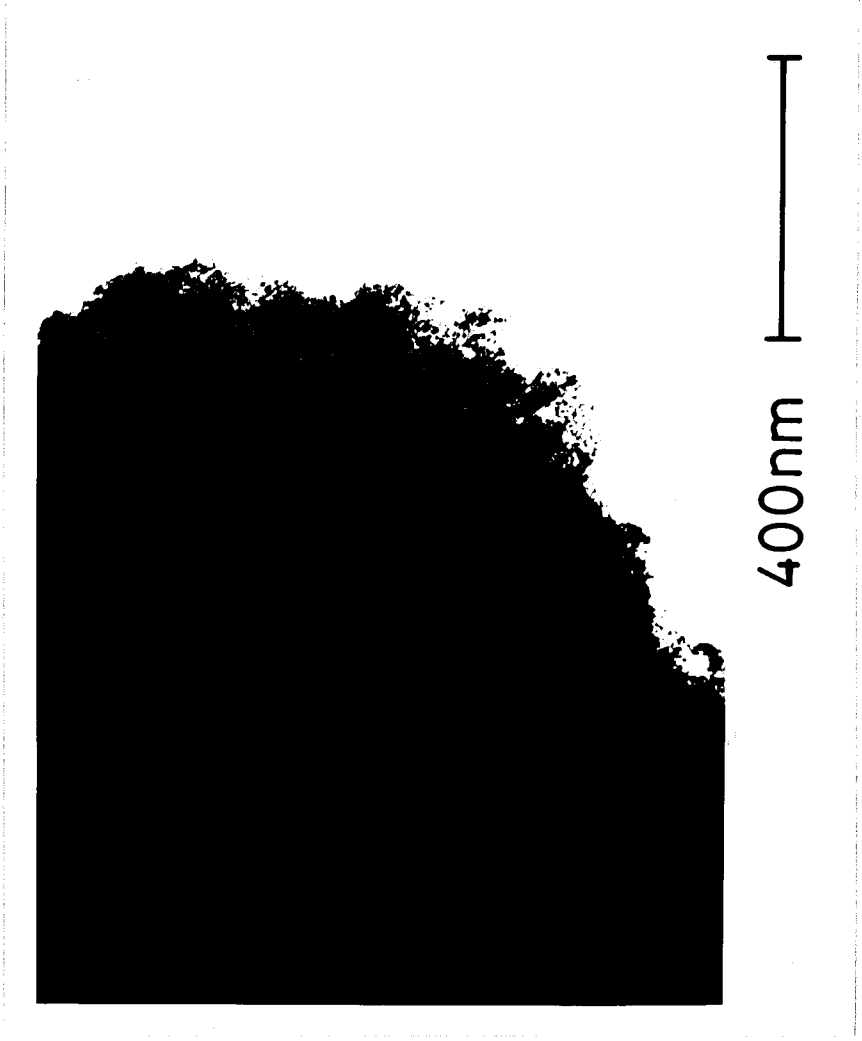

Fig.1-15 (A) TEM micrographs of $MgO-ZrO_2$ grains; treatment conditions are listed in Table 1-11.

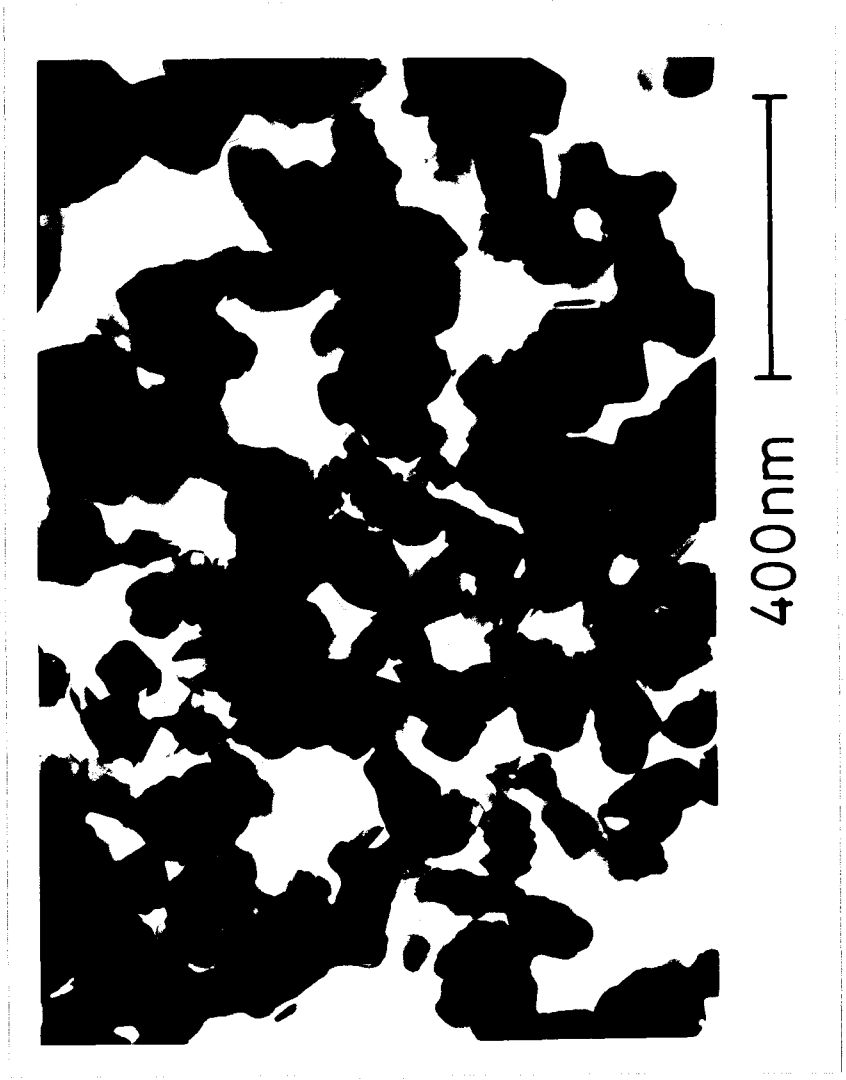

Fig.1-15 (B) TEM micrographs of $MgO-ZrO_2$ grains; treatment conditions are listed in Table 1-11.

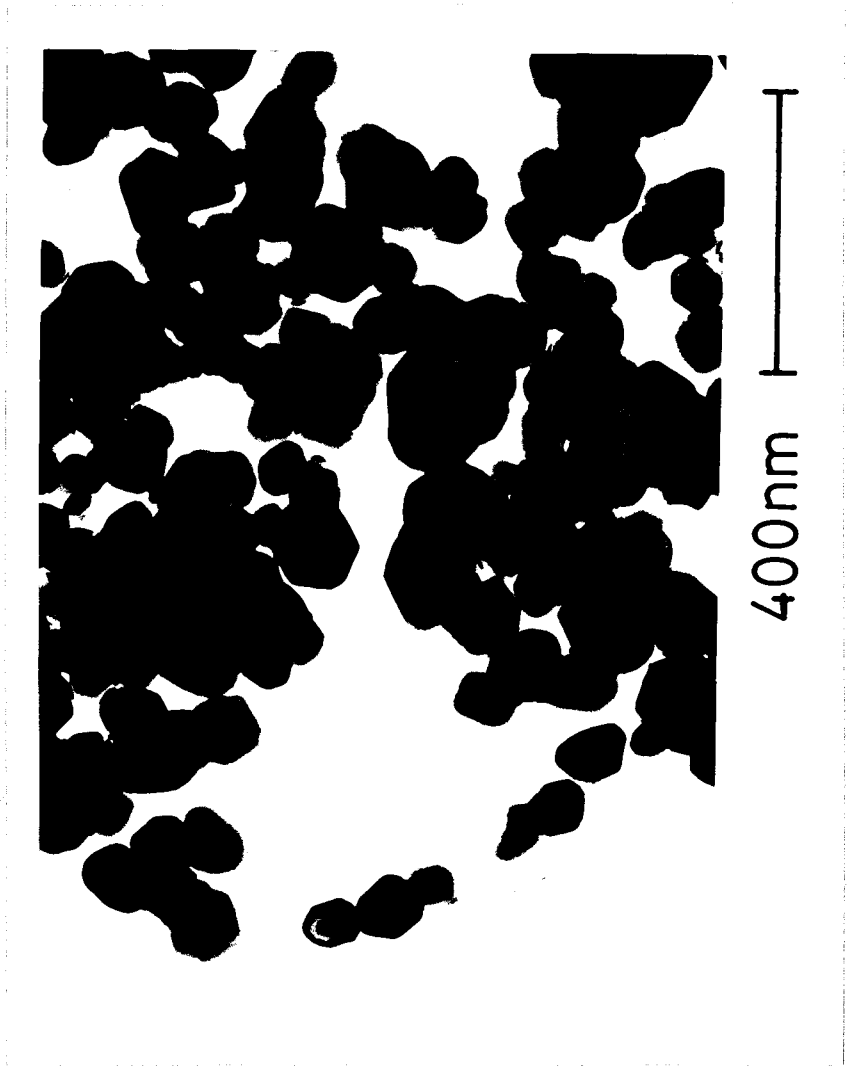

Fig.1-15 (C) TEM micrographs of MgO-ZrO_2 grains; treatment conditions are listed in Table 1-11.

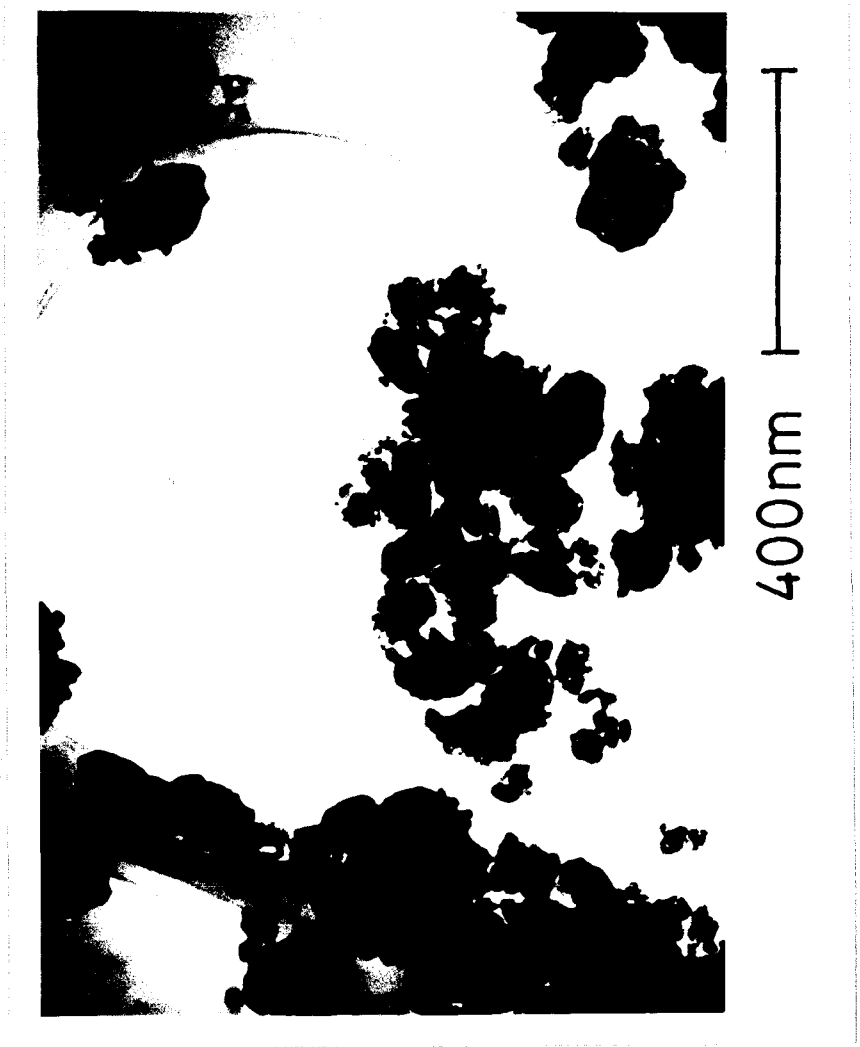

Fig.1-15 (D) TEM micrographs of MgO-ZrO_2 grains; treatment conditions are listed in Table 1-11.

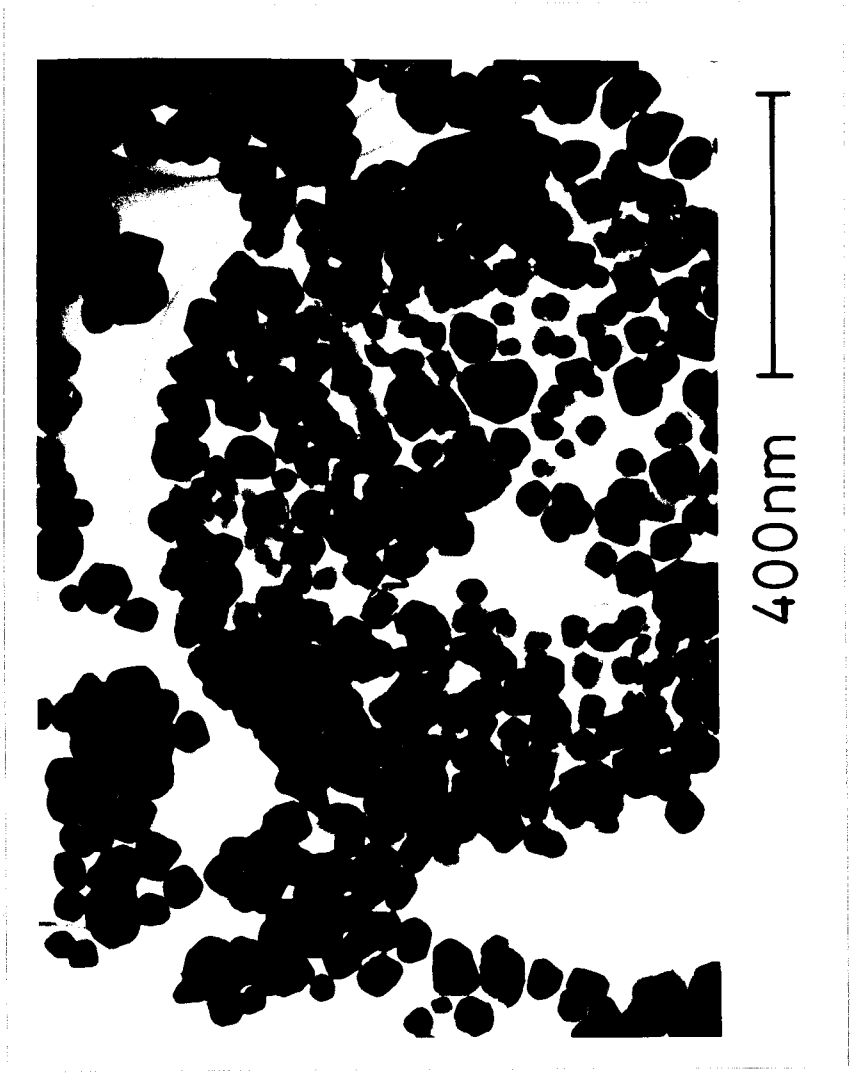

Fig.1-15 (E) TEM micrographs of MgO-ZrO_2 grains; treatment conditions are listed in Table 1-11.

Fig.1-15 (F) TEM micrographs of $MgO-ZrO_2$ grains; treatment conditions are listed in Table 1-11.

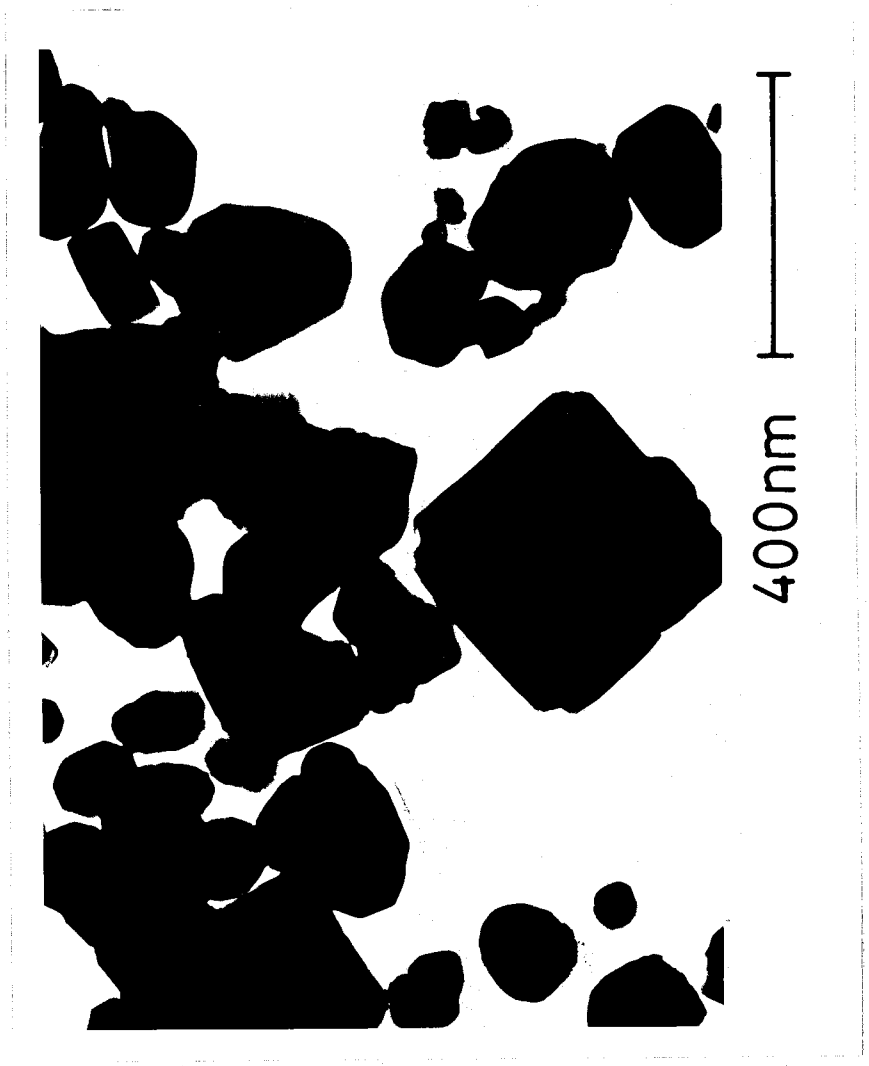

Fig.1-15 (G) TEM micrographs of $MgO-ZrO_2$ grains; treatment conditions are listed in Table 1-11.

Fig.1-15 (H) TEM micrographs of $MgO-ZrO_2$ grains; treatment conditions are listed in Table 1-11.

Fig.1-15 (I) TEM micrographs of $MgO-ZrO_2$ grains; treatment conditions are listed in Table 1-11.

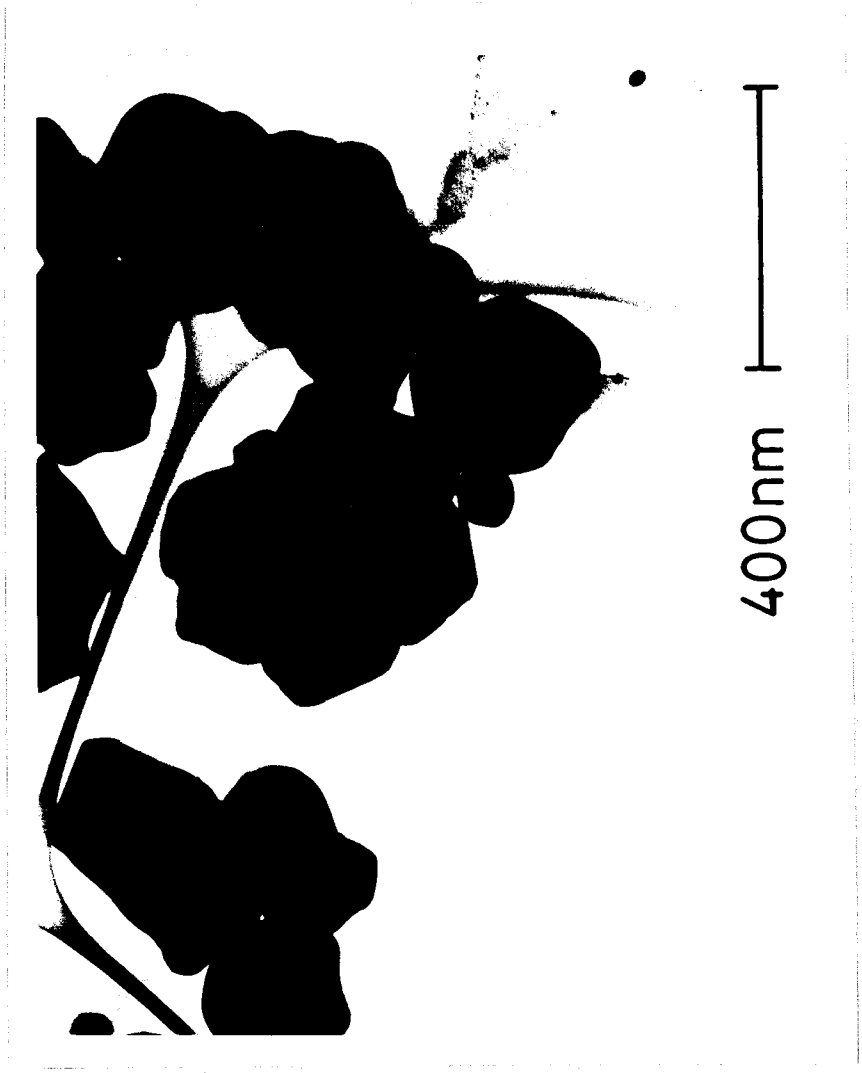

Fig.1-15 (J) TEM micrographs of $MgO-ZrO_2$ grains; treatment conditions are listed in Table 1-11.

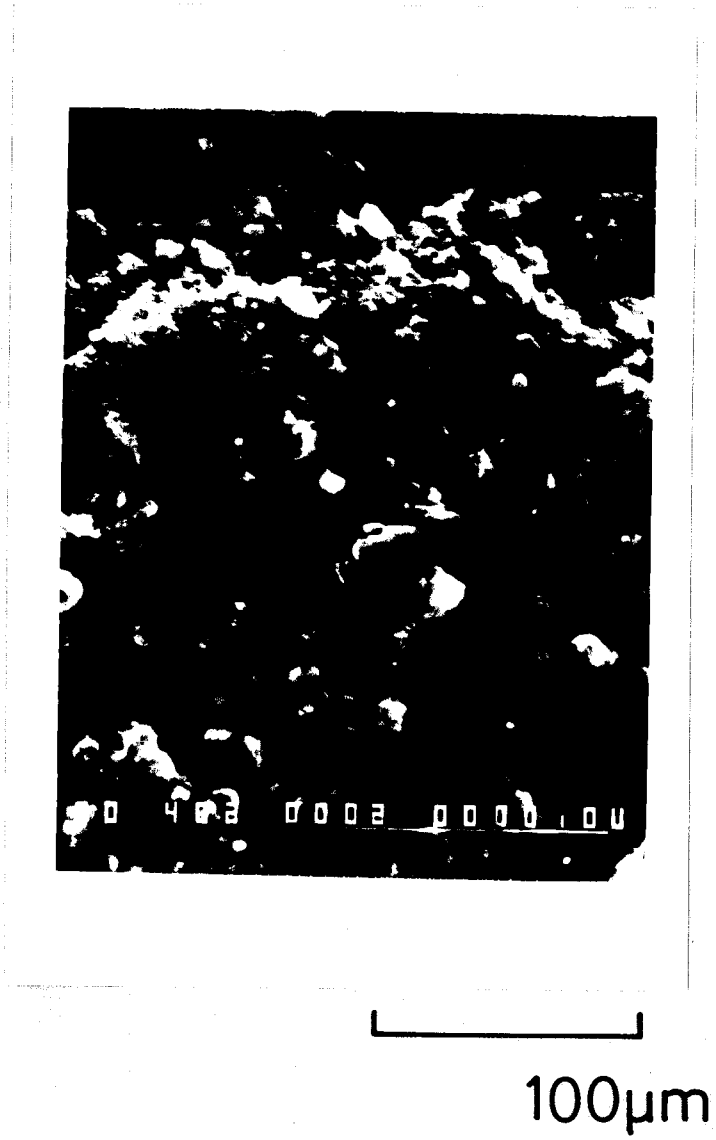

Fig.1-15 (K) SEM micrograph of 6 mol% MgO doped ZrO_2 annealed at 1300℃ for 1hr.

Chapter 2 Neutron Diffraction of Ortho I

Introduction

The crystal structure analysis of ortho I was first performed by Kudoh et al (1986). Using a diamond anvil pressure cell and single crystal X-ray diffraction method, they showed that this high pressure phase has an orthorhombic symmetry and its space group is Pbcm. No other study of the crystal structure analysis using single crystal has been reported since then because of the difficulty of synthesizing single crystal which is large enough for this kind of study.

Suyama et al. (1986) succeeded in synthesizing nearly single phase of very fine powder of ortho I and executed structure refinement by Rietveld analysis. Their result supported that presented by Kudoh et al.

Lee and Heuer (1988) reported that a metastable intermediate stage with orthorhombic symmetry was observed by in-situ observation in TEM in the course of their study of martensitic transformation in tetragonal MgO-Y_2O_3-ZrO_2. This phase with orthorhombic symmetry was also reported by Lenz and Heuer (1982) and Dickerson et al. (1987) in Mg-PSZ and in Ca-PSZ, respectively. Their studies, however, were based on TEM observation and it was difficult to discuss crystal structure any more than the crystal system.

From this state of affairs, the information of the crystal structure of ortho I is considered to be significant when the phase relations among ZrO_2 polymorphs and the toughening mechanism of ZrO_2 ceramics are investigated.

As regards the crystal structure of orthoI , Kudoh et al. (1986) showed that four Zr atoms occupy the 4d site and four O atoms out of eight atoms (denoted as O2) occupy the 4c site and the remaining four O atoms (denoted as O1) occupy half of the positions of the 8e site with equal probability. Their result is based on the following reason: It is difficult to decide the distribution of O1 in 8e site exactly by X-ray diffraction because of the weak diffraction from oxygen atom comparing with that from Zr atom.

The author has carried out a neutron diffraction study of orthoI in order to examine the statistical location of O1 mentioned above and to decide the exact configuration of oxygen. Furthermore, as small amount of water was added to the starting material for high pressure synthesis, there is a possibility that some of the added water remains as absorbed water, water of crystallization and some kinds of hydride. It is interesting to examine this possibility by neutron diffraction since neutron diffraction is sensitive to hydrogen. These results are presented in this chapter.

Experimental

About 1 cm^3 of ortho I was synthesized using cubic anvil type device presented in Chapter 1. Obtained high pressure sample was examined by XRD and EDX to check impurities. As small amount of water was added to the starting material for high pressure synthesis, residual water in such forms as absorbed water, water of crystallization and some kinds of hydride was carefully examined by TG and ^1H NMR as well as by neutron diffraction. The sample was contained in a cylindrical cell made of a 2 μ m thick vanadium foil (1 cm in diameter and 4 cm high) for diffraction data collection.

Neutron diffraction experiment of ortho I at room temperature was performed on the high resolution neutron powder diffractometer (HRP) with a solid methane moderator at pulsed spallation neutron source at National Laboratory for High Energy Physics (Watanabe et al. 1987). The measuring time was about 60 hrs.

In time-of-flight (TOF) neutron diffraction using the pulsed white beam, a detector is set at a fixed scattering angle 2θ , therefore, wave vector, Q, is described as a function of TOF, t. Neutrons with different velocities, v, arrive at the detector after different flight time. The relations among Q, t and λ is given by

$$Q = 4\pi \sin\theta / \lambda \qquad (2\text{-}1)$$

$$\lambda = h/mv = ht/mL \qquad (2\text{-}2)$$

therefore,

$$Q = 4\pi \sin\theta \ * \ mL/h \ * \ 1/t \qquad (2\text{-}3)$$

where L is the total flight path length, m the neutron mass and h Planck constant.

The configuration of HRP is shown in Fig.2-1. The scattered flight path length is 0.8 m and the total flight path length is about 20 m. The diffractometer has two counter banks in both wings ($2\theta \sim 170°$), each of which contains three ^{3}He proportional counters. As a beam monitor, a fission counter is used which is located at the final incident collimator.

By the time-focussing method (Watanabe et al. 1987), data were obtained from three pairs of detectors at three different angles.

The least-squares structure and profile refinements were executed with the Rietveld analysis program, RIETAN, described by Izumi (1985). The diffraction intensity $I_c(t)$ as a function of TOF is calculated by the equation

$$I_c(t)=I_s(t)(A(t)\Sigma_i|F_i|^2 m_i d_i^4 f(\Delta)+Y_b(t)), \qquad (2\text{-}4)$$

where $I_s(t)$ is the incident neutron intensity, A(t) the absorption correction factor, F_i the structure factor for the ith Bragg reflection, m_i the multiplicity, d_i the interplanar spacing, $f(\Delta)$ the peak shape function and $Y_b(t)$ the background.

The incidental neutron spectrum $I_s(t)$ is obtained from incoherent scattering $I_v(t)$ of vanadium. $I_s(t)$ for the sample run is not always the same as $I_v(t)$, but changes in each run. Therefore, $I_s(t)$ for the sample run is determined from $I_v(t)$ by apply-

ing a correction of the monitor spectra $M_s(t)$ and $M_v(t)$ for the sample and vanadium runs, respectively: $I_s(t)=I_v(t)M_s(t)/ M_v(t)$.

The peak shape observed with HRP is governed by the neutron pulse shape, which varies significantly with λ , because HRP covers a wide range of λ . In RIETAN, modified Cole-Windsor function was used for pattern fitting (Izumi 1987).

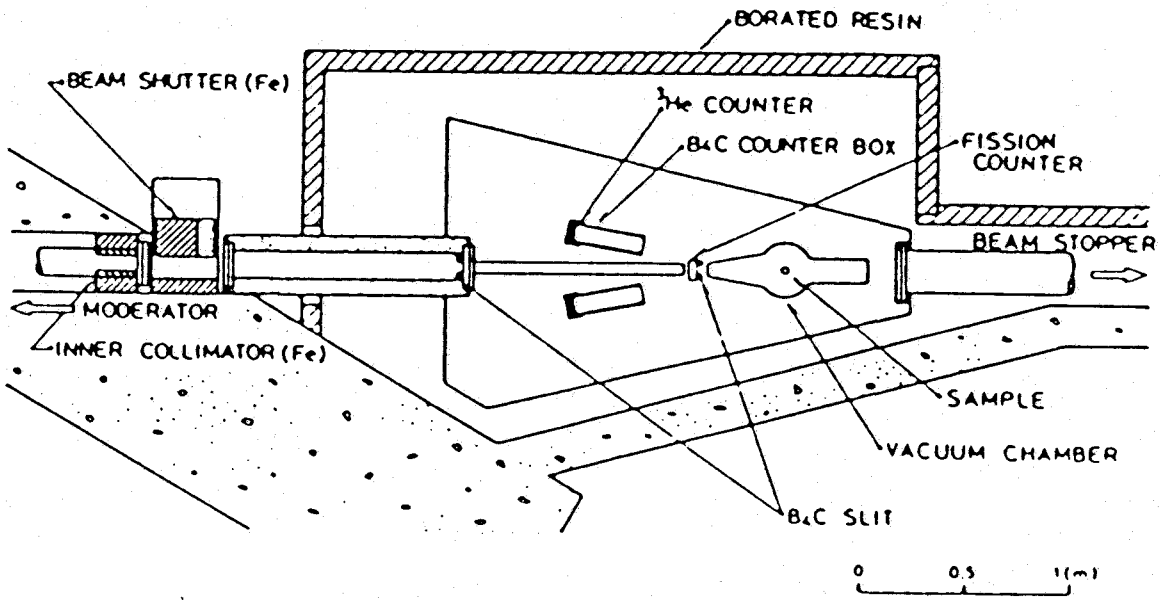

Fig.2-1 Configuration of HRP; after Watanabe et al.(1987)

Results and Discussion

The raw TOF diffraction pattern of ortho-I is shown in Fig.2-2. In spite of the 60 hrs data collection, maximum intensity was about 900 counts because of the small amount of high pressure phase. There was a diffraction with d=0.249 nm which did not appear in case of X-ray diffraction. If space group Pbcm was assumed, this diffraction is not identified. The possibilities which give an interpretation of this diffraction are as follows: ① impurities involved in the high pressure sample. ② diffraction from the attachment of HRP. ③ wrong space group.

As regards ① , possible impurities was BN, graphite, platinum, water and their compounds. XRD and EDX analysis of the same sample that was used in the neutron diffraction study showed no trace of any impurity. Considering the the result of XRD and EDX, impurities, if any, were expected to be some kinds of crystal hydride. Moreover, the amount of crystal hydride was supposed to be large because of the relatively high intensity of the unknown peak in the neutron powder data. Therefore, ^{1}H NMR study was performed. However, no signal attributing to ^{1}H was detected. Concerning ② , there was no substance which gave the diffraction with d=0.249 nm.

Consequently, it is assumed that the adopted space group (Pbcm) was wrong. As mentioned before, there has been only one study of the crystal structure analysis of ortho I (Kudoh et al.1986). It is doubtful whether they collected sufficient number of data to decide the crystal structure under high pressure using a diamond anvil pressure cell because the range for data collection is diminished comparing with the conventional four circle

diffractometer. However, even if the true space group is not Pbcm, it is no doubt that ortho I belongs to a space group very close to Pbcm and has a distorted fluolite structure. This fact is also confirmed by the result of the Rietveld analysis performed by Suyama et al.(1987), who reported that Rwp, Rp and Rb were reduced to 9.84, 7.04 and 3.09 %, respectively by the structure refinement assuming that ortho I belonged to the space group Pbcm.

In the present study, Rwp, Rp and Rb were reduced to 11.25, 7.92 and 7.57, respectively by assuming the space group Pbcm and eliminating the peak with d=0.249 nm as impurities. However, further discussion of the crystal structure is difficult at this moment.

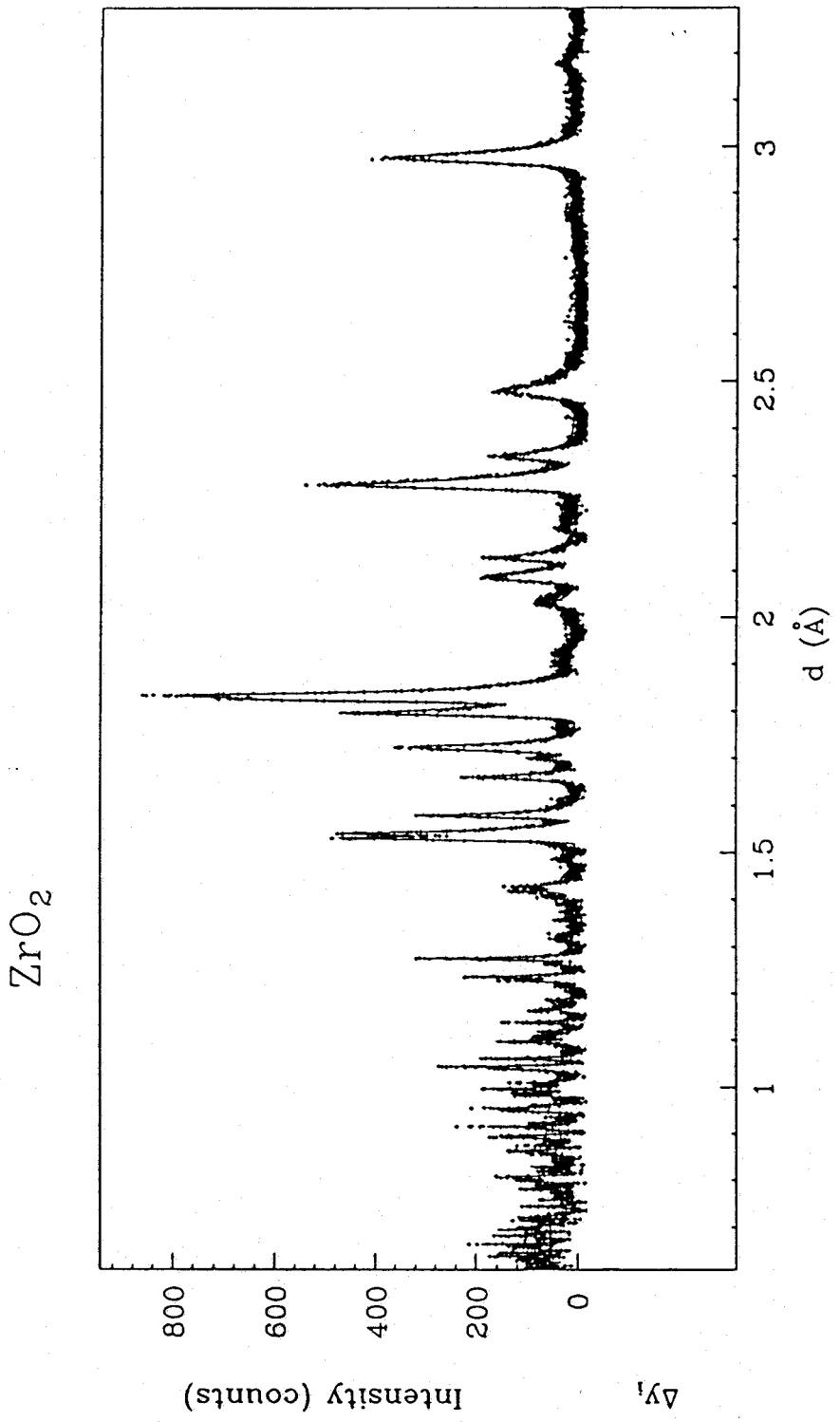

Fig.2-2 Raw data of neutron diffraction of Ortho I

Chapter 3 Synthesis of OrthoII

Introduction

OrthoII was first synthesized by Liu(1980) and its existence was confirmed by Block et al.(1985) and Devi et al.(1987). This phase belongs to the space group Pnma and has a cotunnite ($PbCl_2$) type structure. The polyhedral co-ordination is 9. Though consistent results as to the crystal structure have been reported, stable region of this phase has not been understood well. This is because temperature calibration was not accurate enough to discuss the phase boundaries since their studies of this phase were performed by diamond anvil cell using laser heating method. Furthermore, there is no thermodynamical data at all.

In order to reveal stable region of orthoII and obtain high pressure sample for the thermodynamical experiment, the author has made a series of synthesis experiment. By trial experiments using monoclinic phase as starting materials, the formation diagram of orthoII was obtained to find out optimum conditions for the synthesis of orthoII . According to this diagram, relatively large amount of orthoII was produced to perform thermodynamical experiments. By phase equilibrium experiments, the equilibrium phase boundary was decided.

The stability of Y-ZrO_2 was investigated in the pressure range higher than 10 GPa to show that orthoI do not exist in this case. Synthesis experiment of Ca-orthoII was also attempted using crushed single crystal of CaO doped cubic ZrO_2.

Another experiment to decide the phase boundary between orthoII and its higher temperature phase was performed by in-situ

observation of the electrical resistance change of sample under high pressure and temperature.

Experimental

1. Apparatus for High Pressure Experiment

High-pressure experiments were performed with a uniaxial split-sphere apparatus at the ISEI of Okayama University. The cubic anvil assemble of tungsten carbide is compressed with the aid of a press with power of 1,000 ton (Kawai et al.1973 and Ito and Yamada,1982). Anvils with a 3 mm edge length were used for phase equilibrium experiments, while those with a 5 mm edge length were used for the synthesis of considerable amount of orthoII used for the thermodynamical experiments and also for the electrical resistance measurements.

The specimen assembly is schematically shown in Fig.3-1. The pressure medium was sintered MgO. The powdered sample was put into a cylindrical metal heater embedded in a MgO regular octahedron. As MgO has high thermal conductivity, $LaCrO_3$ sleeve was inserted between the metal heater and MgO as an insulator. Heating materials were platinum for experiments at temperatures lower than 1100 ℃ and tantalum for those higher than 1100 ℃ . Temperature was monitored by the Pt/Pt13%Rh thermocouple with 0.2 mm diameter penetrating at the center of the cylindrical heater. The cold junctions of the thermocouple were taken out of the cubic anvil assembly. No correction was made for the pressure effect on emf.

After being held at a desired condition for a certain duration, the sample was quenched by shutting off the electric power supply. The pressure was released slowly and the product was recovered in the ambient condition.

The generated pressure was calibrated against the supplied

load using several fixed points as shown in Table 3-1.

2. Phase Equilibrium Experiment

Two sets of starting material were prepared for normal and reverse experiments, respectively. The one consisted of monoclinic single phase and the other a 50-50 mixture of orthoII and monoclinic. The samples were held at the desired temperature for a time interval of 45 to 100 min depending on temperature before cooling under pressure.

After the run, the quenched sample was examined with microdiffractometer. In case of the experiments at temperatures higher than 800 ℃ , running time was long enough to ensure the complete conversion to either monoclinic or orthoII . On the other hand, in case of those conducted at temperatures lower than 800 ℃ , running time was not long enough for the complete conversion. However, samples were quenched within 2 hrs. because of the experimental difficulties to keep samples under constant temperature any longer. The individual runs are recorded in Table 3-2 (a)(b).

Referring to the results of normal experiments, orthoII for thermodynamical experiments were synthesized. In these experiments, thermocouple was set outside of the platinum heater so as to prevent the sample from being contaminated.

3. Synthesis of OrthoII of Stabilized ZrO_2

The synthesis of Y_2O_3-orthoII were carried out using 2 and 6 mol%Y_2O_3 (2Y and 6Y) -ZrO_2 fine powder as starting material. 2Y-ZrO_2 consisted of a mixture of the tetragonal and the

monoclinic, while 6Y-ZrO_2 consisted of the cubic. Individual runs are summarized in Table.3-3.

Synthesis experiment of Ca-orthoII was performed by using crushed single crystal of 12 mol% CaO doped cubic ZrO_2 as a starting material. Crushed single crystal (10-1000 μ m) was mixed with NaCl powder used as hydrostatic pressure transmission media and treated at 20 GPa 800 ℃ for 60 min. Recovered sample was washed with water to get rid of NaCl and examined by optical microscopy.

3. Electrical Resistance Measurements

In situ observation of electrical resistance under high pressure and temperature was performed by means of an ohmmeter. Cell assembly for this experiments is illustrated in Fig.3-2. Platinum electrodes with MgO sleeve used as an insulator were inserted into the sample and d.c. electrical resistance was measured between the lead wires which were indirectly connected to platinum electrodes through anvils. Starting material for this experiment was a mixture of orthoII and the monoclinic. In the runs, samples were at first held at 800 ℃ for 30 min to have them transform into orthoII completely. Then, at fixed pressures (16.5 and 18 GPa), the d.c. data were recorded over the temperature range from 600 to 1300 ℃ with an interval of 25 to 100 ℃ for heating and cooling cycles.

Table 3-1 Pressure Calibration

Bi(Ⅰ -Ⅱ)	2.55± 0.06
Bi(Ⅲ -Ⅳ)	7.7± 0.3
Pb(Ⅰ -Ⅱ)	13.6± 0.6
ZnS(metal)	15.6± 0.6
GaAs(matal)	18.7± 0.7

After Akimoto (1979)

Table 3-2(a)

Results of Phase Equilibrium Experiment (Normal Run)

Pressure (GPa)	Temperature (℃)	Duration (min.)	Run Product
20	1100	30	monoclinic
19	1100	30	monoclinic
18	1100	30	monoclinic
19	1000	30	orthoⅡ
18	1000	30	orthoⅡ
17	1000	30	monoclinic
16	1000	30	monoclinic
20	800	40	orthoⅡ
19	800	40	orthoⅡ
17	800	40	orthoⅡ
16.5	800	40	monoclinic
18	600	70	orthoⅡ
17	600	70	orthoⅡ
16	600	70	monoclinic
15	600	90	monoclinic

Table 3-2(b)

Results of Phase Equilibrium Experiment (Reverse Run)

Pressure (GPa)	Temperature (℃)	Duration (min.)	Run Product
17	800	60	orthoⅡ
16	800	60	orthoⅡ
15	800	70	orthoⅡ
14.5	800	60	orthoⅡ
14	800	60	orthoⅡ
13	800	60	monoclinic
13.5	800	60	orthoⅡ
12	600	100	monoclinic
13	600	100	orthoⅡ
11	600	60	monoclinic
14	600	70	orthoⅡ
13.5	600	70	orthoⅡ

Table 3-3 Results of Y_2O_3-OrthoII Synthesis Experiment

Strating Material	Pressure (GPa)	Temp. (℃)	Duration (min.)	Run Product
2mol%Y_2O_3	16	RT	30	no change
2mol%Y_2O_3	14	330	40	no change
2mol%Y_2O_3	18	1000	30	orthoII
2mol%Y_2O_3	14	500	30	no change
6mol%Y_2O_3	12	360	30	no change
6mol%Y_2O_3	18	1000	30	orthoII
# 12mol%CaO	18	800	60	orthoII + Cubic

Y-ZrO_2 is fine powder (< 30 nm)
Ca-ZrO_2 is crushed single crystal

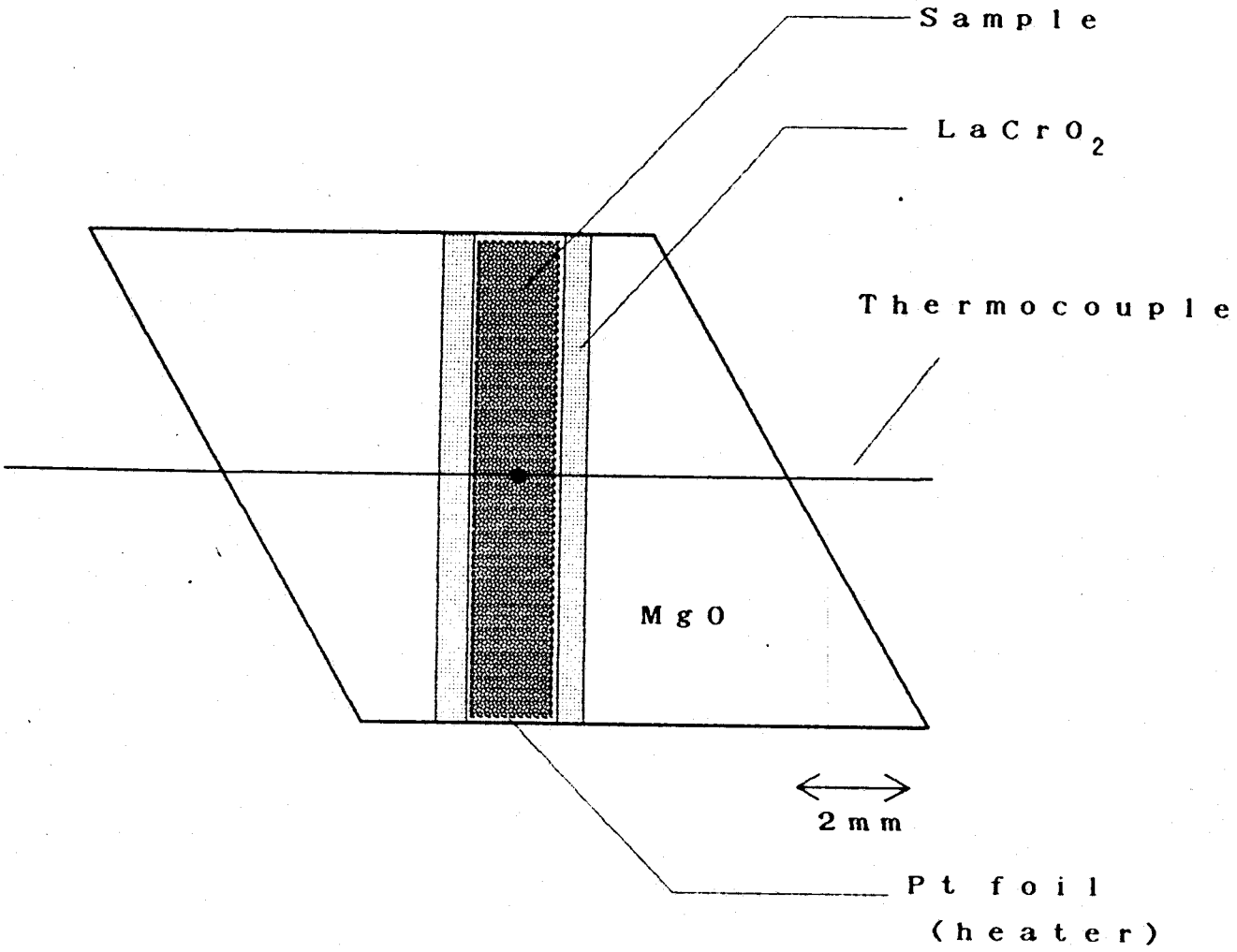

Fig.3-1 Cell assemblage for high pressure synthesis experiment with a uniaxial split-shere apparatus.

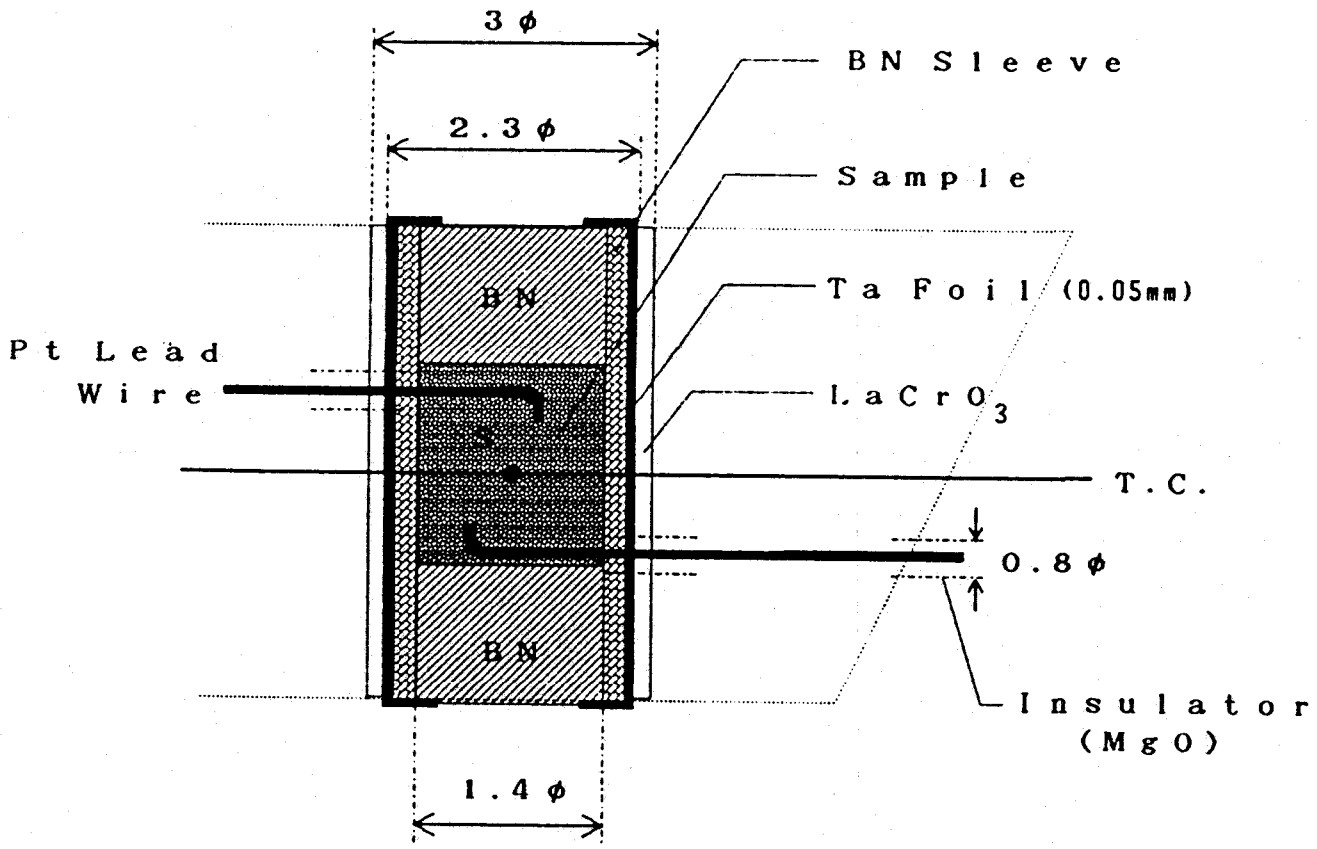

Fig.3-2 Cell assembly for electrical resistance measurement with a uniaxial split-shere apparatus.

Results and Discussion

1. Phase Equilibrium Experiment

Results of phase equilibrium experiment are shown in Fig.3-3, where circles and triangles correspond to the results of the normal and the reverse experiment, respectively. Filled circles (triangles) indicate that recovered sample consisted of orthoII and open circles (triangles) of the monoclinic, respectively.

No orthoI was found in the product of this experiment. This is probably due to the fact that the phase transformation between monoclinic and orthoI is martensitic and orthoI transforms to the monoclinic easily when releasing pressure. Therefore the recovered monoclinic is considered to have been orthoI or another unquencheable polymorph mentioned below when it was subjected to high pressure and temperature and then to revert into monoclinic on decreasing pressure.

In the normal experiment, orthoII appeared above 17 GPa at 800 ℃ and 18 GPa at 1000 ℃ , respectively. However, the recovered sample treated above 18 GPa at 1100 ℃ was not orthoII but monoclinic. This indicates that another kind of high temperature polymorph appears over these conditions. Though there is no identifying the structure of this phase, this phase is believed to be the cubic when the phase relationship of ZrO_2 polymorphs is taken into account.

Because of the experimental difficulty, mainly this is the difficulty to preserve constant temperature, it is hard to keep the sample under experimental conditions for more than 100 min. Consequently it is necessary to keep the sample as high temperature as possible in order to attain equilibrium state within the

relatively short duration of time. On the other hand, as the results of the normal experiment show, another kind of high temperature polymorph which is unquencheable is expected to appear above 1100 ℃ . In order to decide the orthoⅠ -orthoⅡ phase boundary, it is essential to carry out the reverse experiment in the temperature range outside the stable region of this phase. Therefore, two sets of the reverse experiment were executed at 600 ℃ and 800 ℃ to avoid these problems.

In the series of the runs at 800 ℃ , recovered samples consisted of nearly single phase of either the orthoⅡ or the monoclinic. This indicates the transformation of each direction has completed within experimental duration of time and equilibrium state is achieved. The amount of orthoⅡ increased above 13.5 GPa.

In the series of the runs at 600 ℃ , starting material did not transform to either phase completely in duration of time. Considering that some amounts of orthoⅡ involved in the starting material presumably reverted to the monoclinic during compression, there is a probability that these runs at 600 ℃ did not indicate the direction of the reaction properly. Consequently, the phase boundary point in the reverse run was decided to be 13.5 GPa 800 ℃ .

SEM micrographs of the reverse experiment sample before(A) and after(B) the run are shown in Figs.3-4 (A) and (B), respectively. (B) is that of the sample treated at 800 ℃ 16 GPa for 30 min and this shows clearly that newly synthesized orthoⅡ is produced on the surface of orthoⅡ which was mixed in the starting material.

The difference of the phase transformation pressure at the same temperature between the normal and the reverse experiment is due to the energy barrier of the orthoⅠ - orthoⅡ phase transformation. As presented later in this chapter, the orthoⅠ - orthoⅡ transformation occurs by the nucleation and growth process. This process generally has higher activation energy than other phase transformation mechanism such as martensitic transformation. In the present case, higher compression is thought to be necessary for the nucleation of orthoⅡ in the normal runs comparing with the case of the reverse runs. Consequently, the difference of the phase transformation pressure at the same temperature between the normal and the reverse experiment occurred.

At the equilibrium state, reaction does not proceed either direction. Only when excess pressure is generated, the possibility of the transformation from the low pressure phase to the high pressure phase occurs. The probability of the transformation increases as excess pressure is generated.

In case of the normal run, nearly single phase of orthoⅡ, though small crystallite size, was synthesized at 800℃ in 40 min when the sample was subjected to sufficient pressure (>17 GPa), while single phase of the monoclinic was recovered by the run 16.5 GPa 800 ℃ 40 min. It is certain that no long distance diffusion is necessary for this transformation. These views suggest that rate determining step of this transformation is not the growth of nuclei but the rate of nucleation. The probability of the transformation is interpreted as that of occurrence of nuclei which is large enough for growth. Therefore, excess compression to raise this probability was required for the transformation in

case of the normal run.

In the reverse run, orthoII nuclei large enough for growth already exist in the starting material. When these nuclei continue to grow, they are in the stable region of orthoII . From these views, equilibrium pressure is decided to be 13.5 GPa at 800 ℃ .

2. Y_2O_3-OrthoII

Y_2O_3-ZrO_2 was subjected to high pressure and temperature. The results are summarized in Table 3-3. Although stabilized tetragonal and cubic phases have been confirmed not to transform to orthoI , Y_2O_3 doped orthoII was synthesized. and its XRD patterns are illustrated in Fig.3-5. Their lattice parameters are tabulated in Tables 3-4 and -5. The unit-cell volume change of orthoII in non-doped ZrO_2 compared with that obtained by doping with Y_2O_3 is 0.3% and 0.8% for 2Y- and 6Y-ZrO_2, respectively, and these magnitudes are comparable with those when Y_2O_3 is doped to the other polymorphs of ZrO_2, such as those with monoclinic or tetragonal (Ohtaka et al. 1988). While there is no considerable difference in density among orthoI , tetragonal and cubic, about 12 % change is accompanied when these three phases transform into orthoII . Since pressure usually enhances a transformation to denser phase when the density difference is noticeable, stabilized ZrO_2 is considered to transform to orthoII . Same result was reported by Devi et al.(1987). They investigated the structure of Ca-stabilized cubic ZrO_2 with XRD at high temperatures and pressures up to 1000 ℃ and 35 GPa using a diamond-anvil cell interfaced with a YAG laser heating system. They reported that CaO-

stabilized cubic ZrO_2 transforms directly into orthoII . However, in their study, orthoII was not obtained as a single phase but as a mixture of orthoII and the cubic. Considering the inaccuracy of measuring temperature in a diamond anvil cell, it seems that their result implies the possibility of the existence of another phase which appears just above 1000 ℃ because some parts of the sample are considered to be heated excessively with YAG laser. As mentioned before, this high temperature phase is predicted to be cubic.

3. CaO-OrthoII

When recovered sample was examined by microscopy, it was found that the sample consisted of three types of grains; the grain with optical isotropy, that with optical anisotropy and that with their mixture.

Polarizing photomicrographs of grain immersed in methylene iodide are shown in Figs.3-6 and -7. Fig.3-6 (b) shows that the whole grain is optically anisotropic. On the other hand, in Fig.3-7(b), some parts (yellowish part) show the optical anisotropy and other parts of the grain (purple red part) show optical isotropy. Moreover, the yellowish part looks relieving against the matrix and this indicates that the density of this part is higher than the rest.

A crystal with cubic symmetry is optically isotropic and that with orthorhombic symmetry is optically anisotropic. Therefore, three types of grain mentioned above were interpreted as the cubic, orthoII and their mixture, respectively. As there is temperature gradient in the sample chamber, from about 100 ℃ at

the interface with anvil to 800 ℃ in centre, some cubic grains subjected to low temperature are thought to have been remained unchanged or quenched before completing the transformation because of the low reaction rate at low temperature.

From this fact, Fig.3-7 is understood that it represents the intermediate stage from the cubic to orthoⅡ transformation. The shape of orthoⅡ appearing in the cubic matrix is spherical and this indicates that the cubic to orthoⅡ transformation occurs by the nucleation and growth process. Considering the similarity of the crystal structure among orthoⅠ, tetragonal and cubic, all the transformations to orthoⅡ from these phases are concluded to occur by the nucleation and growth process.

4. Electrical Resistance Measurement Experiment

Arrhenius plot of measured data at 16.5 GPa during the heating and cooling cycle and that at 18 GPa during the heating cycle are shown in Figs.3-8 and -9, respectively. There is discontinuity on heating data while cooling data shows continuous change. This discontinuity indicates orthoⅡ to cubic phase transformation. The phase transformation temperatures are 950 to 1050 ℃ at 16.5 GPa and 1000 to 1100 ℃ at 18 GPa,respectively, and these values are in fairly good agreement with the results of synthesis experiment. The slope of the phase boundary seems to have a slight positive value, however, more precise discussion is not possible at this moment because of the uncertainties in estimating temperatures and experimental difficulties to measure the electrical resistance at higher pressure regions.

These figures also show differences in activation energy for

conductivity. Activation energies for conductivities were calculated from the slope of the curve and are summarized in Table 3-6 comparing with those reported previously. Obtained activation energies of cubic phase under high pressure are lower than those in ambient pressure. Furthermore, as the sample is subjected to higher pressure, the activation energy becomes lower. Since ZrO_2 behaves like semiconductor at high temperature, this result is reasonably understood through the fact that electrical conductivity of semiconductor is generally promoted by compression. In the case of the activation energy of orthoII , same tendency was observed.

In the cooling cycle shown in Fig.3-5, no discontinuous change in electrical resistance is observed. This result indicates that the cubic to orthoII reverse phase transformation do not occur at a certain temperature during the cooling cycle. Furthermore, the recovered sample was not a single phase of orthoII but the mixture of orthoII and the monoclinic. There seems to be two possible explanations about this fact: One is super-cooling of the cubic, that is, some amount of the cubic remains to be transformed after shutting off the electric power supply and transforms directly to the monoclinic when pressure is released. The other is pressure leak in sample chamber caused by the contraction of pressure medium and reverse transformation of some amount of the cubic. Some parts in sample chamber become stable condition for orthoI by this pressure leak. Consequently, recovered sample becomes the mixture of orthoII and the monoclinic.

Table 3-4 Y-OrthoII Lattice Parameters

	2Y-OrthoII			6Y-OrthoII		
hkl	obs/nm	I/I102	dcal/nm	dobs/nm	I/I102	dcal/nm
011	0.2970	45	0.2967	0.2978	37	0.2974
102	0.2813	100	0.2803	0.2806	100	0.2805
111	0.2621	73	0.2620	0.2625	80	0.2625
112	0.2147	12	0.2146	0.2152	11	0.2150
202	0.2114	6	0.2115	0.2115	5	0.2117
211	0.2034	59	0.2033	0.2037	50	0.2036
013	0.1814	36	0.1814	0.1817	35	0.1816
113	0.1725	15	0.1725	0.1726	18	0.1727
020	0.1669	21	0.1669	0.1673	19	0.1673
004	0.1621	20	0.1620	0.1623	21	0.1622
302	0.1614	30	0.1614	0.1615	28	0.1615
311	0.1577	25	0.1576	0.1578	25	0.1578
213	0.1521	31	0.1521	0.1523	29	0.1523
220	0.1434	26	0.1432	0.1435	28	0.1435
204	0.1401	7	0.1401	0.1402	9	0.1403
400	0.1395	8	0.1396	0.1397	7	0.1397

Table 3-5 X-ray Data for Orthorhombic ZrO_2

	#OrthoI	#OrthoII	2Y-OrthoII	6Y-OrthoII
a(nm)	0.50364	0.55807	0.5582	0.5587
b(nm)	0.52546	0.33312	0.3338	0.3346
c(nm)	0.50855	0.64744	0.6482	0.6488
V(nm^3)	0.13458	0.12036	0.12088	0.12129
D(g/cm^3)	6.08	6.80	6.76	6.68

After Suyama et al. (1987)

Table 3-6 Activation Energy of Electrical Conduction

phase	pressure (GPa)	temp. range (℃)	activation energy (eV)
cubic	16.5	1100-1300	0.80
cubic	18.0	1100-1300	0.60
orthoII	16.5	600-1100	0.72
orthoII	18.0	600-1100	0.40
cubic	ambient	400-1000	0.96 (1)
cubic	ambient	700-1000	0.92 (2)

(1) 8.0 mol%-Y_2O_3 Jayaratna et al. (1987)
(2) 8.7 mol%-Y_2O_3 Badwal (1984)

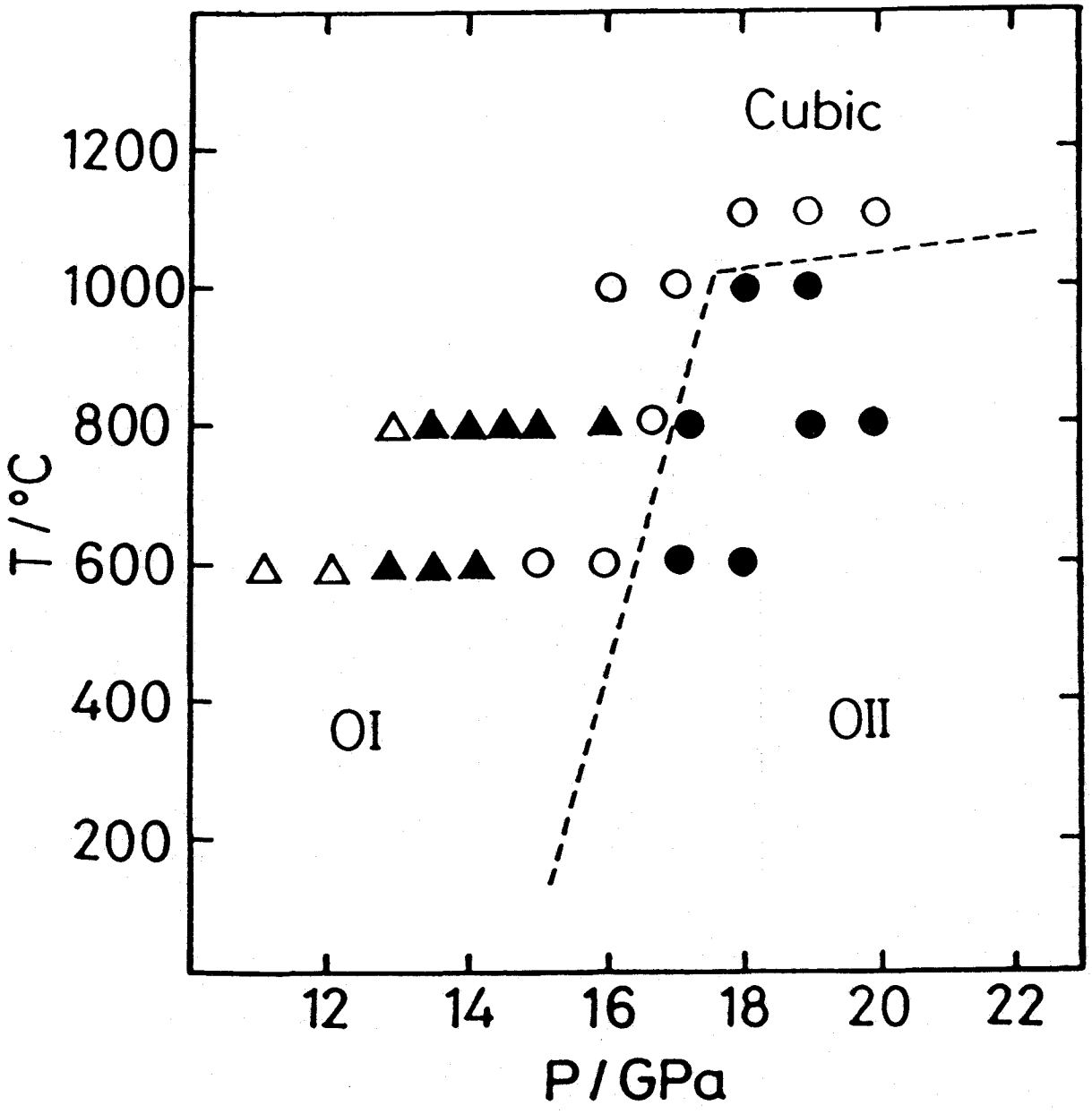

Fig.3-3 Results of phase equilibrium experiments: Circles are the results of the normal run and triangles are those of the reverse run. (●) and (▲) orthoII ; (○) and (△) the monoclinic.

Fig.3-4 (A) SEM micrograph of starting material for reverse experiment.

Fig.3-4 (B) SEM micrograph of product for reverse experiment.

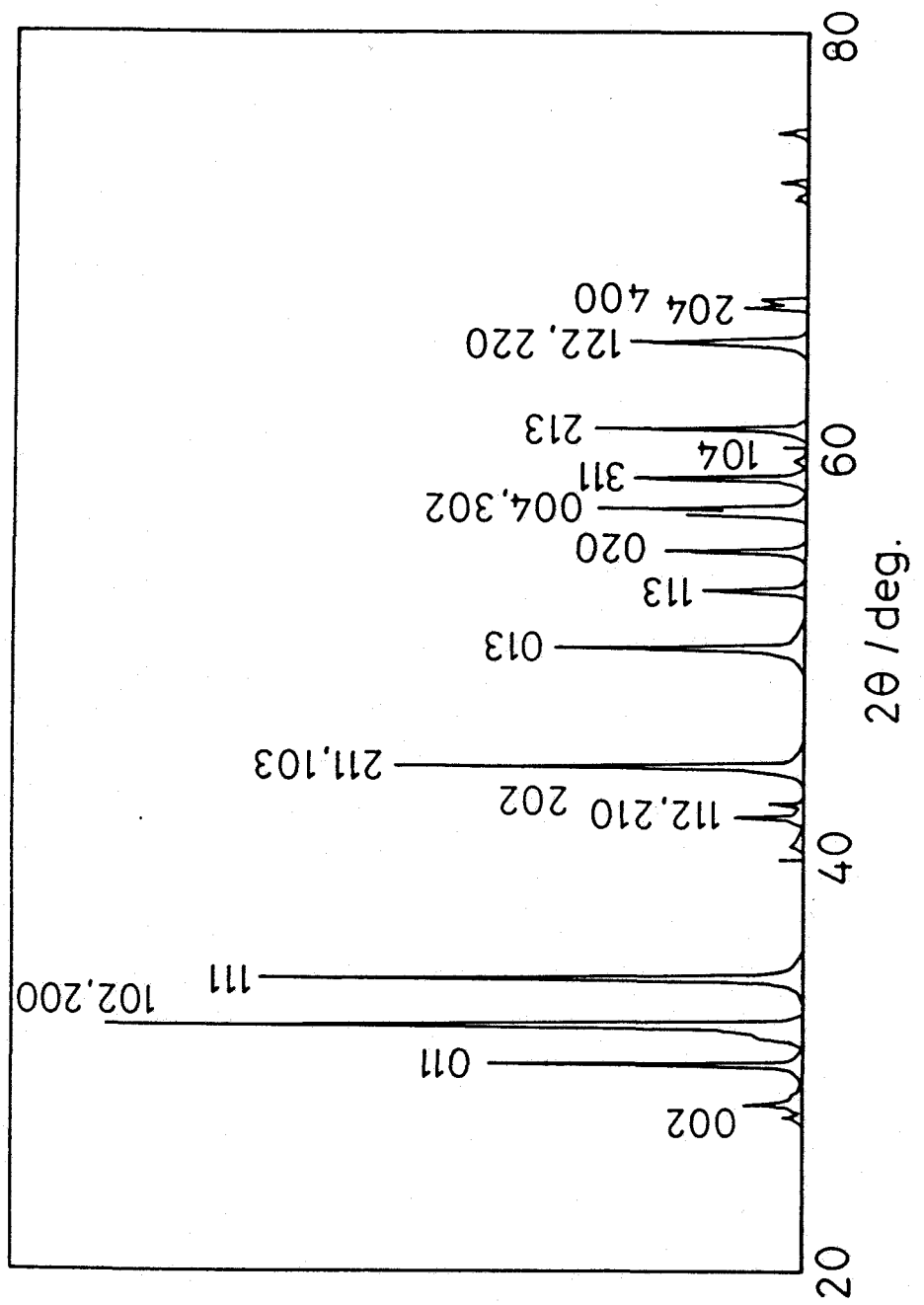

Fig.3-5 XRD pattern of 2Y-orthoⅡ .

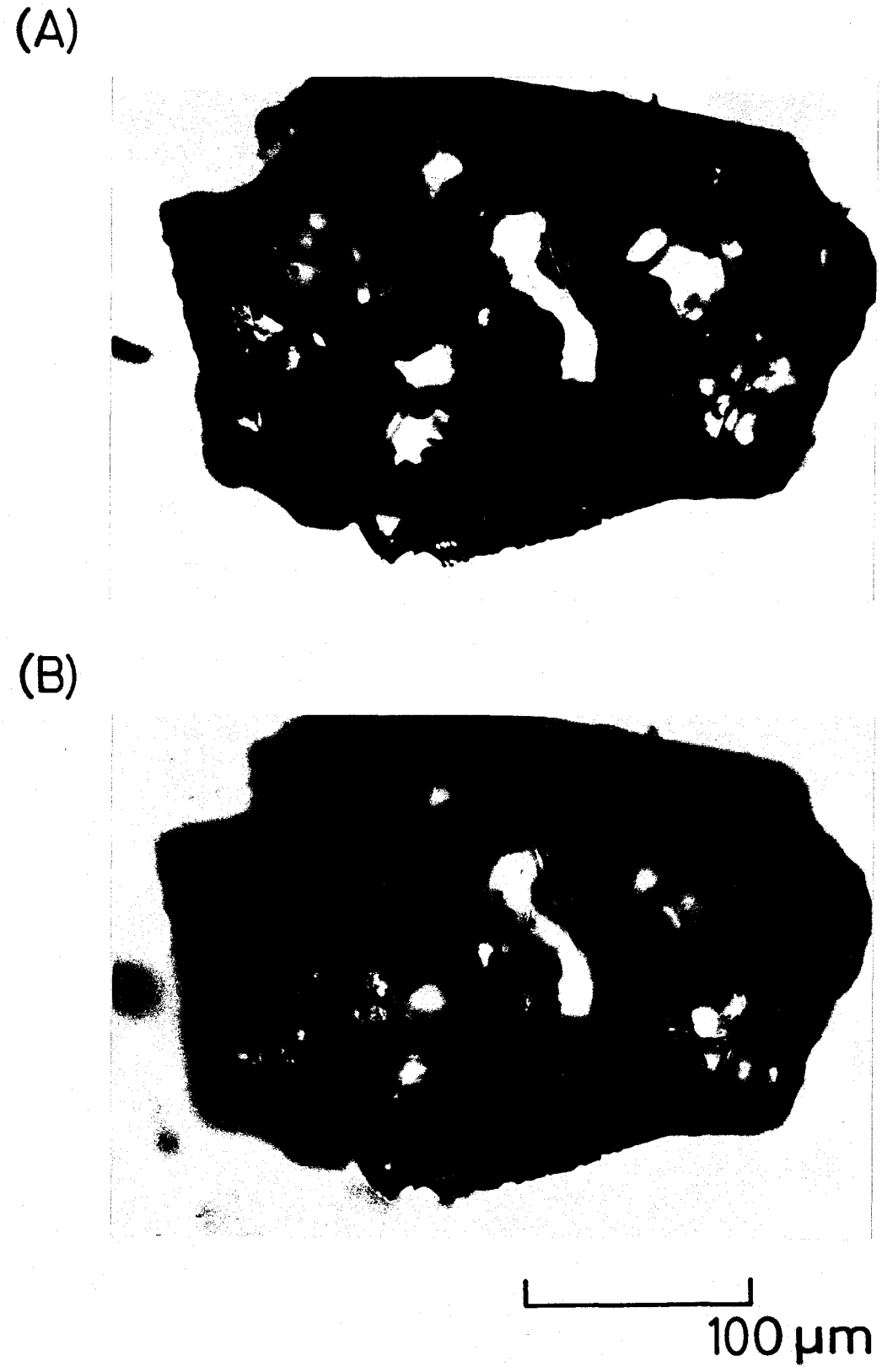

Fig.3-6 Polarizing microscope photos of the cubic and orthoII mixture (A) crossed parallel (B) crossed polars with Gypsum Plate.

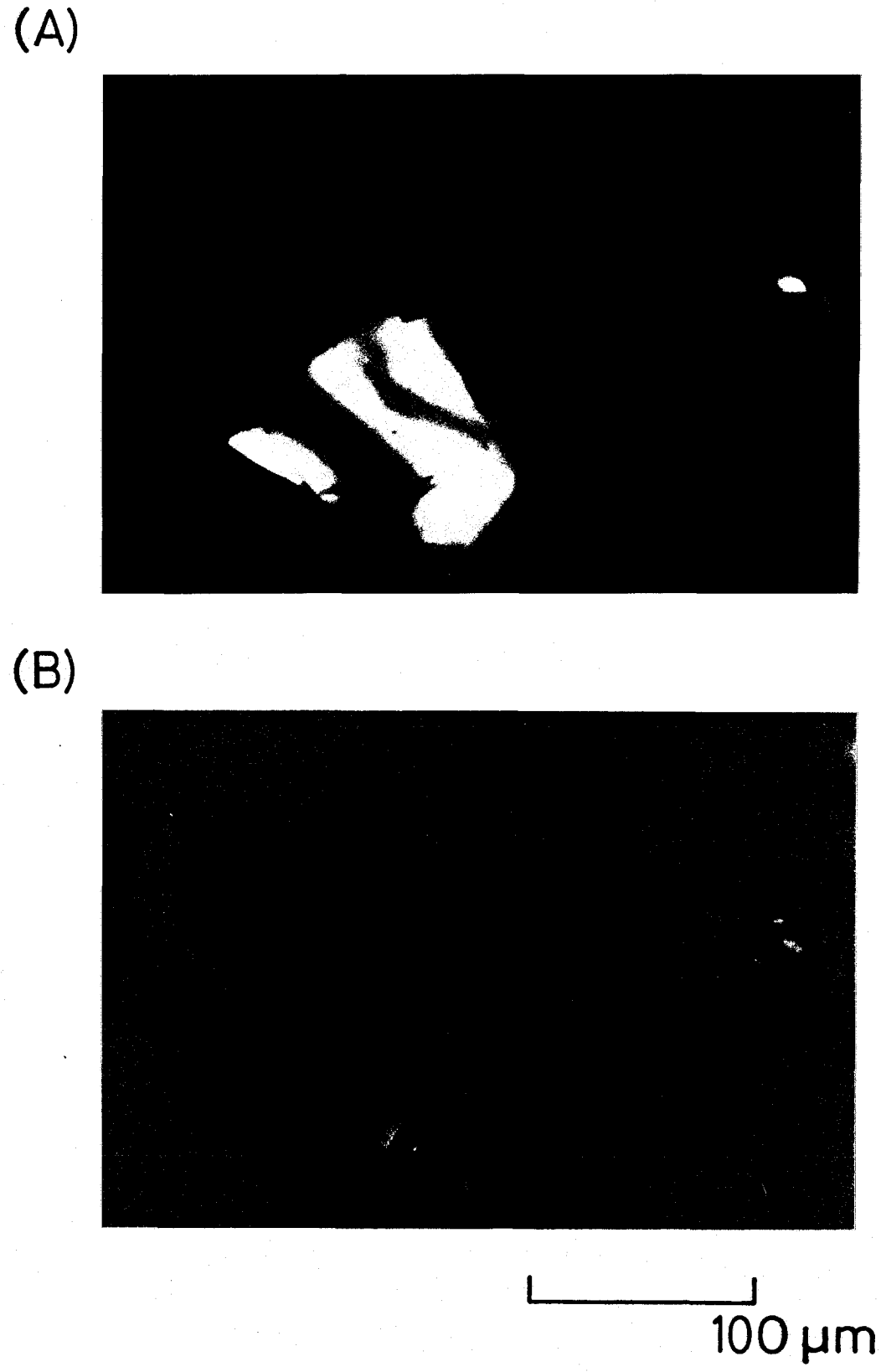

Fig.3-7 Polarizing microscope photos of orthoⅡ single grain (A) crossed parallel (B) crossed polars with Gypsum Plate.

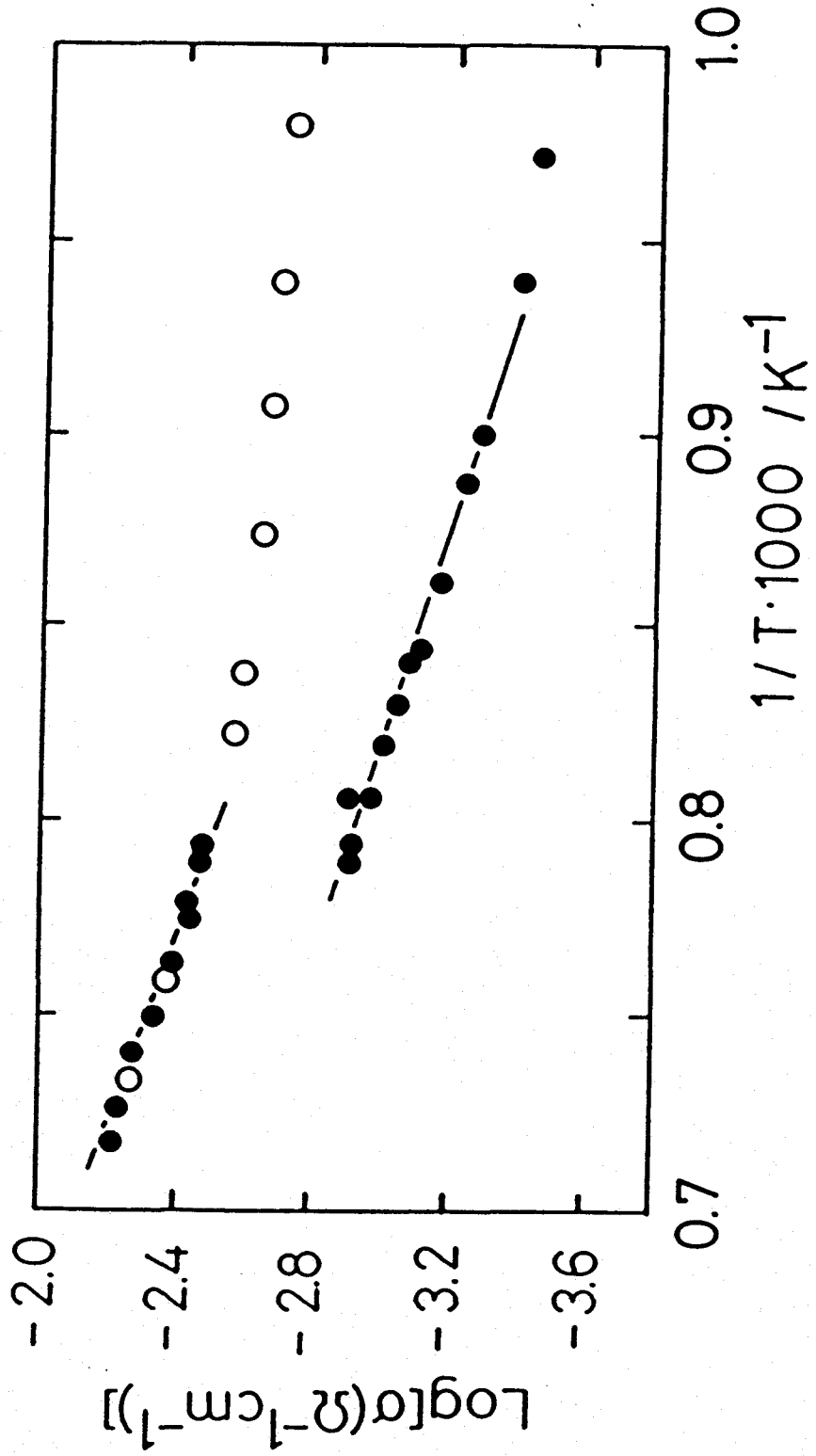

Fig.3-8 Arrhenius plot for the heating (●) and cooling (○) cycle of ZrO_2 at 16.5 GPa.

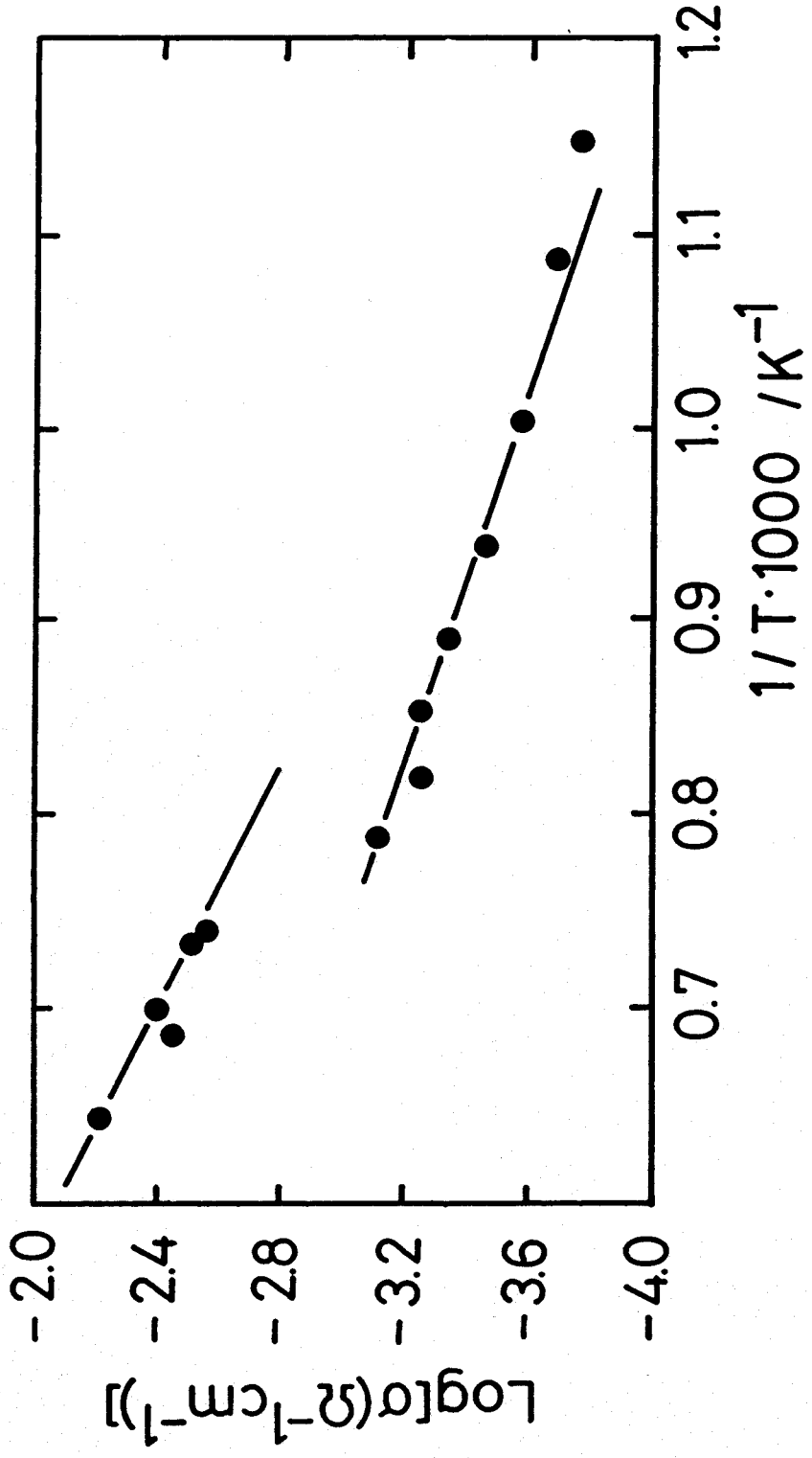

Fig.3-9 Arrhenius plot for the heating cycle of ZrO_2 at 18 GPa.

Chapter 4 Thermodynamics of ZrO_2 High Pressure Phase

Introduction

Thermodynamical data of ceramic materials are indispensable to the evaluation of their stability and the phase relations.

There are a lot of synthesis experiments performed for investigating phase transformations and reactions among ceramic materials under high pressure, however, it is doubtful whether their results indicate the equilibrium conditions. Especially when experiments are carried out under relatively low temperature range, there are often the cases that the deviations from the equilibrium state are not negligible because reactions usually proceeds slowly on such conditions.

On the other hand, using enthalpies of transformation or formation, it can be estimated whether the synthesis experiments indicates the equilibrium state or not. It is practically impossible to obtain the precise phase boundary under high pressure over a wide range just by the repetition of synthesis experiments. On the contrary, it will be more practical to calculate the phase boundary combining a few reliable data obtained by synthesis experiment and thermodynamical data. Therefore, thermodynamical data is believed to be essential to obtain precise equilibrium phase diagrams.

So it is with ZrO_2 high pressure polymorphs. In case of them, however, there was no thermodynamical data because of the difficulty of preparing high pressure sample for the experiments. Previously reported studies on ZrO_2 P-T phase diagram are two; one is the formation phase diagram up to 6 GPa (Bocquillon and

Sussee 1969) and the other is the monoclinic - orthoI boundary obtained by in-situ observation (Block et al. 1985).

By the series of synthesis experiments, high pressure sample in good quality and quantity for thermodynamical experiments has become obtainable. The author has carried out the thermodynamical study of ZrO_2 high pressure polymorphs. The enthalpies of phase transformation were measured with calorimeter. The entropies of phase transformation were estimated by combining the phase equilibrium data with enthalpies. The results are reported in this chapter. Furthermore, the stability of ZrO_2 high pressure polymorphs in the P-T diagram is discussed on the basis of the results of both thermodynamical and synthesis experiment.

Experimental

1. Sample Preparation

High pressure polymorphs of ZrO_2 were prepared as follows. All the samples were characterized by both XRD and microscopic observation. Starting material was ZrO_2 fine powder (grain size < 30 nm) offered by Tosoh Co.

OrthoⅠ (about 150 mg) was synthesized using a cubic anvil type high pressure device operated at 6 GPa and 500 ℃ for 1hr. XRD data for synthesized sample are shown in Fig.4-1(a). All lines in the pattern are indexed as orthoⅠ except for a slight trace of monoclinic.

OrthoⅡ (about 150 mg) was synthesized using a uniaxial split-sphere type high pressure apparatus in ISEI Okayama University. The starting material was put into a cylindrical platinum heater and was held at 18 GPa and 1073 K for 1hr. The sample was quenched and examined by XRD. The result is shown in Fig.4-1(b). The product was well crystallized orthoⅡ with a small amount of monoclinic.

Synthesized orthoⅠ and orthoⅡ contained small amount of monoclinic. As these high pressure phases easily reverse to monoclinic by thermal treatment or shear stress, detected monoclinic is considered to be produced by the shear stress during releasing pressure or even when the product was ground to powder for calorimetry experiment. No correction was made for this monoclinic because its amount was small and its effect on the calculations of entropies and slope of phase boundaries was negligible when uncertainties involved in other parameters such as pressure and temperature of phase equilibrium experiment data

were estimated.

The reverse transformation of the high pressure phases to monoclinic with annealing at calorimetric temperatures was examined by XRD and the results are shown in Fig.4-2 for orthoⅠ and in Fig.4-3 for orthoⅡ respectively. While orthoⅡ completely transforms to monoclinic within 10 min. at 700 ℃, orthoⅠ remains for 20 min. at 700 ℃. However, almost all of orthoⅠ transforms to monoclinic within 20 min at 784 ℃.

Obtained high pressure sample was dried at 110 ℃ for 24 hrs. to get rid of absorbed vapor. However, heating the samples at higher temperature to burn off some contamination which might happen to be included could not be done because of the instability of the samples. Therefore, contaminations other than absorbed vapor were checked by measuring the weight of the sample before and after the calorimetry experiment.

2. Calorimetry

Calorimetric measurements were made using a Calvet-type high temperature microcalorimeter described in Fig.4-4 (Navrŏtsky 1977). From the results of observing reverse transformation with annealing, the temperature of the calorimetry was set at 784 ℃. At this temperature, both of orthoⅠ and orthoⅡ are not stable and reverse rapidly to monoclinic within 20 min, therefore, drop calorimetry method was adopted to measure the heat of phase transformation at room temperature between these phases. In the runs, powder sample was put into a thin platinum tube and was dropped from room temperature to platinum crucible in the calorimeter at 780 ℃. Typical example of recorded data is shown

in Fig.4-5. Slashed area corresponds to the total heat content caused by a dropped sample in which heat content of a platinum tube and the sample and the enthalpy of phase transformation is involved. Subtracting the heat content of the platinum tube from the total heat content, heat content attributed to the sample is obtained. Calorimetric cycle used to calculate the enthalpies of phase transformation is as follows;

$$\text{ortho I}_{RT} = \text{monoclinic}_{1057K} \qquad \Delta H_1 \qquad (4\text{-}1)$$

$$\text{ortho II}_{RT} = \text{monoclinic}_{1057K} \qquad \Delta H_2 \qquad (4\text{-}2)$$

$$\text{monoclinic}_{RT} = \text{monoclinic}_{1057K} \qquad \Delta H_3 \qquad (4\text{-}3)$$

$$\text{monoclinic}_{RT} = \text{ortho I}_{RT} \qquad \Delta H_4 = \Delta H_3 - \Delta H_1 \qquad (4\text{-}4)$$

$$\text{ortho I}_{RT} = \text{ortho II}_{RT} \qquad \Delta H_5 = \Delta H_1 - \Delta H_2 \qquad (4\text{-}5)$$

ΔH_1, ΔH_2 and ΔH_3 are measured by dropping ortho I , ortho II and monoclinic sample, respectively. The enthalpies of phase transformation (ΔH_4 and ΔH_5) are calculated by combining measured values.

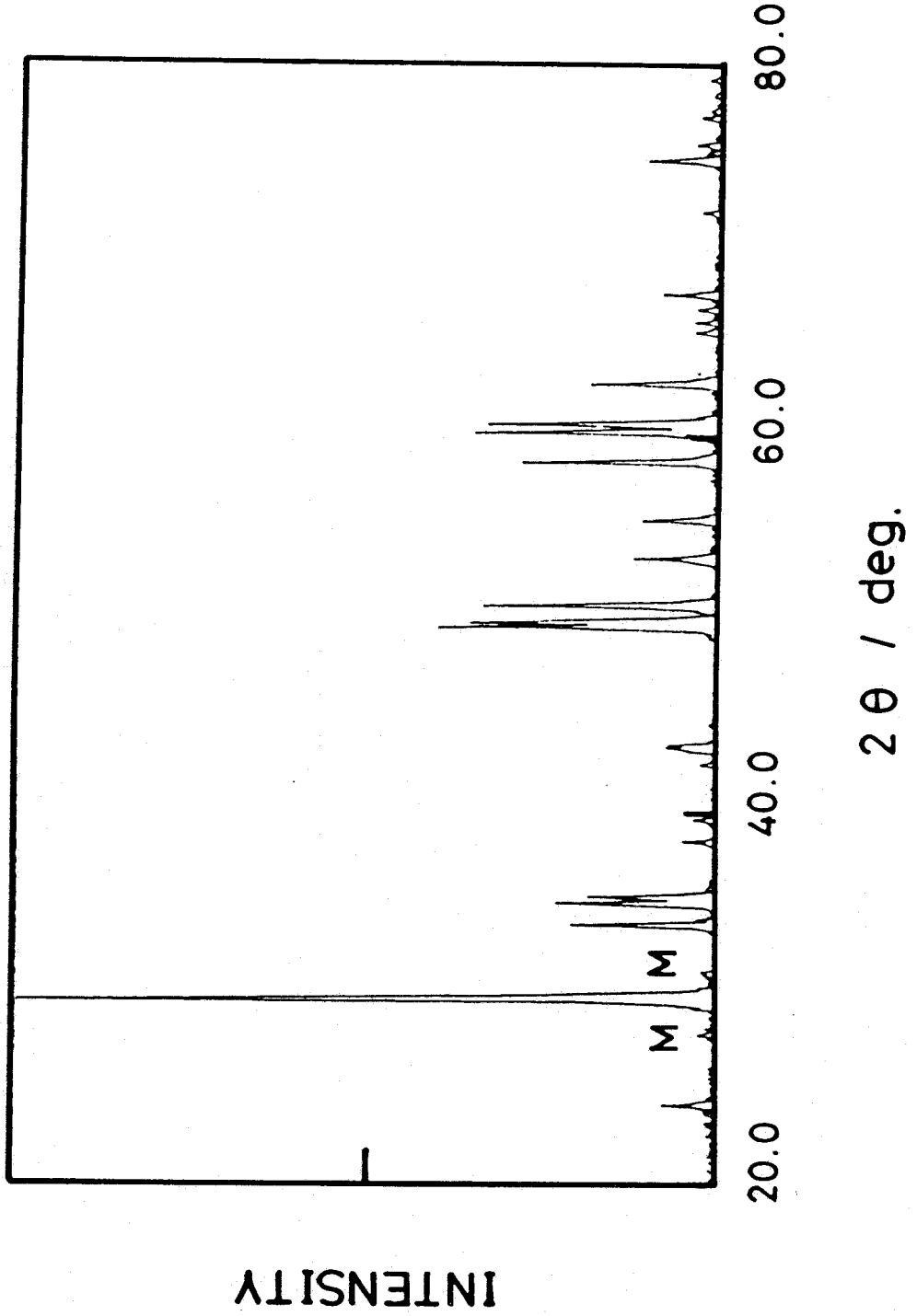

Fig.4-1(A) XRD pattern of orthoI sample for calorimetry experiments

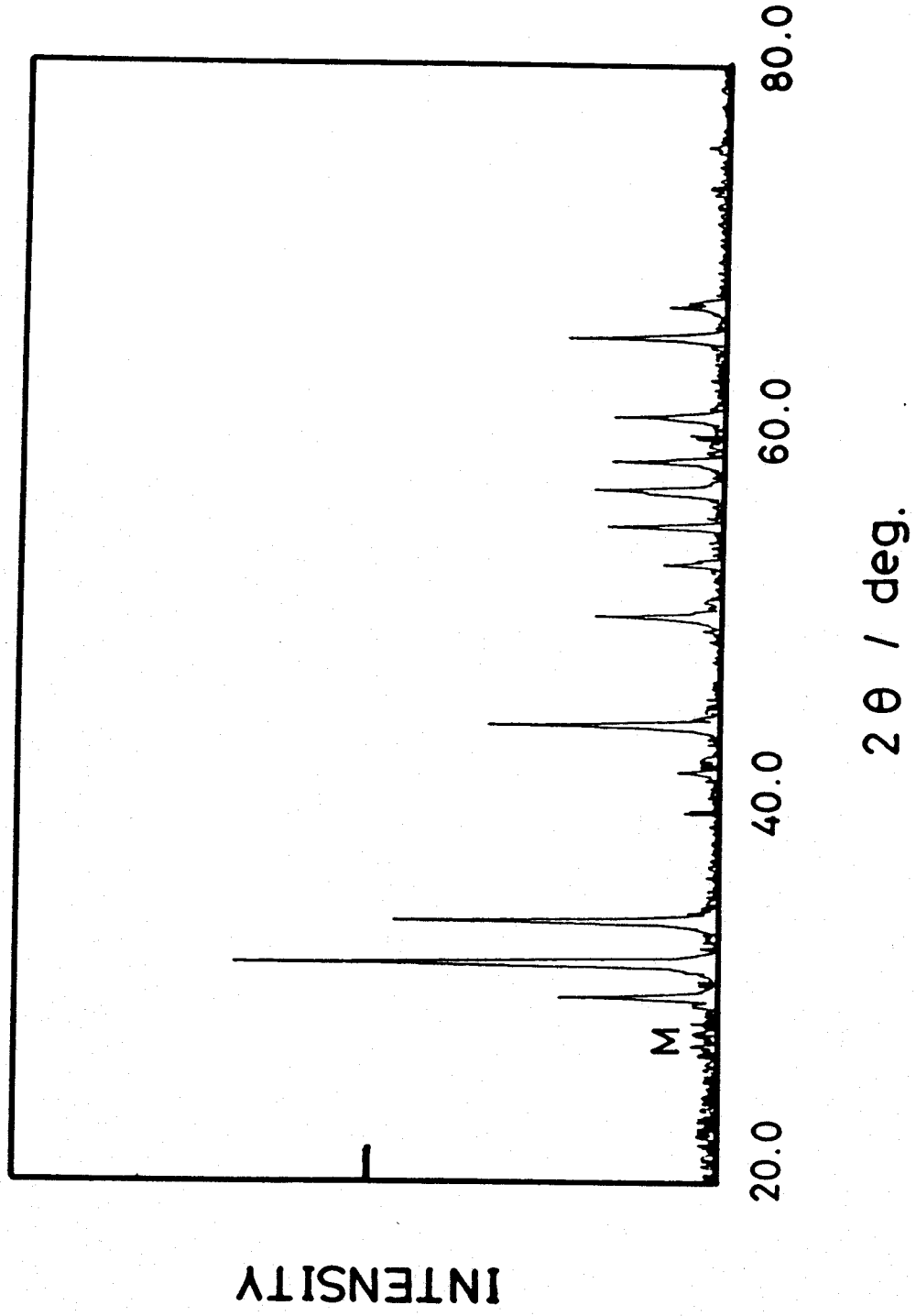

Fig.4-1(B) XRD pattern of orthoⅡ sample
for calorimetry experiments

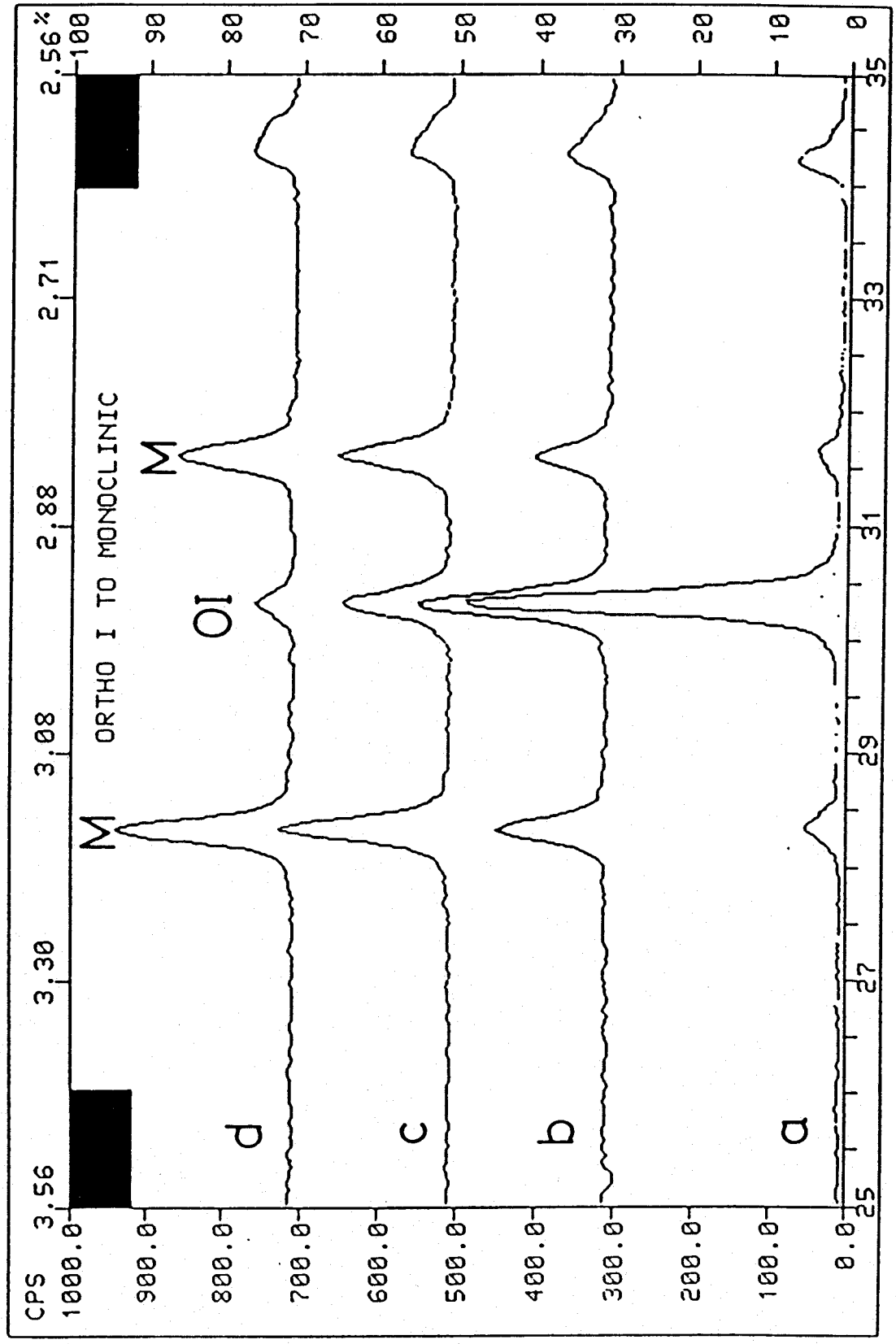

Fig.4-2 Reverse transformation of orthoI by annealing a:25 ℃, b:700 ℃ *10 min., c:700 ℃ *30 min. and d:780 ℃ *20 min.

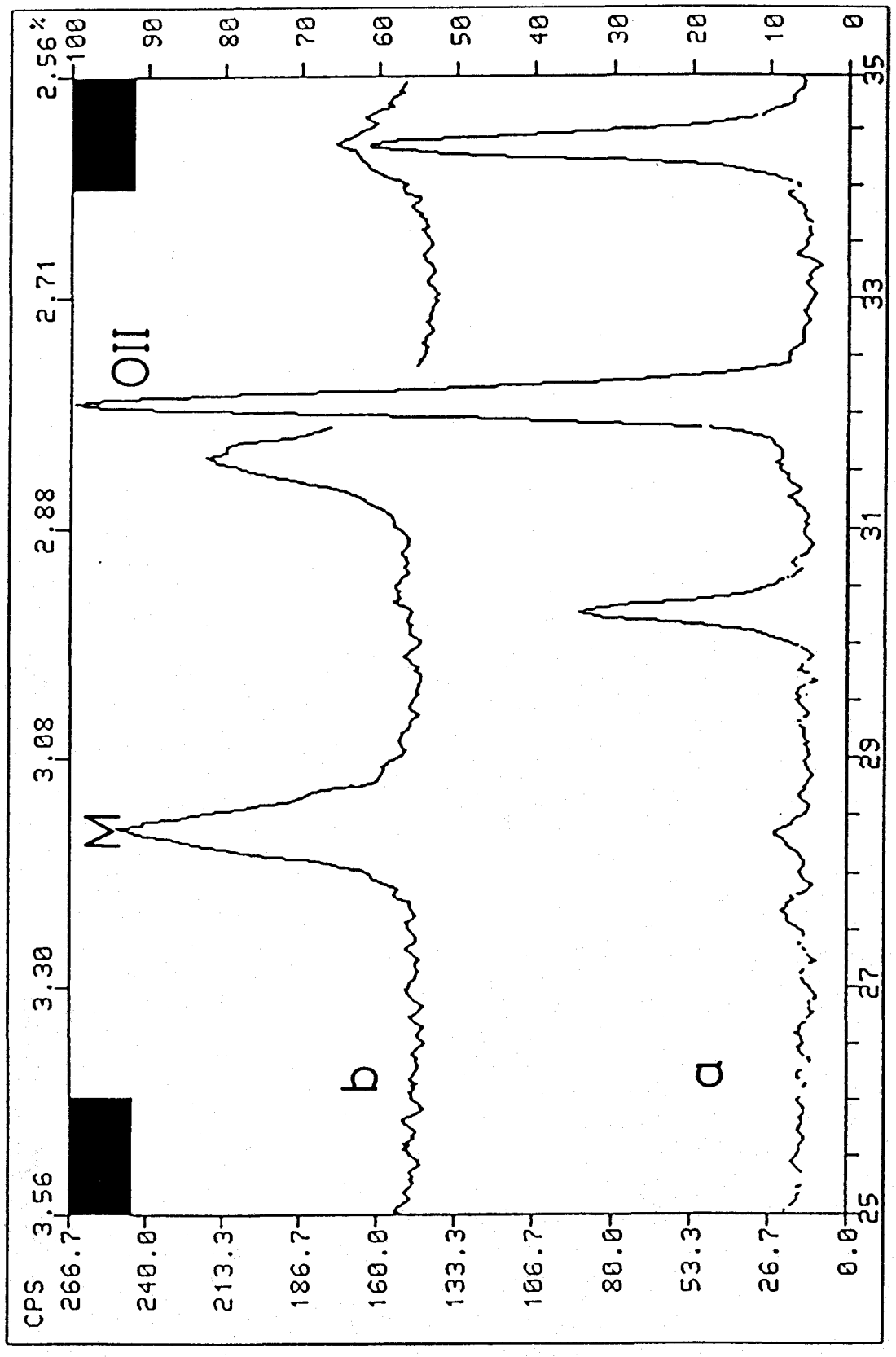

Fig.4-3 Reverse transformation of orthoⅡ by annealing

a: a:25 ℃ , b:700 ℃ *10 min.

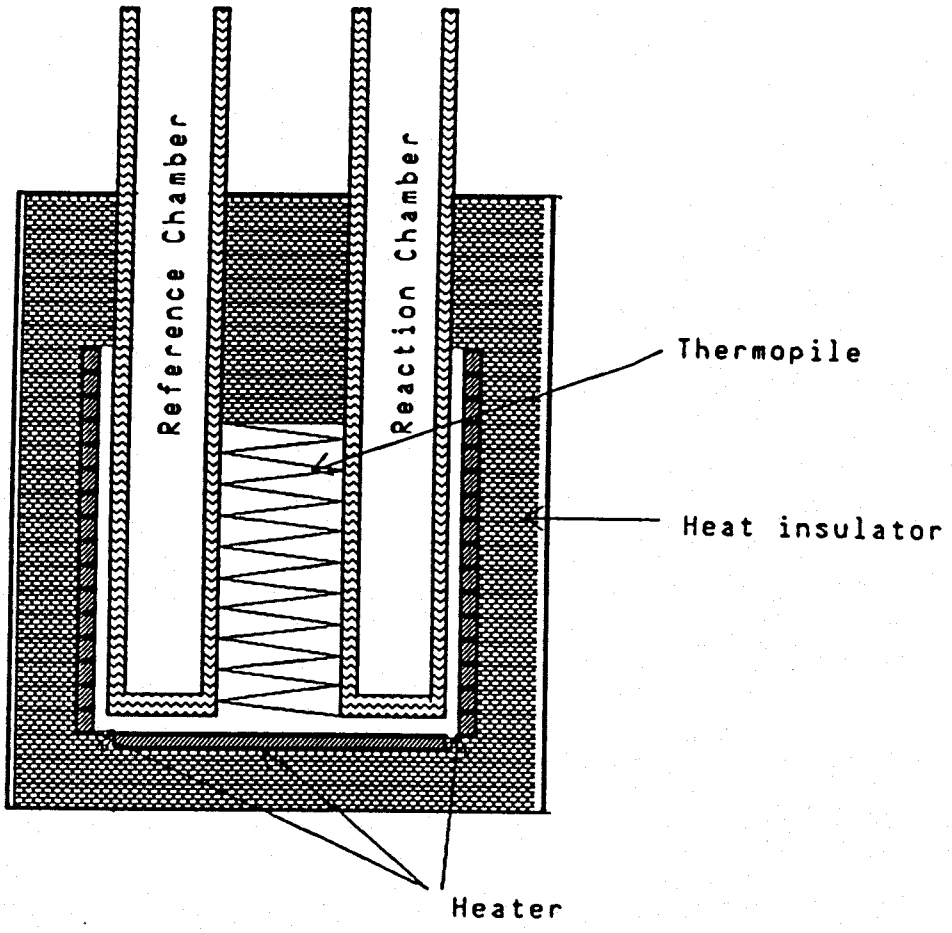

Fig.4-4 Calvet-type high temperature microcalorimeter

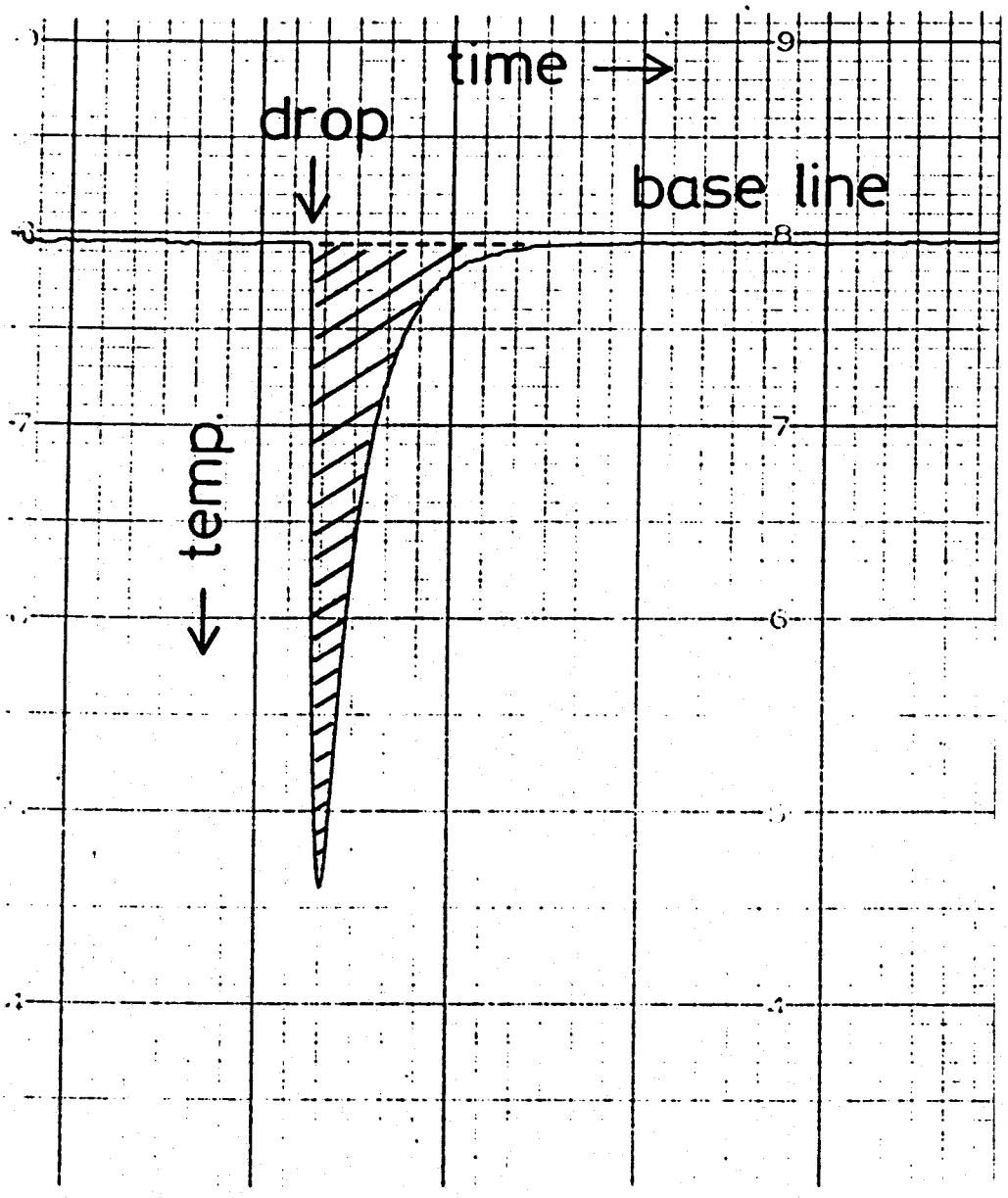

Fig.4-5 Calorimetry chart

Results

1. Thermodynamical Data

Enthalpies measured by the drop calorimetry of monoclinic, ortho I and ortho II are summarized in Table 4-1. The enthalpies in Table 4-1 were obtained by subtracting heat content of platinum tube from the measured heat effect of the sample plus platinum tube. Therefore, the enthalpy data in Table 4-1 are the sum of heat content plus heat of transition of ZrO_2 high pressure phases at room temperature. The enthalpies of the phase transformation were calculated using the calorimetric cycle.

2. Calculation of the Phase Boundary

Using enthalpy data, slopes of the boundaries can be calculated. To locate the phase boundaries in pressure-temperature diagram, the value of the standard free energy for the phase transformation or the equilibrium pressure at one temperature is essential. Regarding the monoclinic-ortho I phase boundary, equilibrium pressure reported by Block et al. (1985) was used. As to the ortho I -ortho II phase boundary, the results of the phase equilibrium experiment presented in Chapter 3 were used. The equilibrium pressures used for the calculation were 3.28 GPa at 298 K and 13.5 GPa at 1073 K for the monoclinic-ortho I and the ortho I - ortho II boundary, respectively. With these phase transformation pressures, entropy changes and P-T slopes of boundaries were calculated by following thermodynamical equation;

$$\Delta G_{P,T} = \Delta H_T - T\Delta S_T + \int^P \Delta V dP = 0 \qquad (4\text{-}6)$$

where ΔG_{PT} and ΔV_{PT} are free energy and molar volume changes, respectively at P (atm) and T (K), and ΔH_T and ΔS_T are enthalpy and entropy changes, respectively at T (K) and 1 atm.

In the calculations, ΔH_T and ΔS_T were assumed to be independent of temperature in the temperature range of interest, because no experimental data for heat capacity of ZrO_2 high pressure phases are available.

In case of the monoclinic to orthoⅠ phase transformation, the effect of pressure on V was corrected using compressibility data reported by Kawasaki (1989). Since there is no data of the thermal expansion of both orthoⅠ and orthoⅡ, values of V at ambient pressure were used for the orthoⅠ to orthoⅡ phase transformation assuming that ΔV attributing to the compression compensate that attributing to the thermal expansion. The unit cell volumes and the compressibilities used in the calculations are summarized in Table 4-2. Obtained thermodynamical data are listed in Table 4-3.

Table 4-1 Enthalpies Measured by Drop Calorimetry of ZrO_2

Sample weght (mg)	Δ W (mg)	Δ H (kJ/mol)	Sample weight (mg)	Δ W (mg)	Δ H (kJ/mol)
ortho I		ΔH_1	monoclinic[a]		ΔH_3
20.26	0.02	41.76	20.24	0.03	52.17
20.70	0.05	40.78	20.65	0.01	52.20
19.62	0.02	42.00	19.60	0.02	52.74
18.27	0.04	40.95	18.23	0.01	51.66
		Av.41.37			Av.52.19
ortho II		ΔH_2	monoclinic[b]		ΔH_3
34.49	0.09	32.23	34.46		52.43
27.41	0.22	32.26	27.35		53.50
39.58	0.00	33.03	39.58		52.55
19.68	0.10	32.55	19.66		51.72
		Av.32.52			Av.52.55
			monoclinic[c]		ΔH_3
			25.00	0.17[d]	52.55
			25.86	0.06	51.85
			27.63	0.03	53.41
			25.65	0.18[d]	52.06
			19.87	0.08	49.65
					Av.52.49
				total	Av.52.42[e]

These are a combination of heat contents and enthalpy of phase transformation

(a) Recovered sample after the drop of ortho I
(b) Recovered sample after the drop of ortho II
(c) Starting material for high pressure phase synthesis
(d) Leak on the recovered platinum tube was detected
(e) Average of (a)+(b)+(c)

Table 4-2 Molar Volume and Bulk Modulus Data of ZrO_2

phase	V_{298} (cm^3/mol)	bulk modulus (GPa)
monoclinic	22.16[a]	116.2[b]
ortho I	20.22[a]	181.4[b]
ortho II	18.12[a]	

a Suyama et al. (1986)
b Kawasaki (1989)

Table 4-3 Obtained Thermodynamical Data of ZrO_2

Transformation		ΔV_{298} (cm^3/mol)	ΔH_{298} (J/mol)	ΔS_T (J/molK)	dP/dT ($x10^{-3}$GPa/K)
monoclinic -ortho I	A	-1.82 (3.28 GPa)	11050	17.06	-9.25
monoclinic -ortho I	B	-1.47 (6.00 GPa)	11050	7.09	-4.76
ortho I -ortho II		-2.10 (1 atm)	8850	-18.52	8.70

Equilibrium points used in the calculations are 3.28GPa*R.T.(A), 6.00GPa*R.T.(B) and 13.5GP*1073K for the mono-ortho I (A),(B) and the ortho I -ortho II , respectively.

Discussion

1 Monoclinic-Ortho I Phase Boundary

When crystal structures of the monoclinic and ortho I are compared, the entropy of configuration of ortho I is found to be larger than that of the monoclinic, therefore, a positive value of calculated ΔS is reasonable.

Calculated slope of the phase boundary at room temperature is plotted in Fig.4-6 together with the results of in-situ observation reported by Block et al. (1985) for comparison. Obtained slope is much shallower than that reported. Some possibilities which give rise to this discrepancy between calculated and experimental data are considered to be like this: ① Some impurities involved in the sample though constant values of ΔH were obtained through all runs. ② some problems with hysteresis, shear stress etc. which make experimental boundary wrong. ③ The effect of surface energy on the measured enthalpies which was ignored in the calculation.

As regards the impurities, no evidence of their existence was observed by XRD, OM, TEM, EDX, TG, ^{1}H NMR and Raman spectra.

In case of most thermodynamical studies of solid, the contribution of surface energy to total free energy is negligibly small comparing with that of the free energy of bulk. When a specimen consists of ultra fine powder (approximately smaller than 100 nm), however, the effect of surface energy on the total free energy becomes significant. As shown in Chapter 1, the stability of the very fine tetragonal powder at room temperature is explained by considering the difference in the surface energy between the tetragonal and the monoclinic. The difference in total

free energy (ΔG_{total}) between A and B phases is described as following equation;

$$\Delta G_{total} = (G^c_A - G^c_B) + (\gamma'_A - \gamma'_B)$$
$$= \Delta G_{bulk} + \Delta \gamma' \qquad (4\text{-}7)$$

where G^c is molar free energy of bulk (J/mol) and γ' is surface energy (J/mol). Conventional unit of surface energy is erg/cm^2, however, molar unit is used in this equation for the convenience. Therefore, γ' changes with grain size. Strain energy is neglected here. In most cases, ΔG_{bulk} is much larger than $\Delta \gamma'$, therefore, $\Delta \gamma'$ is negligible. However, in case of tetragonal very fine powder, $\Delta \gamma'$ must be considered. At room temperature, $\Delta \gamma'$ has a positive value and this value increases as grain size decreases while ΔG_{bulk} has a constant negative value. ΔG_{total} becomes 0 at certain grain size (d_c) and then has positive in the range $d<d_c$. This means that very fine powder of the tetragonal ($d<d_c$) is stable at room temperature.

Present experiments were performed using ultra fine powder of ZrO_2(crystallite size was about 20-30 nm). If there is difference in surface energy between the monoclinic and orthoI as well as in case of the tetragonal and the monoclinic, this difference will make the value of ΔG_{total} different from that of bulk sample.

Kawasaki (1989) performed in situ observation of the monoclinic to orthoI phase transformation at room temperature using a diamond anvil pressure cell. He showed that pressure at which orthoI appears shifts to high pressure side as crystallite size is decreased. There are two possible explanations for this

result: One is that activation energy for the transformation increases as crystallite size decreases and that excess compression is required for the transformation. The other is the equilibrium pressure, at which $\Delta G_{total} = 0$, shifts because of the remarkable contribution of $\Delta \gamma'$. He reported that ZrO_2 fine powder crystallite size, which was 20-30 nm, transformed to orthoI within a few seconds at 6.6 GPa while even slight trace of orthoI did not appear after holding the sample at 5.75 GPa for more than 1 day. This result is unreasonable to be explained only by the high activation energy. If the equilibrium pressure is about 3 GPa, 5.75 and 6.6 GPa are stable region of orthoI . Even if there is high activation energy for the phase transformation, it is most unlikely to occur that the transformation rate differs so drastically between 5.75 and 6.6GPa. Therefore, it seems more practical to explain his result by the shift of equilibrium pressure.

Assuming the shift of equilibrium pressure by the contribution of surface energy term in equation (4-5), the phase boundary was calculated using measured enthalpy. The transformation pressure used was 6 GPa reported by Kawasaki for fine powder with the same crystallite size as the present study. Obtained thermodynamical data are listed in Table 4-3. Calculated slope of the phase boundary is plotted in Fig.4-6. Comparing with the value calculated at 3.28 GPa, this value of the slope is close to that reported by Block et al. (1985). Furthermore, obtained stable region of fine powder of orthoI is relatively consistent with the results of synthesis experiments using same size of powder as shown in Fig.1-9 in Chapter 1.

Using newly calculated value, ΔG_{total} at 3.28 GPa was calcu-

lated from equation (4-6) to be 2889 (J/mol). As shown in equation (4-7), calculated ΔG_{total} corresponds to $\Delta \gamma$ ', because the value of ΔG_{bulk} at 3.28 GPa is 0. Using $\Delta \gamma$ ', the difference in the surface energy between the monoclinic and orthoI was estimated. Following equation was used;

$$4\pi r^2 \cdot A \cdot M^{-1} \cdot 10^{-21} \Delta \gamma = 2889 \text{ (J/mol)} \qquad (4\text{-}8)$$

where r is radius of a grain (Spherical grain is assumed. Grain size is assumed to be equal to crystallite size because of ultra fine powder). A and M are Avogadro's constant and number of molecule involved in one grain, respectively. $M=(4/3 \cdot \pi r^3)V^{-1} \cdot 4$, V is unit cell volume (nm^3). The difference of V between the monoclinic and orthoI is ignored here because of its small value, 6 %. $\Delta \gamma$ is the difference of surface energy between the monoclinic and orthoI (erg/cm^3). Substituting appropriate value to each parameter, r=12.5, V=0.143 and $A=6.02 \times 10^{23}$, $\Delta \gamma$ was calculated to be 560 (erg/cm^2). Considering that $\Delta \gamma$ is 430 (erg/cm^2) in case of the tetragonal very fine powder, obtained value seems to be acceptable. However, as there is no data of this kind available, further discussion is impossible.

Following is the conclusion: Values calculated with considering the effect of surface energy are more consistent with results obtained by other studies than those without consideration of surface energy. Therefore, there seems to be remarkable effect of surface energy on the total free energy when grain size of sample is very small.

2 Ortho I in Stabilized ZrO_2

Lee and Heuer (1988) reported that a metastable intermediate stage with orthorhombic symmetry was observed in the course of their study of martensitic transformation in tetragonal MgO-Y_2O_3-ZrO_2. They performed in situ observations of the martensitic transformation in a TEM by adjusting current and illumination conditions of the electron beam; the localized beam heating generated thermomechanical stresses which induced the transformation. This phase with orthorhombic symmetry was also reported by Lenz and Heuer (1982) and Dickerson et al. (1987) in Mg-PSZ and in Ca-PSZ, respectively. All of their studies were carried out by TEM observation and Lee and Heuer (1988) stated that this phase was interpreted as a metastable polymorph of ZrO_2 which occurred in various forms of t-ZrO_2 as an artifact during TEM examination.

It is interesting to discuss this phase with orthorhombic symmetry referring to the present studies of ortho I . Though the result of thermodynamical study shows the extension of the stable region of ortho I to lower pressure part than those reported previously, ortho I is unlikely to be stable at ambient pressure since ortho I transforms to the monoclinic by annealing in the temperature range from 300 to 1000℃ . Their report that the phase was a intermediate stage between the tetragonal and the monoclinic opposes present result that the stabilized tetragonal does not transform to ortho I .

Considering the results of present study, the phase with orthorhombic symmetry is explained as follows: By localized beam heating, thermomechanical stresses are induced in the heated area and consequently transformation from the tetragonal to the

monoclinic occurs. In addition to the thermal expansion on the heated area, about 6 % volume change is accompanied with this transformation. Consequently, total expansion causes high stress fields on the heated area. No data evaluating the magnitude of this stress is available, however, the value is expected to be above 1 GPa considering that the reported value of the surface stress induced by grinding is about 1 GPa for 40vol%Al_2O_3-60vol%ZrO_2 with 3.6mol%-Y_2O_3 (Green et al. 1984). This magnitude of stress is thought to be high enough to give rise to the monoclinic to ortho I phase transformation at elevated temperature. Therefore, the phase presented by Lee and Heuer is considered to be ortho I . They stated that some tetragonal grain, which were in the thinnest part of the sample foil and showed less strain than adjacent grains, underwent a different phase transformation (t-o-m), and also showed different twining behavior. This statement is explained as follows: Under high strain, the monoclinic reduces the strain energy by twining. On the other hand, if there is less strain, in other words, under pseudo-hydrostatic pressure, the monoclinic transforms to ortho I as shown by Chapter 1.

Following is the conclusion: The phase with orthorhombic symmetry observed in TEM sample is ortho I , however, the tetragonal does not transform to ortho I but to the monoclinic at first and then the monoclinic transforms to ortho I .

3 Ortho I - Ortho II Phase Boundary

Ortho I -ortho II phase boundary obtained thermodynamically is illustrated in Fig.4-7 with the results of phase equilibrium experiments for comparison. The slope of the boundary obtained thermodynamically is a little shallower than that by synthesis experiment and it is seen that the stable region of ortho II extends below 10 GPa at room temperature. Block et al. (1985) reported that ortho II started to appear at 16.6 GPa and this transformation was not complete until 22 GPa when pressure was increased at room temperature. These results indicate that there exists high energy barrier between ortho I and ortho II . Therefore, at low temperature, phase transformation proceeds slowly and this makes observed boundary shift toward higher pressure region. When the crystal structures of the monoclinic, ortho I and ortho II are compared (shown in Fig.4-8), it is apparent that reconstruction of lattice is necessary for the ortho I - ortho II phase transformation while the monoclinic-ortho I phase transformation occurs with slight displacement of each atom. This fact also supports the existence of high energy barrier between ortho I and ortho II .

Combining with the result of electrical resistance measurement, the stable region of ortho II is determined as shown in Fig.4-7 (solid line).

4. Quenching of Ortho I

As shown in Chapter 1, ortho I is quenchable only when its grain size is very small. This phenomenon is tentatively explained by the activation energy of the ortho I to monoclinic phase transformation. Regardless of grain size, the monoclinic is the stable phase at ambient pressure and room temperature. Quenched ortho I do not reverse to the monoclinic because of high activation energy. The result that quenching of ortho I depends on grain size indicates the difference in activation energy with grain size.

As the ortho I to monoclinic phase transformation occurs martensitically, the activation energy of this reaction is assumed to be the energy which is necessary for slight displacement of atoms (ions). This phase transformation accompanies about 6 % volume expansion, therefore, the direction of the displacement is that results in volume expansion.

A small grain has relatively high surface energy. To decrease its relative surface energy, small grain generally tends to aggregate each other, absorb impurities on its surface, cause grain growth at elevated temperature, and contract.

Generally surface is the site for nucleation or starting point of newly transformed phase because it has relatively low energy comparing with bulk. In case of martensitic transformation, it can be said that transformation rate at surface regulates the whole transformation because once transformation begins it proceeds immediately over the grain.

In case of the ortho I to monoclinic phase transformation with small grain size, relatively high surface energy is thought to work significantly to prevent the transformation. This is be-

cause the phase transformation occurring on surface enlarges surface area and consequently raises relative surface energy. As grain size increases, effect of surface energy is weakened and ortho I reverses to the monoclinic with ease.

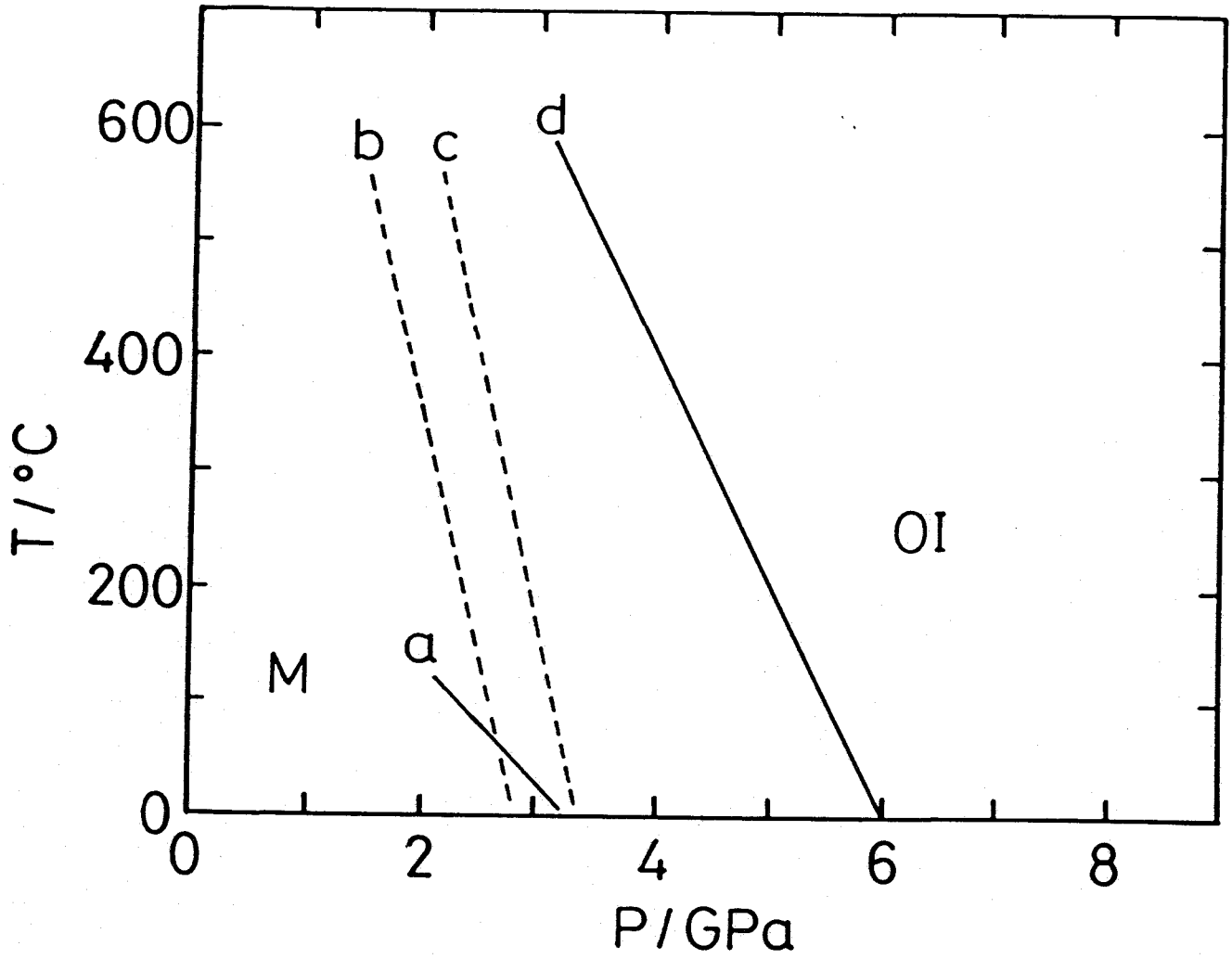

Fig.4-6 Monoclinic-Ortho I boundary

(a) calculated phase boundary assuming Δ G=0 at 3.28 GPa

(b) transformation pressure on increasing pressure

(c) reverse transformation with decreasing pressure

(d) calculated phase boundary assuming Δ G=0 at 6.0 GPa

(b) and (c): after Block et al. (1985)

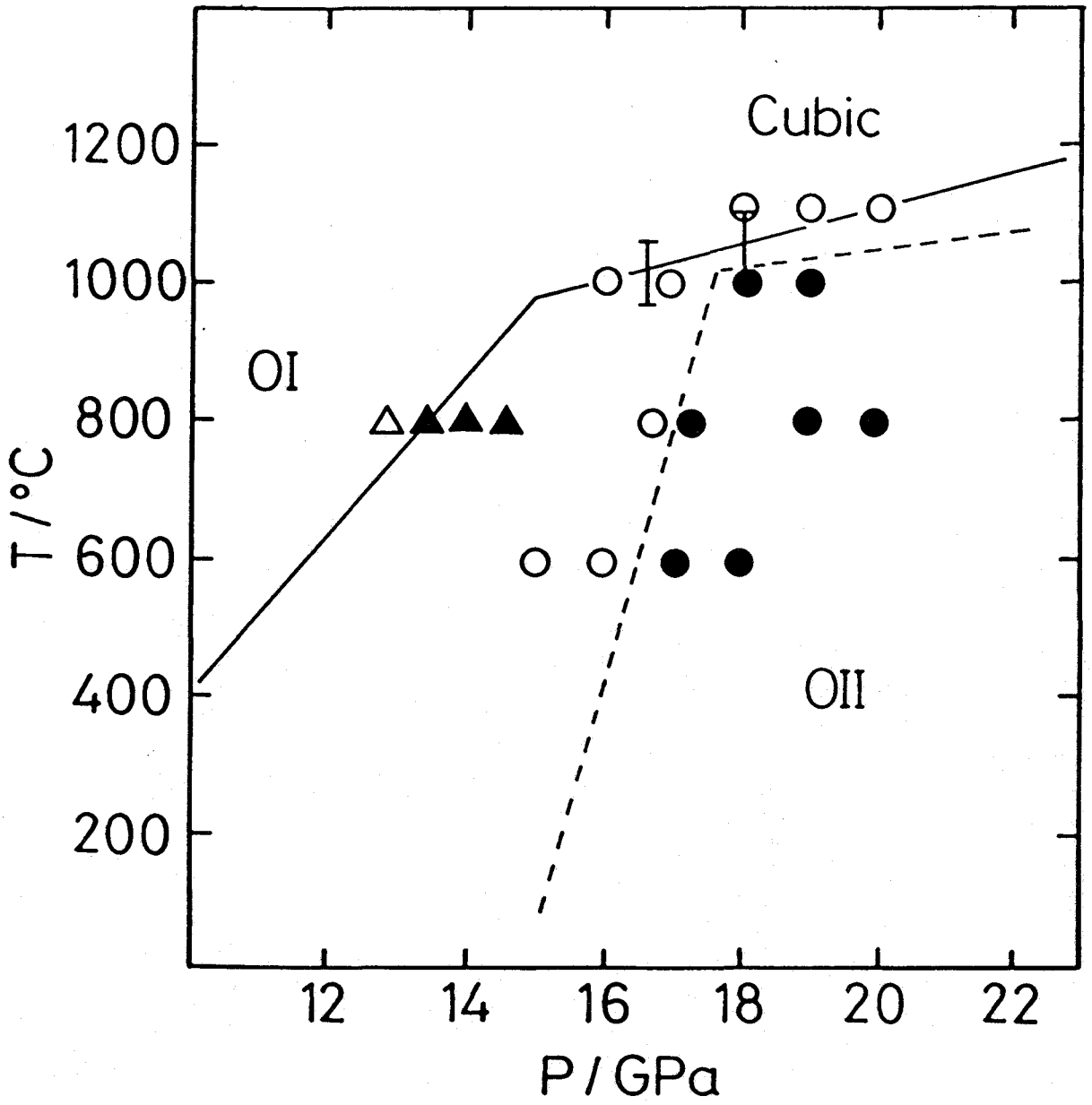

Fig.4-7 Stable region of orthoII

Solid line is obtained phase boundary: OrthoI -orthoII is calculated by thermodynamical data. OrthoII -cubic is determined by electrical resistance measurement (experimental data are shown as I). Results of phase equilibrium experiments are also shown for comparison: Circles are the results of the normal run and triangles are those of the reverse run. (●) and (▲) orthoII ; (○) and (△) the monoclinic.

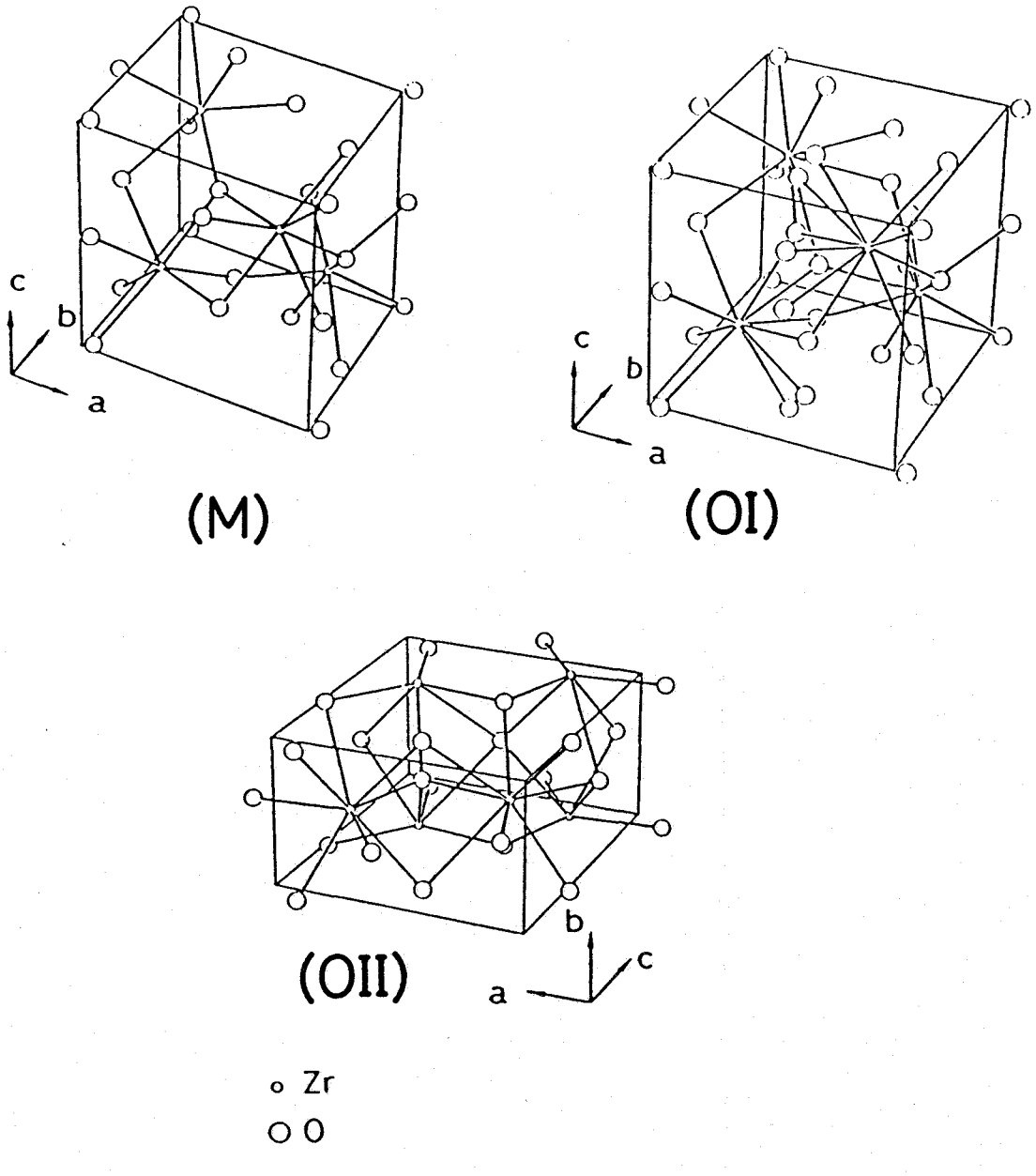

Fig.4-8 Crystal structure of monoclinic, OrthoⅠ and OrthoⅡ after Suyama (1986)

Summary

The present study on the orthorhombic forms of ZrO_2 gives the following results:

1) Ortho I was synthesized using very fine powder (maximum crystallite size was about 60 nm). Considering the relation between crystallite size and surface energy, difference in total free energy between monoclinic and ortho I was evaluated.

2) High temperature phases stabilized by additives did not transform to ortho I because of the small difference in density among these phases.

3) The neutron diffraction study of ortho I indicated the possibility that space group to which ortho I belongs is not Pbcm but one with lower symmetry.

4) The phase equilibrium point between ortho I and ortho II was decided by the phase equilibrium experiments. The synthesis experiment using single crystal of the cubic demonstrated that the transformation to ortho II occurs by the nucleation and growth mechanism.

5) The phase boundary between ortho II and its high temperature phase was fixed by electrical resistance measurements under pressures up to 18 GPa and temperatures up to 1300 ℃.

6) Enthalpies of phase transformation among the monoclinic, ortho I and ortho II were measured with Calvet-type microcalorimeter. Combining measured enthalpies and results of synthesis experiments, entropies of phase transformation and slopes of phase boundary were obtained. From these results, stable regions of ortho I and ortho II was determined.

Acknowledgments

The author heartily wishes to thank Professor S. Kume for the valuable discussion, supervision in the course of the investigations and careful reading the manuscripts.

He wishes to express his thanks to Associate Professors H. Takubo and T. Yamanaka for their instructive advices.

He wishes to thank Professor. A. Navrotsky for giving him the opportunity to perform calorimetry study in her laboratory. He is very much grateful to Associate Professor E. Ito for his kind supervision on high pressure experiments.

Sincere thanks go to Professor K. Urabe, and Associate Professor H. Toraya and Dr. F. Izumi for their helps on high resolution TEM, WPPD and neutron diffraction studies, respectively. Thanks are also due to Drs. K. Nobugai and T. Karasawa for their helps in TEM and Raman spectroscopy studies, respectively.

He wishes to thank Professor F. Kanamaru and Associate Professors Y. Miyamoto and S. Kikkawa for the helpful discussion and suggestion.

He thanks to Dr. T. Ashida for his occasional to-the-point advices. The author is much obliged to Mr. T Iwami for his help on the study of Y-orthoI . Messrs. S. Kuge and S. Kawasaki are thanked for discussion and the preparation of figures . Mr.Katsura is also thanked for his help on high pressure experiments in ISEI.

The author heartily appreciate Ms. M. Nakai's kindnesses.

References

Anderson,C.A. and Gupta,T.K.,(1981) Phase stability and transformation toughening in zirconia,:184-201 in Advances in Ceramics, Vol.3, Science and Technology of zirconia, Edited by A.H.Heuer and L.W.Hobbs, Am.Ceram.Soc., Columbus, OH

Arashi,H. and Ishigame,M.,(1982) Raman spectroscopic studies of the polymorphism in ZrO_2 at high pressures, Phys.Stat.Sol., 71:313-321

Benson,G.C.,Freeman,P.I. and Dempsey,E.,(1963) Calculation of cohesive and surface energies of thorium and uranium oxides, J.Am.Ceram.Soc.,46:43

Block,S., Da Jornada,J.A.H. and Piermarini,G.J.,(1985) Pressure-temperature phase diagram of zirconia, J.Am.Ceram.Soc.,68:497-499

Bocquillon,G., Sussee,C. and Vodar,B.,(1968) Allotropie de l'oxyde d'hafnium sous haute pression, Rev.Int.Hautes Temper. et Refract,5:247-251

Boquillon,G. and Sussee,C.,(1969) Diagramme de phase de la zircone sous pression, ibid.,6:263-266

Devi,S.R.U.,Ming,L.C. and Manghnani,M.H.,(1987) Structural transformation in cubic zirconia,J.Am.Ceram.Soc.,70:C-218

Dickerson,R.M.,Swain,M.V. and Heuer,A.R.,(1987) Microstructural evolution in Ca-PSZ and the room temperature instability of tetragonal ZrO_2, J.Am.Ceram.Soc.,70:214-220

Endo,T.,(1974) Dr.Thesis, Fac. Engineering Sci., Osaka Univ., Osaka Japan

Garvie,R.C.,(1965) The occurrence of metastable tetragonal zirconia as a crystallite size effect, J.Phys.Chem.,69:1238

Green,D.J.,Lange,F.F. and James,M.R.,(1984) Residual surface stresses in Al_2O_3-ZrO_2 composites, in Advances in Ceramics, Vol.12, Science and Technology of ZirconiaⅡ , Edited by Claussen,S.,Ruhle,M. and Heuer,A.H.,Am.Ceram.Soc.,Columbus, OH :240-250

Howard,C.J.,Hill,R.J. and Reichert,B.E.,(1988) Structures of the ZrO_2 polymorphs at room temperature by high-resolution neutron powder diffraction, Acta Cryst.,B44:116-120

Izumi,F.,(1985) A software package for the Rietveld analysis of X-ray and neutron diffraction patterns, Nippon-Kessho-Gakkai-Shi,27:23-31

Jura,G. and Garland,C.W.,(1952) The experimental determination of the surface tension of magnesium oxide, J.Am.Chem.Soc.,74:6033

Kawasaki,S.,(1989) M.Thesis, Fac. Engineering Sci., Osaka Univ., Osaka Japan

Keramidas,V.G. and White,W.B.,(1974) Raman scattering study of the crystallization and phase transformations of ZrO_2, J.Am.Ceram.Soc.57:22-24

Kudoh,Y.,Takeda,H. and Arashi,H.,(1986) In situ determination of crystal structure for high pressure phase of ZrO_2 using a diamond anvil and single crystal X-ray diffraction method, Phys.Chem.Minerals,13:233-237

Lee,R. and Heuer,A.H.,(1988) In situ martensitic transformation in a ternary MgO-Y_2O_3-ZrO_2 alloy: I,Transformation in tetragonal ZrO_2 grains, J.Am.Ceram.Soc.71:694-700

Lenz,L.K. and Heuer,A.H.,(1982) Stress-induced transformation during subcritical crack growth in partially stabilized zirconia, J.Am.Ceram.Soc.,65:C-192

Liu,L.,(1980) New high pressure phase of ZrO_2 and HfO_2, J.Phys.Chem.Solids,41:331-334

Livey,D.T. and Murray,P.,(1956) Surface energies of solid oxides and carbides, J.Am.Ceram.Soc.,39:363

Ming,L.C. and Manghnani,M.H.,(1985) Solid State Physics under

Pressure: Recent Advance with Anvil Devices,:135-140,KTK Scientific Publishers, Tokyo

Navrotsky,A.,(1977) Progress and new directions in high temperature calorimetry, Phys.Chem.Minerals 2:89-104

Ohtaka,O.,Iwami,T.,Urabe,K. and Kume,S.,(1988) Synthesis of the orthorhombic phase of 2Y-ZrO_2,J.Am.Ceram.Soc.,71:C-164

Ohtaka,O.,Toraya,H. and Kume,S.,(1988) Lattice parameters of the orthorhombic phase of 2Y-ZrO_2,Abstract, 12th Annual Conference on Composites and Advanced Ceramics, Am.Ceram.Soc. Cocoa Beach, FL, Jan. 17-20

Pawley,G.S.(1981) Unit-cell refinement from powder diffraction scans,J.Appl.Cryst.,14:357-361

Stokes,A.R.,(1955):413-415 in X-ray Diffraction by Polycrystalline Materials edited by Peiser,H.S., The institute of physics London (1955)

Suyama,R.,(1986) M.Thesis, Fac. Engineering Sci., Osaka Univ., Osaka Japan

Suyama,R.,Ashida,T. and Kume,S.,(1985) Synthesis of the orthorhombic phase of ZrO_2,J.Am.Ceram.Soc.,68:C-314

Suyama,R.,Horiuchi,H. and Kume,S.,(1987) Structural refinement of

ZrO_2 and HfO_2 treated at 600 ℃ 6 GPa, Yogyo-Kyokai-Shi, 95:567-568

Toraya,H.,Yoshimura,M. and Somiya,S.,(1984) Calibration curve for quantitative analysis of the monoclinic-tetragonal ZrO_2 system by X-ray diffraction, J.Am.Ceram.Soc.,67:C-119

Toraya,H.,(1986) Whole-powder-pattern fitting without reference to a structural model: Application to X-ray powder diffractometer data,J.Appl.Cryst.,19:440-447

Toraya,H.,Ohtaka,O. and Kume,S.,(1987) Unit cell parameters of non-doped and 2 mol% Y_2O_3 doped orthorhombic (high pressure form) ZrO_2, Mineral.J.,13:500-504

Watanabe,N.,Asano,H.,Iwasa,H.,Satoh,S.,Murata,H.,Karahashi,K., Tomiyoshi,S., Izumi,F. and Inoue,K.,(1987) High resolution neutron powder diffractometer with a solid methane moderator at pulsed spallation neutron source, Jap.J.Appl.Phys.,26: 1164-1169

Witney,E.D.,(1962) Effect of pressure on monoclinic-tetragonal transition of zirconia; thermodynamics, J.Am.Ceram.Soc.,45:612

Witney,E.D.,(1965) Electrical resistivity and diffusionless phase transformations of zirconia at high temperatures and ultrahigh pressures, J.Electrochem.Soc.,112:91-94